



### This is to certify that the

#### thesis entitled

#### Equilibria and Kinetics of Nonionic Organic Compound Sorption in Soil Organic Matter

presented by

Tyler Thomas Ames

has been accepted towards fulfillment of the requirements for

M.S.	degree in _	CHE	

Dennis J Miller Major professor

Date \_\_\_\_8/2/94

O-7639

MSU is an Affirmative Action/Equal Opportunity Institution



PLACE IN RETURN BOX to remove this checkout from your record.

TO AVOID FINES return on or before date due.

DATE DUE	DATE DUE	DATE DUE

MSU is An Affirmative Action/Equal Opportunity Institution cylerolatedus.pm3-p.1

# EQUILIBRIA AND KINETICS OF NONIONIC ORGANIC COMPOUND SORPTION IN SOIL ORGANIC MATTER

Ву

Tyler Thomas Ames

#### **A THESIS**

Submitted to
Michigan State University
in partial fulfillment of the requirements
for the degree of

MASTER OF SCIENCE

Department of Chemical Engineering

1994

#### **ABSTRACT**

# EQUILIBRIA AND KINETICS OF NONIONIC ORGANIC COMPOUND SORPTION IN SOIL ORGANIC MATTER

By

#### **Tyler Thomas Ames**

While it is known that soil organic matter (SOM) is responsible for nonionic organic compound sorption in water-saturated soil, the equilibria and kinetics of this process are not fully understood. Regarding equilibria, a method of predicting SOM-water partition coefficients for nonionic organic compounds is successfully developed from the UNIFAC type models of Gmehling et al. (1993) and Kontogeorgis et al. (1993). Regarding kinetics, desorption is examined with a goal of developing a fundamental mass transfer model. A gas purge apparatus is critically analyzed and used to collect kinetic data while scanning electron microscopy and x-ray fluorescence spectroscopy are used to examine soil morphology. A spherical geometry, Fickian diffusion model is used to determine effective diffusion coefficients. Kinetic and morphological data indicate soil organic matter may be appropriately modeled as organic-mineral aggregates or solid particles. Steam explosion is used to modify soil morphology as demonstrated with mercury porosimetry.

#### **ACKNOWLEDGEMENTS**

I would like to express my gratitude to Dr. Eric Grulke for guidance and support throughout my Masters program. I also thank Dr. Dennis Miller for advising, as well as Dr. R. Mark Worden for help with mathematical modeling.

I am grateful to Dr. Steven Boyd for use of the MSU gas purge apparatus as well as his expertise in soil science. I thank Dr. Thomas Benzing for instruction with the gas purge apparatus as well as many discussions. I also thank Michael Rich for his skill and patience with scanning electron microscopy of soil samples.

I am perhaps most thankful for my loved ones who have provided encouragement and understanding. I am forever grateful to my mother, my father, and Krista for sharing my achievements as well as tribulations.

# **TABLE OF CONTENTS**

List of Tables		vii
List of Figures		ix
Nomenclature		xi
Chapter 1: Literature	Review and Research Objectives	1
1.1 Introduction	on	1
1.2 Significan	ce of soil organic matter	2
1.3 Models fo	r sorption kinetics	4
1.4 Equilibriu	m of saturated soil organic matter systems	7
1.5 Group con	tribution activity coefficient models	8
1.6 Research	objectives	12
Chapter 2: Solute pha	se equilibria in soil organic matter and water	14
2.1 Introduction	on	14
2.2 Materials	and methods	17
2.2.1	Literature data	17
2.2.2	A modified ELBRO-FV model for prediction of equilibrium	17
	2.2.2.1 Model soil organic matter molecules	17
	2.2.2.2 Model development	19
2.3 Results an	d Discussion	24
2.3.1	Preliminary Results	24
2.3.2	Partition Coefficients from the modified ELBRO-FV model	28
2.3.3	Partition Coefficients using literature activity coefficients	31
2.4 Conclusio	ns	35

Chapter 3: Desorption	n kinetics	37
3.1 Introduction	on	37
3.2 Materials	and metho	ods38
3.2.1	Gas pur	ge system38
	3.2.1.1	Apparatus38
	3.2.1.2	Experimental procedure40
	3	3.2.1.2.1 Solute-soil equilibration40
	3	3.2.1.2.2 Batch stripping of soil sample41
	3	3.2.1.2.3 Heated re-stripping42
3.2.2	Soil sam	aple preparation43
3.2.3	Model d	evelopment and implementation44
	3.2.3.1	Head space45
	3.2.3.2	Gas phase
	3.2.3.3	Liquid phase46
	3.2.3.4	Solid phase47
	3.2.3.5	Multiple solid phases49
	3.2.3.6	IMSL solution of differential equations50
	3.2.3.7	Data analysis52
3.3 Results an	d Discuss	ion54
3.3.1	Apparat	us analysis54
3.3.2	Soil sam	ple analysis57
	3.3.2.1	Virgin and steam exploded Colwood A57
	3.3.2.2	Size fractions of organic enriched Colwood A59
	3.3.2.3	Heated re-stripping analysis61
	3.3.2.4	Total mass removed
	3.3.2.5	Parameter sensitivity65
	3	3.3.2.5.1 Mass transfer coefficient

	3.3.2.5.2 Effective diffusion coefficient	3
3.4 Conclusion	ns71	l
Chapter 4: Soil Morp	hology73	3
4.1 Introduction	on73	3
4.2 Materials	and Methods73	3
4.2.1	Sample preparation	3
4.2.2	Scanning electron microscopy74	ł
4.2.3	X-ray fluorescence spectroscopy74	ł
4.2.4	Steam explosion	5
4.2.5	Mercury porosimetry76	5
4.3 Results an	d Discussion77	7
4.3.1	Scanning electron microscopy77	7
	4.3.1.1 Particle morphology77	7
	4.3.1.2 Steam explosion	3
	4.3.1.3 Particle shearing during batch stripping80	)
4.3.2	X-ray fluorescence spectroscopy	3
4.3.3	Mercury porosimetry84	ŀ
4.4 Conclusion	ns85	5
Conclusions and Reco	ommendations87	7
Appendix A: Sub-gro	oup representations for model SOM molecules91	l
Appendix B: MathCa	d worksheets for activity coefficients calculations93	3
Appendix C: FORTR	AN code for batch stripping simulation	)4
Appendix D: Phase ed	quilibrium calculations for batch stripping experiment 11	10
List of References	11	12

# LIST OF TABLES

Table 1: SOM-water partition coefficients for propylbenzene, concentration basis	15
Table 2: UNIFAC sub-group representation for Stevenson model	20
Table 3: Summary of method for predicting activity coefficients	24
Table 4: List of solutes used in equilibrium calculations	24
Table 5: Predicted and experimental octanol-water partition coefficients, mole fraction basis.	28
Table 6: Predicted and experimental SOM-water partition coefficients, mole fraction basis.	29
Table 7: UNIFAC vs. modified ELBRO-FV partition coefficient predictions for Stevenson SOM model, mole fraction basis.	31
Table 8: Predicted vs. literature solute activity coefficients in water	32
Table 9: Predicted octanol-water partition coefficients using activity data, mole fraction basis.	33
Table 10: SOM-water partition coefficients for Bondi molar group volumes, mole fraction basis.	34
Table 11: SOM-water partition coefficients for Gmehling molar group volumes, mole fraction basis.	34
Table 12: Organic carbon content of soil samples.	43
Table 13: Ideal vs. actual head space break-through times in seconds	45
Table 14: Hypothetical morphologies of soil organic matter and respective material balance equations.	48
Table 15: Batch stripping model parameters	52
Table 16: Henry's law coefficients for alkylbenzenes	53

Table 17: Fitted model para	ameters for batch stripping experiment	56
Table 18: Percent of total pr	ropylbenzene removed for batch stripping runs	65
	ule sub-group representation for Bondi molar group	91
	ule sub-group representation for Gmehling molar grou	•
	sub-group representation for Bondi molar group	92
	sub-group representation for Gmehling molar group	92

# **LIST OF FIGURES**

Figure 1: Humic acid structure from Aiken et al. (1985)	18
Figure 2: Humic acid structure of Stevenson (1982)	19
Figure 3: VLE vs. LLE parameter predictions of octanol-water partition coefficients, mole fraction basis.	25
Figure 4: VLE vs. LLE parameter predictions of SOM (Aiken model)-water partition coefficients, mole fraction basis.	26
Figure 5: VLE vs. LLE parameter predictions of SOM (Stevenson model)-water partition coefficients, mole fraction basis.	26
Figure 6: Stevenson vs. Aiken partition coefficient predictions using UNIFAC (Sandler, 1989), concentration basis.	27
Figure 7: Gas purge system for batch stripping experiments.	39
Figure 8: Stripping gas propylbenzene concentration vs. time for blank runs at 100 mL/min flow rate	54
Figure 9: Stripping gas propylbenzene concentration vs. time for blank runs at 600 mL/min flow rate	55
Figure 10: Stripping gas propylbenzene concentration vs. time for virgin and steam exploded Colwood A at 100 mL/min flow rate.	58
Figure 11: Stripping gas propylbenzene concentration vs. time for three soil sample particle sizes at 600 mL/min flow rate	60
Figure 12: Stripping gas propylbenzene concentration vs. time for initial stripping at 600 mL/min flow rate, 25 degrees Celsius	62
Figure 13: Stripping gas propylbenzene concentration vs. time for heated restripping at 600 mL/min flow rate, 75 degrees Celsius.	63
Figure 14: Stripping curve dependence on mass-transfer coefficient for no-soil runs at 100 mL/min flow rate.	66

Figure 15: Stripping curve dependence on mass-transfer coefficient for no-soil runs at 600 mL/min flow rate.	67
Figure 16: Stripping curve dependence on effective diffusion coefficient (cm <sup>2</sup> /min) for 280 micron spheres at 100 mL/min flow rate and k <sub>L</sub> a=69 1/hr	69
Figure 17: Stripping curve dependence on effective diffusion coefficient (cm <sup>2</sup> /min) for 280 micron spheres at 600 mL/min flow rate and k <sub>L</sub> a=69 1/hr	70
Figure 18: Virgin and steam exploded Colwood samples at 35 X magnification	79
Figure 19: Pulverization effects of batch stripping on 250-500 micron Colwood samples.	82
Figure 20: Incremental pore volumes for virgin and steam exploded Colwood samples.	84

#### **NOMENCLATURE**

#### **Abbreviations**

CSTR	continuous stirred tank reactor
NMR	nuclear magnetic resonance

PFR plug flow reactor SE steam explosion

SEM scanning electron microscopy

SOM soil organic matter

XRF x-ray fluorescence spectroscopy

#### **Symbols**

a gas-liquid interfacial area per volume of liquid (1/cm)

 $A_s$  total surface area of solid phase (cm<sup>2</sup>)

 $C_g$  solute concentration in stripping bubbles (g/mL)

 $C_{g,in}$  solute concentration in gas entering stripping flask (g/mL)

 $C_h$  solute concentration in head space (g/mL)  $C_l$  solute concentration in liquid phase (g/mL)  $C_s$  solute concentration in solid phase (g/mL)

 $C_s^m$  solute mass fraction in soil

 $D_{agg}$  diffusion coefficient for soil aggregate

 $D_{disp}$  head space dispersion coefficient (cm<sup>2</sup>/min)

 $D_{eff}$  solid phase effective diffusion coefficient (cm<sup>2</sup>/min)

 $D_{SOM}$  diffusion coefficient for soil organic matter

F stripping gas flow rate (mL/min)

Henry's law coefficient (dimensionless)partition coefficient (dimensionless)

 $K_d$  solute partition or dispersion coefficient for soil (dimensionless)

 $k_L$  gas-liquid mass transfer coefficient (cm/min)

 $k_L a$  gas-liquid mass transfer coefficient (1/min)

 $K_x$  mole fraction partition coefficient (dimensionless)

 $M_s$  mass of soil (g)

 $m_T$  total solute added to stripping flask (g)

P pressure

R radius of solid phase (cm)

r spatial variable over radius of solid phase (cm)

 $\overline{r}$  spatial variable over radius of solid phase (dimensionless)

 $R_i$  inner radius (cm)  $R_o$  outer radius (cm)

temperaturetime (minutes)

 $V_{
m f}$  pure component molar free volume

 $V_g$  volume of stripping bubbles (mL)

 $V_l$  volume of liquid phase (mL)

x mole fraction

z spatial variable over length of head space (cm)

#### **Greek letters**

γ solute activity coefficient

 $\gamma^{tv}$  free volume contribution to activity coefficient

 $\gamma^{res}$  residual contribution to activity coefficient

 $\phi^{fv}$  free volume fraction

 $V_h$  gas velocity in head space (cm/min)

#### **CHAPTER 1: LITERATURE REVIEW AND RESEARCH OBJECTIVES**

#### 1.1 Introduction

Soil and groundwater contamination by man-made chemicals is a leading environmental problem for government, industry and the public. An important class of contaminants is nonionic organic compounds. This broad classification includes gasoline constituents, industrial solvents, pesticides and herbicides. Many of these compounds are susceptible to microbial degradation and therefore have been targeted for bioremediation. Microbial degradation kinetics are well understood for many combinations of organisms and pollutant compounds. However, solute mass transport and equilibria in a soil-water system play an equally important role and are only partially understood. Successful implementation of bioremediation methods depends on kinetic models which include mass transport as well as microbial degradation. Such models will be able to accurately predict solute concentrations and removal rates.

Pollutant interaction with the soil and water has two important aspects: equilibria and kinetics. Pollutant degradation involves a series of steps including: desorption from soil into the aqueous phase, transport in the aqueous phase to the microorganisms, and microbial degradation. Thermodynamic equilibrium provides limiting case information as to solute concentrations in the soil and aqueous phases. One such limiting case would result if solute desorption from soil was rapid relative to degradation. Solute concentrations would be governed by soil-water equilibria. In contrast, desorption and degradation rates may be on the same order of magnitude. Solute concentrations would be determined by the kinetics of both processes. In any case, soil concentrations are required parameters for determining the level of contamination and if clean-up criteria have been met. Aqueous phase concentrations are needed to determine if the substrate

concentration is sufficient for efficient microbial degradation, but not so high that toxicity is a problem.

Both the equilibria and kinetics of nonionic organic compounds in soil-water systems are addressed in this work. A group contribution activity coefficient model has been adapted to predict solute partition coefficients between soil and water. Soil organic matter, which is responsible for nonionic compound sorption in saturated systems, constitutes the soil phase. Predictions are made for several compounds including halogenated hydrocarbons and pesticides. The work demonstrates the feasibility of modeling soil organic matter with a single molecule and predicting equilibria.

A fundamental mass transport model is needed for soil organic matter. Development of a model in this work is approached from two angles: analysis of kinetic data and physical probing of soil morphology. Insight to the morphology of soil organic matter is gained by batch stripping propylbenzene from soil and analyzing the results with a simple Fickian diffusion model. Microscopic and spectroscopic techniques are used to visually examine soil samples. Conclusions about hypothesized soil models can be drawn with kinetic and visual information.

#### 1.2 Significance of soil organic matter

A great deal of research has been aimed at predicting the sorptive behavior of organic pollutants in soil. One of the most significant concepts resulting from research is the key role that soil organic matter plays in sorption of nonionic organic compounds. Although soil is a complex and heterogeneous mixture, its components can be classified as organic or mineral matter. Soil organic matter is the decomposition products of living organisms, and is a complex and heterogeneous mixture. It has been reported as a flexible, cross-linked, branched, amorphous (noncrystalline), polyelectrolytic polymeric substance (Brusseau et al., 1991). Most important is the difference between organic and mineral matter with respect to water. Organic matter is considered hydrophobic while

polar mineral surfaces are hydrophilic due to strong polar interactions with water (Chiou, 1990). The consequence of water's preference for mineral matter and the polymeric nature of soil organic matter have been uncovered in numerous publications as described hereafter.

The direct correlation between soil organic matter content and sorption capacity has been established by many researchers (Brusseau and Rao, 1989; Chiou et al., 1979; Chiou, 1990; Lambert et al., 1965; Lambert, 1968). The correlation agrees with the physical concepts of the system. In a water saturated system, water will wet the mineral surfaces due to polar interactions. The sorption of the organic solute to the mineral matter is therefore extremely hindered. Sorption of the organic solute to hydrophobic soil organic matter is not hindered. The sorption capacity of the soil organic matter is far greater than that of the few sorption sites on hydrated mineral surfaces, thus the correlation between sorption capacity and soil organic matter. Only polar groups on the organic solute would be attracted to the mineral surfaces. The situation is quite different for dry or nonsaturated soils. The organic solute can freely adsorb to the mineral surfaces. In general, the sorptive capacity of the abundant mineral surfaces is much greater than of the small amounts of soil organic matter. As a result, the sorption capacity of dry soils is higher than that of saturated soils. Starting with saturated soil, water vapor was found to sharply reduce sorption capacities by about two orders of magnitude (Chiou and Shoup, 1985). At about 90% relative humidity, sorption isotherms were comparable to that of an aqueous system. The strong interaction between water and mineral surfaces is further demonstrated by wetting dry soils to which an organic solute has been sorbed. The water displaces the organic solute from the mineral surfaces (Chiou, 1990).

It should be noted that the preceding discussion on the role of sole organic matter is only valid for nonionic organic compounds. A ionic compound will interact with mineral surfaces in a manner similar to water. Additionally, experimental results may deviate from the soil organic matter correlation with increasing polarity. As solute

polarity increases, the solute will adsorb in increasing quantity to the polar mineral surfaces. While sorbate molecular structure has been found to have minimal impact on sorption for nonionic, low polarity compounds, structure becomes more important for complex molecules such as pesticides (Brusseau and Rao, 1991). While the soil organic matter correlation still holds for complex or polar molecules, some variation from nonpolar molecule behavior can be seen in equilibrium and rate studies.

#### 1.3 Models for sorption kinetics

With a basic knowledge of the role of soil organic matter in sorption, the aspect of sorption kinetics can be addressed. In the effort to predict and explain the nonequilibrium sorption of organic compounds, many researchers have presented conceptual models for rate limited desorption. Brusseau et al. (1991) divided rate limiting processes into two useful classifications: transport related processes and sorption related processes. Transport related processes can be defined as physical non-equilibrium resulting from a heterogeneous flow domain. Rate limitation by transport processes has been handled either by including it in the models, or designing experiments in which it is insignificant. An example of the prior is including film diffusion and/or axial and radial diffusion in a model for a soil column experiment. An example of the latter is a well mixed batch stripping experiment such as the gas purge apparatus found in the literature (Benzing, 1993; Brusseau et al., 1990).

Regardless of how transport limitations are handled, sorption related processes have also been divided into two classes: chemical nonequilibrium and physical nonequilibrium. Chemical nonequilibrium is assumed to be the result of a time-dependent sorption reaction at the sorbent surface (Brusseau and Rao, 1989). Chemical nonequilibrium would result from strong sorbate-sorbent interactions such as covalent or ionic bonding, not expected with nonionic organic compounds and soil organic matter. The literature is consistent that chemical nonequilibrium is probably not important for

nonionic organic compounds in an aqueous system (Brusseau and Rao, 1989; Brusseau et al., 1991; Chiou, 1990). The body of literature which addresses physical nonequilibrium, however, is large and appears to have developed in somewhat independent circles with no consensus on the specific mechanism for sorption.

Chemical engineering models for diffusion in catalyst pellets have provided ideas for modeling diffusion in soil. The catalyst pellets consist of crystalline catalyst particles compressed together. The void space between the particles constitutes macropores, while the crystalline particles themselves are porous, constituting micropores. Wakao and Smith (1962) presented a theoretical model for predicting diffusion rates in catalyst pellets dividing the pellet into a homogeneous macropore fraction and a homogeneous micropore fraction. A more conceptually correct model was proposed by Ruckenstein et al. (1971). The model includes radial macropore diffusion into the pellet and radial micropore diffusion into particles which is dependent on the radial position of the particle. A diffusion model for activated carbon was presented by Peel et al. (1981). The model accounted for film diffusion, macropore and micropore diffusion, with a first-order rate expression for transfer between macropores and micropores. A comparison of diffusion models was provided by Miller and Weber (1986) for soil systems. The study compared three models: a first-order rate expression, a first-order rate expression with a parallel instantaneous equilibrium term, and a dual resistance model with film diffusion and Fickian particle diffusion in series. The dual resistance model was not only more conceptually correct but provided the best fit to data.

The concepts of the previously mentioned diffusion models were applied to a soil system by Crittenden et al. (1986). The model included film diffusion, macropore diffusion, surface diffusion (micropore diffusion), and axial/radial dispersion as the study was conducted in soil columns. The study noted that all of the rate-limiting mechanisms are important and cannot be completely ignored. In a follow-up paper, experimental results for the model were presented (Crittenden et al., 1986). The authors noted mixed

satisfaction with the predictive capabilities of the model. It should be pointed out that despite the model's conceptually sound basis, the role of organic matter versus mineral matter in the soil was not considered.

A physical diffusion model which considers the role of soil organic matter was presented by Wu and Gschwend (1986). The sorption is described by radial diffusion into the soil aggregate, modified by a retardation factor reflecting microscale partitioning of the solute between the pore fluid and soil organic matter. The organic matter could be interpreted as coating on pore walls or as organic particles in an aggregate of both organic and mineral matter. Adjustment of the one fitting parameter, the effective diffusion coefficient, provided good fit to experimental data. A similar model was presented by Ball and Roberts (1991b) where hindered pore diffusion due to restrictive pore sizes was considered. Models of this type are typically referred to as retarded intraparticle diffusion.

While first-order rate-expression models have been used to approximate physical diffusion, they are also somewhat synonymous with intraorganic matter diffusion. The intraorganic matter diffusion model comes from the visualization of soil organic matter as a polymeric partition medium. The conceptual model parallels the observation that the majority of the solute sorbs (or desorbs) very quickly while the remainder sorbs (or desorbs) over a long period of time (Robinson et al., 1990). The soil organic matter is then visualized as having a fraction where sorption (or desorption) of the solute is instantaneous and the remainder is rate-limited. The model can be thought of as having three well mixed boxes or phases. The first box is the aqueous phase. The second box is the fraction of the soil organic matter which is in equilibrium with the aqueous phase. The third box is the remainder of the soil organic matter. Movement of the solute between the second and third box is described by a first-order rate expression.

#### 1.4 Equilibrium of saturated soil organic matter systems

In the effort to predict the behavior of organic compounds in soil, a great number of researchers have determined and analyzed equilibrium conditions for organic pollutants in soil. Studying equilibrium behavior not only gives sorption capacities but gives insight into the mechanism of sorption. A study of equilibrium conditions typically results in a sorption isotherm. The isotherm is graphical representation of amount solute sorbed versus the amount of solute in solution or solute activity. Data points are taken at several solution concentrations to produce a curve.

The shape of a sorption isotherm gives information about the system being studied. The sorption of nonionic organic compounds onto saturated soil (sorption onto soil organic matter) has been found to have linear isotherms (Chiou et al., 1979; Chiou, 1990; Karickhoff et al., 1979; Robinson et al., 1990). This is in contrast to the five general classes of Brunauer sorption isotherms. A Henry's law constant can then be used to predict the amounts of solute in the soil and aqueous phases at equilibrium. Linear isotherms are considered supporting evidence for the role played by soil organic matter. The polymeric organic matter is viewed as a partition medium as opposed to a conventional solid sorbent which would fit a Brunauer isotherm classification. Additionally, studies have shown small heats of sorption and the absence of competition between solutes supporting the argument of a partition medium (Chiou, 1990). Although the concept of soil organic matter as a polymeric partition medium is fairly well accepted, absolute linearity of the isotherms has been questioned. Kyle (1981) commented that linearity of the isotherms had not been clearly established relative to scatter in the data. Isotherms have been reported as nonlinear at higher solute concentrations (Ball and Roberts, 1991a; Voice et al., 1983; Weber et al., 1983).

As previously mentioned, Henry's law has been used to represent linear isotherm data. However, other models have been used in the literature. Nonlinear isotherms have been fit with success by the Langmuir and Freundlich models (Ball and Roberts, 1991a).

The Flory-Huggins model has also been applied (Chiou et al., 1983). The use of the Flory-Huggins model makes sense as it was derived for polymer systems. The model was used by Chiou with assumptions for low solute concentration including a polymer volume fraction of unity, giving a linear isotherm.

A final consideration in regards to equilibrium is that of time. Equilibrium of an organic solute in a soil-water system can take a long time to reach. In a study of toluene adsorbing to soil concentrations appeared steady after 45 days (Robinson et al., 1990). However, analysis after 5 months showed sorption into the soil had not reached equilibrium as previously thought. Ball and Roberts (1991a) reported that contact times of tens to hundreds of days were required to reach equilibrium in the system which gave nonlinear isotherms. Steinberg et al. (1987) reported half-equilibration times of 2-3 decades. Generally, the papers with linear isotherms reported equilibration times less than three days.

#### 1.5 Group contribution activity coefficient models

Phase equilibrium for gases and liquids has been predicted with great success using UNIFAC, a group contribution method for determining activity coefficients. UNIFAC is a powerful predictive tool, as only the structural formula of the mixture components is required. A given compound is represented by a relatively small number of functional groups. Activity coefficients are calculated with only molar areas and volumes of these groups as well as interaction parameters for the groups, which have been fit with existing equilibrium data. While UNIFAC was developed for vapor-liquid equilibrium correlations, it has been expanded to liquid-liquid and polymer-solvent equilibria. It is reasonable then to apply UNIFAC to organic solute-water-soil organic matter equilibrium if soil organic matter is viewed as a polymeric substance. The following review provides background for this application.

Oishi and Prausnitz (1978) modified the UNIFAC model for application to solvent activities in polymer solutions. The modification accounted for free volume effects. The UNIFAC model does not account for changes in free volume due to mixing, as appropriate for ordinary liquid mixtures. Free volume effects are significant for polymer-solvent solutions, however, as polymer molecules are much more tightly packed than solvent molecules (Oishi and Prausnitz, 1978). These effects were accounted for by adding a free volume contribution term to the combinatorial and residual terms. The free volume term requires the external degrees of freedom of the solvent molecule and a proportionality factor which were picked to give good results. Predicted activities were good for the nonpolar systems tested.

With increased interest in applying UNIFAC to liquid-liquid equilibria (LLE) systems, Magnussen et al. (1981) developed a parameter table for liquid systems. A new parameter table was needed as quantitative predictions of multicomponent LLE from binary data only or LLE compositions using vapor-liquid equilibrium (VLE) parameters were not possible (Magnussen et al., 1981). The LLE parameters were moderately successful, but likely suffered from a lack of LLE data for parameter calculation. With the strength of a group contribution method depending on the equilibrium data available, several VLE parameter table updates were made for UNIFAC (Gmehling et al., 1982; Macedo et al., 1983; Tiegs et al., 1987; Hansen et al., 1991). Updates included modified interaction parameters based on increasingly available equilibria data as well as new main groups.

An alternative approach is to focus on parameter sets for specific classes of systems. Hooper et al. (1988) developed temperature dependent interaction parameters for water-organic liquid systems. Agreement with experimental data was very good, but the trade-off is limited application due to a small number of main groups. Similar approaches were taken by Cooling et al. (1992) for water-unsaturated chlorinated

hydrocarbons, and by Abed et al. (1992) for water-sucrose-glucose and water-sucrose-fructose systems.

Efforts were also directed toward improvement of the UNIFAC model itself. Larsen et al. (1987) made two modifications. The group interaction parameters were made temperature dependent, and the combinatorial term was modified. The Staverman-Guggenheim combinatorial expression, used in UNIFAC, was found to lead to negative values for combinatorial excess entropy and thus dropped for the simpler Flory-Huggins combinatorial expression. These changes along with rearrangement of some groups and new parameter fitting made for improved predictions over UNIFAC.

Changes to the UNIFAC-FV model were made by Iwai and Arai (1989) for application to hydrocarbon vapors in molten polymers. The combinatorial and residual terms were that of Oishi and Prausnitz (1978) while the free volume term was modified. In previous papers, the Bondi (1968) method was used to calculate specific hard-core volumes. The authors state that the dead-space of large, branched molecules is difficult to estimate by this method. Instead they estimated hard-core volumes from specific volumes at 0 K, estimated by the method of Biltz (1934). The external degrees of freedom were determined from heat of vaporization data of the pure solute. This method seems to have more of a conceptual basis than the approach of Oishi and Prausnitz (1978). Despite use of original UNIFAC parameters (Fredenslund et al., 1977), the results were quite good even at elevated temperatures (130 - 175 degrees Celsius). When the predictions were in error, the activities were usually underestimated.

Doong and Ho (1991) addressed the sorption of organic vapors in semicrystalline polyethylene. Only amorphous domains are thought to be accessible, but the presence of crystalline domains appears to affect sorption. The authors present a theoretical model which includes free energy contributions from combinatorial entropy, free volume, interactional-enthalpy (from UNIFAC), and elastic factors. The model contains one adjustable parameter, characteristic of a given polymer and independent of concentration

and temperature. The elastic term in the equation accounts for the crystalline domains affecting the tension or tightness (constraining) of the amorphous chains.

A final modification of the UNIFAC model for solvent-polymer systems, leading to a simpler result, is that of Kontogeorgis et al. (1993). Their ELBRO-FV activity coefficient model contains a residual UNIFAC term and a free volume term given by Elbro et al. (1990). The free volume term is derived from a generalized van der Waals partition function and accounts for both combinatorial and free volume contributions. The ELBRO-FV model offers: (i) a single expression for combinatorial-free volume effects, (ii) no adjustable parameters as used by Oishi and Prausnitz (1978), and (iii) linear temperature dependent interaction parameters (Kontogeorgis et al., 1993). Evaluation with a large variety of polymer solutions showed good experimental agreement and compared favorably with UNIFAC-FV (Oishi and Prausnitz, 1978) predictions.

Gmehling et al. (1993) presented a modified UNIFAC model, which can be viewed as the current update for VLE and LLE applications. The combinatorial term was empirically modified to deal with compounds very different in size, and an extensive data base of VLE, LLE, molar excess enthalpy, and infinite dilution activity coefficient data was used to fit interaction parameters. The temperature dependence of the interaction parameters was also modified from linear to a second-order polynomial. In previous UNIFAC models, the molar group volume and area parameters were obtained from van der Waals group volumes and areas as given by Bondi (1968). Gmehling et al. (1993) fit the parameters using the extensive database. The combination of these factors makes this the group contribution model of choice for VLE or LLE equilibria.

#### 1.6 Research objectives

 To demonstrate the feasibility of using a group contribution activity coefficient method for predicting pollutant partition coefficients between soil organic matter and water.

A UNIFAC type method will be developed for predicting solute activity coefficients in soil organic matter and water. Soil organic matter will be modeled using molecules proposed for humic acid in the literature. Corrections developed for polymer solution systems will be applied. Success of predictions compared to literature data will be quantified.

2. To mathematically model and determine the limitations of the gas purge apparatus as a tool for developing a fundamental mass transfer model for soil organic matter.

The batch stripping experiment (gas purge apparatus) must be accurately modeled before soil analysis can be done. Existence of rate limited gas-liquid mass transfer needs to be determined and quantified. Limitations of the experiment are to be explored including ability to discern between particles of different size or diffusion coefficient and complete a mass balance.

3. To develop a mass transport model for solute desorption from soil organic matter based on morphological information.

Desorption data will be obtained with a batch stripping experiment. As a first approach, a spherical geometry Fickian diffusion model will be tested for ability to predict

desorption curves. Effective diffusion coefficients will be estimated. While this model is similar to that of Wu and Gschwend (1986) as well as Ball and Roberts (1991b), efforts will be made to understand soil organic matter morphology as needed for a good mass transport model. Soil organic matter general morphology is hypothesized as solids, coatings, or aggregates. Microscopy and spectroscopy will be used to visualize morphology. Desorption data will be used to deduce sample characteristics using virgin, organic enriched and sieved, as well as steam exploded soil samples.

# CHAPTER 2: SOLUTE PHASE EQUILIBRIA IN SOIL ORGANIC MATTER AND WATER

#### 2.1 Introduction

The equilibrium concentrations of a nonionic organic solute partitioned between soil organic matter and water is the first of two system aspects which must be addressed when considering a bioremediation process. The thermodynamic equilibrium provides limiting case information as to solute concentrations in the soil and aqueous phases. The soil concentration is a required parameter for determining the level of contamination and if clean-up criteria have been met. Aqueous phase concentrations are needed to determine if the substrate concentration is sufficient for efficient microbial degradation, but not so high that substrate toxicity is a problem.

The distribution of a solute between two phases, such as soil and water, can be conveniently described by a partition coefficient. The partition coefficient is typically the ratio of solute mole fractions or concentrations in the two phases. As described later, the partition coefficient is a function of solute activity coefficients in each phase. In typical environmental systems, solute concentrations are low and the activity coefficients in both phases are essentially constant with respect to concentration and equal to infinite dilution activity coefficients. This conveniently allows the use of a single partition coefficient which does not depend on solute concentration. While infinite dilution systems are evaluated in this work, the theory is applicable to non-dilute systems as well.

As previously outlined in the literature review, soil organic matter is the specific soil component responsible for nonionic compound sorption in aqueous systems. Experimental data does exist for partition of organic solutes between soil organic matter and water, but it is limited. Additionally, the heterogeneous nature of soil organic matter

leads to varied partition data depending on the source of the soil sample. Table 1 illustrates propylbenzene partition coefficient differences between soil samples.

**Table 1:** SOM-water partition coefficients for propylbenzene, concentration basis.

Soil	<u>K<sub>OM</sub></u>	
Capac A	158	
Colwood A, whole soil	209	
Colwood A, 53-125 micron, SOM enriched fraction	295	
Colwood A, 250-500 micron, SOM enriched fraction	331	
(Source: Benzing, 1993)	331	

The sparse and varied nature of partition data provides motivation for development of a method of predicting equilibrium. Such a method would allow for equilibrium predictions where data was not available. Equilibrium could be predicted for engineered compounds in the developmental stage, such as new pesticides. Ideally, the method would also correctly predict equilibrium differences due to variations in chemistry of soil organic matter. Available information such elemental analysis and percent carbon aromaticity could correlate predictions. A group contribution method such as UNIFAC is a prime candidate for meeting the above criteria. Only limited information is required to predict activity coefficients such as structural formula and molar volume. Differences in elemental content and aromaticity are also accounted for by UNIFAC.

This work develops a method for predicting partition coefficients for nonionic organic solutes in soil organic matter and water. In general, the partition coefficient of an organic solute between two phases can be described by Equation 1 from Sandler (1989).

$$K = \frac{\text{concentration of solute in phase I}}{\text{concentration of solute in phase II}}$$
 (1)

For a solute which is completely dissolved between two immiscible phases, equilibrium is described by Equation 2.

$$x_1^I \gamma_1^I (T, P, x_1^I) = x_1^{II} \gamma_1^{II} (T, P, x_1^{II})$$
 (2)

where (x) is the mole fraction of the solute, gamma is the activity coefficient of the solute, (T) is temperature and (P) is pressure. Equation 2 can be rearranged to the very useful form of Equation 3.

$$\frac{x_1^I}{x_1^{II}} = K_x = \frac{\gamma_1^{II}(T, P, x_1^{II})}{\gamma_1^I(T, P, x_1^I)}$$
(3)

The distribution or partition coefficient for the solute mole fractions is equal to the reciprocal of the ratio of the solute activity coefficients in the two phases.

Octanol-water partition coefficients were calculated in addition to soil organic matter-water partition coefficients. Solute equilibrium between SOM and water has been correlated to equilibrium between octanol and water in a linear fashion (Chiou, 1990; Chiou et al., 1983; Karickhoff et al., 1979). As octanol is a pure component organic phase, group contribution method predictions of partition equilibrium are expected to be good. The quality of octanol-water predictions qualitatively represents the most which could be expected of SOM-water predictions. In other words, if octanol-water predictions averaged 20% error then SOM-water predictions would not be reasonably expected to have only 10 or 15% error. The quality of SOM-water predictions can be measured against that of octanol-water predictions.

#### 2.2 Materials and methods

#### 2.2.1 Literature data

Experimental data from the literature was collected in order to develop and test a group contribution activity coefficient model for soil organic matter-water systems. Data collected includes infinite dilution activity coefficients, octanol-water partition coefficients, and soil organic matter-water partition coefficients. Partition coefficient data was taken from Chiou et al. (1983), Briggs (1981), and Benzing (1993). This data was compared to predicted partition coefficients obtained from the ratio of predicted solute activity coefficients in each phase. While this is a comparison of the desired quantity, the predicted value depends on two variables (the two activity coefficients). Two given models may yield similar partition coefficients, but very different activity coefficients. It is valuable to have a direct measure of a model's predictive capability of the activity coefficient for at least one of the two phases. Infinite dilution activity coefficient data was collected in order to make this comparison. Data was taken from Hwang et al. (1992b) and Cooling et al. (1992).

#### 2.2.2 A modified ELBRO-FV model for prediction of equilibrium

#### 2.2.2.1 Model soil organic matter molecules

The predictive value of UNIFAC and similar group contribution methods lies in the fact that relatively little knowledge is required about components in the system to be modeled. In the case of UNIFAC models, only the structural formula is required in order to specify the number of each sub-group in the compound. The ELBRO-FV model (and other polymer-solvent models) also requires the pure component molar volume for each component. This information is readily available for water, octanol, and many solutes.

Soil organic matter, however, is far from a pure component, and assumptions must be made in order to provide a structural formula and molar volume.

Two structural models were chosen for the calculations. The first is a tetramer structure proposed for humic acid from Aiken et al. (1985) shown in Figure 1.

Figure 1: Humic acid structure from Aiken et al. (1985).

The Aiken model is based on a variety of information including elemental analysis, titration data, and NMR analysis as well as the assumption of a lignin pre-cursor backbone. A value of n=1 was used for the repeating hydrocarbon chain. The second model is a hypothetical humic structure of Stevenson (1982) which is shown in Figure 2.

One additional assumption is required to obtain a pure component molar volume. A density of 1.1 g/mL was arbitrarily chosen. This is comparable to the value assumed by Chiou et al. (1983) of 1.2 g/mL. The molar volume is given by the molecular weight (from the structural model) divided by the density. The molar volume can also be determined experimentally by measuring the specific gravity of a soil organic matter sample.

Figure 2: Humic acid structure of Stevenson (1982).

#### 2.2.2.2 Model development

As a preliminary examination, the BASIC program for UNIFAC of Sandler (1989) was used to calculate solute activity coefficients in the three phases: water, octanol, and soil organic matter. The Sandler UNIFAC program was chosen as it provided quick preliminary calculations. Both the Stevenson and Aiken models were used for soil organic matter. Benzene, toluene, ethylbenzene, and propylbenzene were used as solutes. Additionally, a second analysis was done with the parameter set for liquid-liquid equilibrium of Magnussen (1981). The LLE parameter set was chosen as the SOM-water system is solid-liquid system. A solid-liquid system would seemingly be better modeled as a liquid-liquid system opposed to a vapor-liquid system. The main group parameters (van der Waals areas and volumes for combinatorial term calculations) as well as interaction parameters (for residual term calculations) were changed to those of Magnussen (1981).

Inputs to the BASIC program were the UNIFAC sub-group representations for each component. As an example, the Stevenson model representation used with the Sandler (1989) UNIFAC is shown in Table 2.

**Table 2:** UNIFAC sub-group representation for Stevenson model.

UNIFAC sub-group	Frequency
CH <sub>2</sub>	1
CH	3
ACH	15
AC	22
ОН	4
ACOH	13
CH <sub>2</sub> CO	2
CHO	1
НСОО	5
СН-О	6
CH <sub>2</sub> NH	1
ACNH <sub>2</sub>	1
CHNH	11

It should be noted that exact representations of the model soil organic matter molecules were not possible with most sub-group sets, as required sub-groups were not available. An example is quinone which was represented by an aromatic carbon and a hydroxyl. The result is representations which vary slightly depending on the set of groups and sub-groups used. Also, as the SOM molecules are quite large, multiple representations are possible with a given set of sub-groups. Sub-group representations for both SOM molecules applicable to the final modified ELBRO-FV method of this work are listed in Appendix A.

Solute activity coefficients as a function of solute concentration were determined by the BASIC program. A greatly simplifying assumption was that solvent phases (SOM, water or octanol) were pure. In other words, any limited mutual solubilities were ignored. In reality, the water phase would have a small amount of octanol while the octanol phase would have a small amount of water. The mutual solubilities, if accounted for, would depend on solute concentrations. This assumption was checked for octanol-water partitioning. Predicted partition coefficients decreased by less than 3% when octanol-water solubility was accounted for. Additionally, solvent phase mixing is considered negligible for SOM-water as soil organic matter is a cross-linked, polymeric substance.

A polynomial curve fitting program (Polymath) was used to represent the activity coefficients as a function of concentration with fifth-order polynomials. Microsoft Excel was used to iteratively solve for solute concentrations in each phase, e.g. Stevenson SOM and water, and thus the partition coefficient. As mentioned in the introduction, the analysis thus far is applicable to non-dilute as well as dilute systems as activity coefficients are a function of concentration. However, as concentrations of interest were low, the solute activity coefficients were found to be independent of solute concentration and equal to the infinite dilution activity coefficients. Therefore, infinite dilution activity coefficients were calculated in future work using a solute mole fraction of 0.00001.

After preliminary calculations were reviewed, an improved method of calculation was developed based on literature for polymer-solvent systems. A simple approach would be to choose one of the literature models for all calculations. However, combining elements of different models may lead to better predictions. For example, the residual contribution term to the activity coefficient is common to all models. As described in the literature review, the interaction parameters used to calculate this term are updated over time as databases expand or have been fit for specific classes of compounds. Activity coefficient predictions may be improved by using an interaction parameter set other than that which was published with a given model.

The ELBRO-FV model of Kontogeorgis et al. (1993) was chosen as a basis for calculation of solute activity coefficients in the soil organic matter phase. Strengths of the model include a simplified derivation of a single free volume and combinatorial contribution term as well as proven predictive capabilities. ELBRO-FV was evaluated with polymer solution data from athermal to strongly polar systems. Predicted infinite dilution activity coefficients were in very good agreement with experimental data, and predictions compared favorably with UNIFAC-FV (Kontogeorgis et al., 1993).

In the ELBRO-FV model (Kontogeorgis et al., 1993) the predicted activity coefficient ( $\gamma$ ) is the sum of the free volume term and the residual term as given by Equation 4 for a given component (i).

$$\ln \gamma_i = \ln \gamma_i^{\text{fv}} + \ln \gamma_i^{\text{res}} \tag{4}$$

The free volume term is given by Equation 5 from Elbro et al. (1993). The free volume fraction is given by Equation 6.

$$\ln \gamma_i^{\text{fv}} = \ln \frac{\phi_i^{\text{fv}}}{x_i} + 1 - \frac{\phi_i^{\text{fv}}}{x_i}$$
 (5)

$$\phi_i^{\text{fv}} = \frac{x_i V_{\text{f},i}}{\sum_i x_j V_{\text{f},j}} \tag{6}$$

(x) is the component mole fraction, (j) ranges from one to the number of components, and  $(V_{f,i})$  is the component molar free volume. The molar free volume is given by the difference between the pure component molar volume and the van der Waals volume as calculated by the method of Bondi (1968). However, Gmehling et al. (1993) published a set of fitted molar volumes in place of the traditional van der Waals molar volumes. Therefore, the free volume term could be calculated with group molar volumes taken from:

- (i) van der Waals molar volume parameters based on the method of Bondi (1968)
- (ii) fitted/optimized molar volumes of Gmehling et al. (1993)

Both sets of values were used in partition calculations in order to determine if one set was more successful in predictions than the other.

The residual term of the ELBRO-FV model is given by UNIFAC from Fredenslund et al. (1977). It is logical to replace the outdated 1977 interaction parameter

set used to calculate this term with a more appropriate one. As seen in the literature review many sets are available, some with broad application while are some specific. Three options were identified:

- (i) the most recent database parameters of Gmehling et al. (1993)
- (ii) the LLE database parameters of Magnussen et al. (1981)
- (iii) the water-organic liquid database parameters of Hooper et al. (1988)

The Gmehling et al. (1993) set was ultimately chosen as the database used to fit parameters is the largest and most recent. The LLE parameters of Magnussen et al. (1981) seemed a logical choice as the solute-SOM-water system is solid-liquid-liquid being modeled as a liquid-liquid-liquid system. However, the preliminary results showed that even the outdated VLE parameter set used by Sandler (1989) had significantly greater success with the solute-SOM-water system than the Magnussen et al. (1981) set. While the specific focus of the Hooper et al. (1988) parameter set was appropriate, it was rejected as it lacked too many groups required for modeling of soil organic matter.

A final model adjustment was made based on the following preliminary study. Activity coefficients were calculated on MathCad worksheets for benzene, toluene, and ethylbenzene in octanol, water, and the Stevenson SOM phase. The ELBRO-FV free volume contribution was apparently not appropriate for the aqueous phase. Predicted activity coefficients were two to three orders of magnitude too low. Residual term contributions alone were close to experimental values, but free volume term contributions were negative. The rectify this problem, the modified ELBRO-FV model was used only for SOM phase predictions while the modified UNIFAC model of Gmehling et al. (1993) was used for water and octanol phase predictions. While it is surprising that the ELBRO-FV model does not handle an aqueous phase well, it should be noted that predictions with an aqueous phase were not evaluated by Kontogeorgis et al. (1993). Table 3 summarizes the final modified ELBRO-FV model used for calculating partition coefficients.

**Table 3:** Summary of method for predicting activity coefficients.

Phase	Method
Solute in soil organic matter	Modified ELBRO-FV (Kontogeorgis et al., 1993)  - Molar group volumes by:  (a) Method of Bondi (1968)  (b) Fitted Gmehling et al. (1993)  - Interaction parameters of Gmehling et al. (1993)
Solute in water	Modified UNIFAC (Gmehling et al., 1993)
Solute in octanol	Modified UNIFAC (Gmehling et al., 1993)

The completed model was used to predict partition coefficients for a wide variety of pollutant compounds. A complete list is given in Table 4. Effort was made to test a set of compounds which was diverse as possible, while constrained by the limited literature SOM partition data. The group includes several important pollutants as well as pesticides. Calculations were performed on MathCad worksheets. Worksheets for benzene calculations are included in Appendix B. Predicted activity coefficients and partition coefficients were compared to experimental values using Microsoft Excel.

**Table 4:** List of solutes used in equilibrium calculations.

1,2,4-trichlorobenzene	ethylbenzene
2-chloro biphenyl	hexachlorobenzene
4-bromo nitrobenzene	m-toluidine
aniline	methyl tert-butyl ether
benzene	n-propyl-N-phenylcarbamate
captan	naphthalene
carbaryl	nitrobenzene
chlorobenzene	phenol
ethyl-N-phenylcarbamate	

#### 2.3 Results and Discussion

## 2.3.1 Preliminary Results

Preliminary work was done in order to determine the feasibility of applying a group contribution approach such as UNIFAC to soil organic matter-water systems. The

partition coefficients predicted with UNIFAC (Sandler, 1989) were in reasonably good agreement with experimental data. Additionally, the VLE parameter set of Sandler (1989) was superior to the LLE set of Magnussen (1981). The results for the octanol-water system are shown in Figure 3. Results for the Aiken and Stevenson model molecules are shown in Figure 4 and Figure 5 respectively.

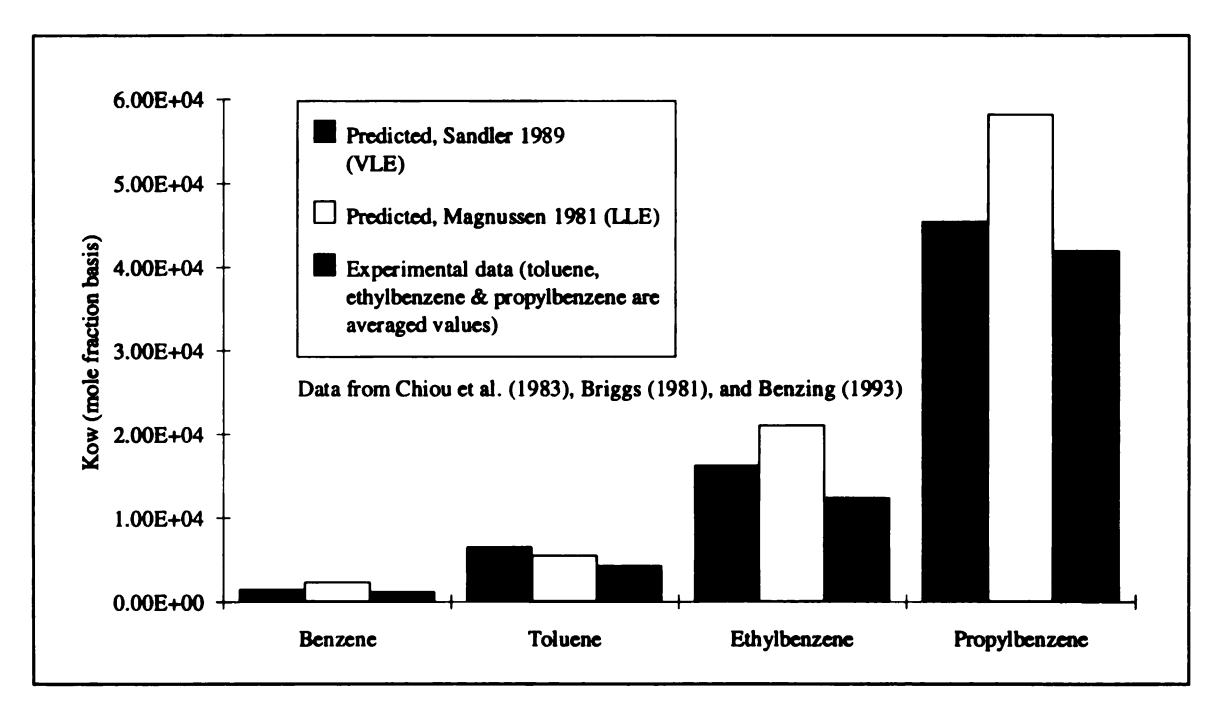


Figure 3: VLE vs. LLE parameter predictions of octanol-water partition coefficients, mole fraction basis.

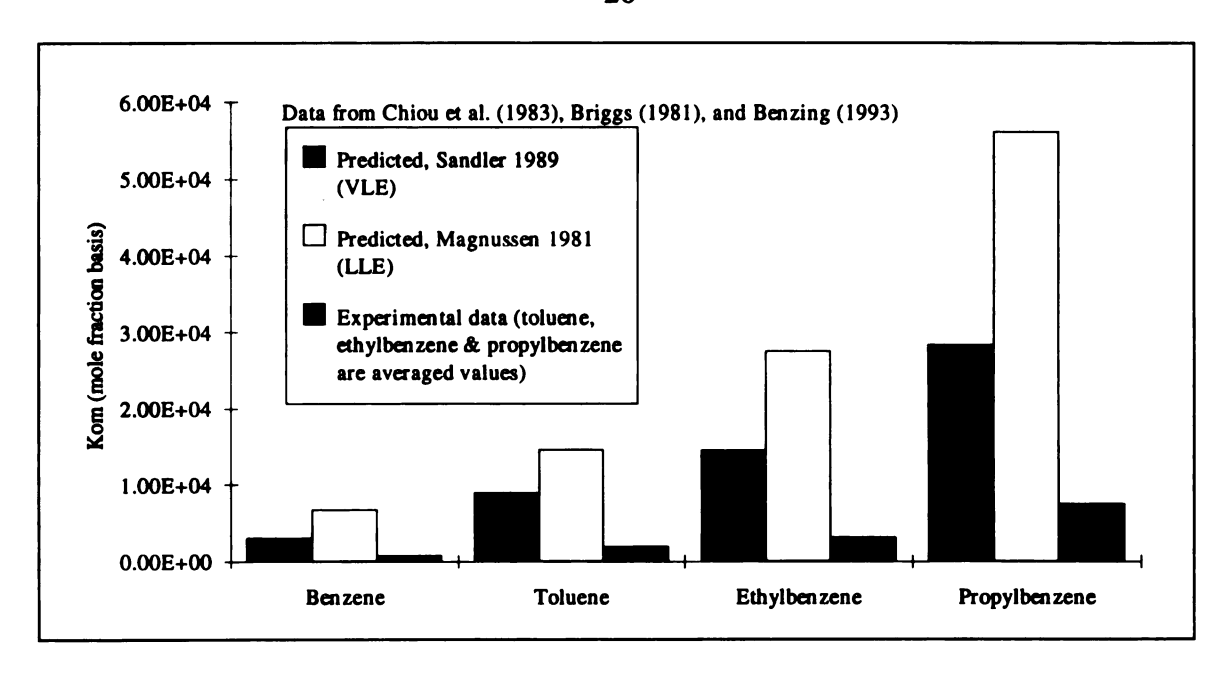


Figure 4: VLE vs. LLE parameter predictions of SOM (Aiken model)-water partition coefficients, mole fraction basis.

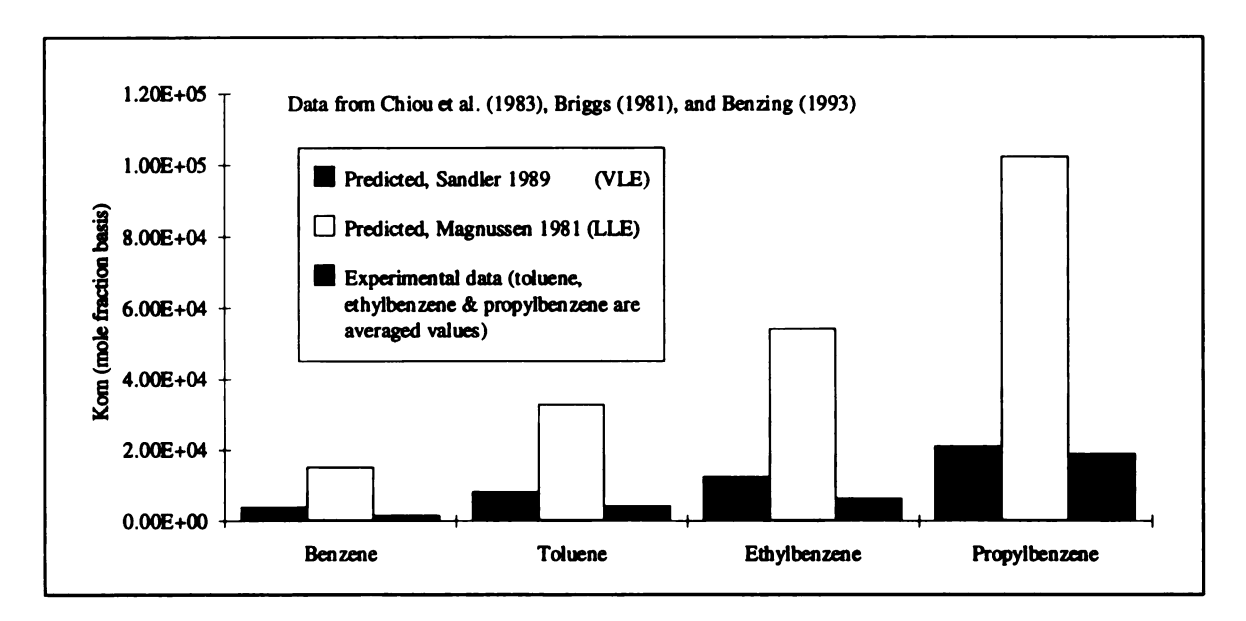


Figure 5: VLE vs. LLE parameter predictions of SOM (Stevenson model)-water partition coefficients, mole fraction basis.

Octanol-water partition coefficients are included as a reference for SOM-water results.

UNIFAC predictions for octanol-water systems were expected to be in good agreement with experimental data and they are. Figure 3 shows that the VLE parameter set is better

than the LLE parameter set. This was not expected as the experimental data is for LLE equilibrium. The VLE set superiority is likely due to the larger number of data sets used in parameter fitting and their diversity. The trend is even more significant in SOM-water predictions. The results imply that parameter sets based on the most diverse and numerous data sets should be used when possible.

A second important result of preliminary work is the difference in predictions made with the Stevenson and Aiken model SOM molecules. As seen in Figure 4 and Figure 5, predictions made with the Stevenson model are much closer to experimental values than the Aiken model predictions. Another illustration of the results is provided in Figure 6.

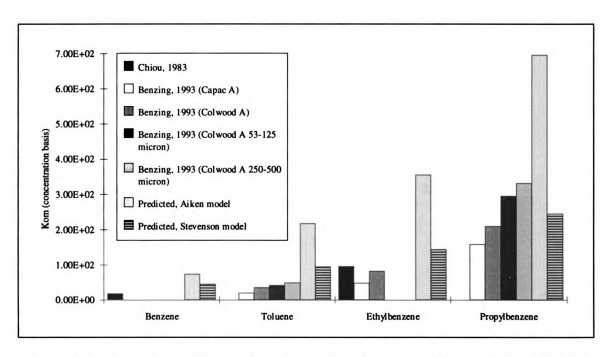


Figure 6: Stevenson vs. Aiken partition coefficient predictions using UNIFAC (Sandler, 1989), concentration basis.

Individual experimental values are shown to illustrate the variation in the data depending on the soil. The results indicate that the Stevenson molecule may be more representative of actual soil organic matter. The primary difference between the two molecules is aromaticity, as seen in Figure 1 and Figure 2, suggesting that aromaticity may be an important factor in SOM chemistry related to equilibrium.

## 2.3.2 Partition Coefficients from the modified ELBRO-FV model

The modified ELBRO-FV method developed in this work was used to predict partition coefficients for a variety of solutes. Accuracy varied greatly with solute. As a reference, octanol-water partition coefficients are shown in Table 5 along with the ratio of predicted to experimental values.

**Table 5:** Predicted and experimental octanol-water partition coefficients, mole fraction basis.

Solute	Predicted	Experimental	Ratio
мтве	113	N/A	N/A
Benzene	1,185	1,178	1.01
Ethylbenzene	12,420	12,336	1.01
Propylbenzene	39,173	41,800	0.937
Naphthalene	46,399	20,006	2.32
1,2,4-Trichlorobenzene	5,459	91,446	0.0597
Hexachlorobenzene	25,844	2,405,280	0.0107
2-Chloro-biphenyl	15,278,592	302,807	50.5
Phenol	72	252	0.286
Chlorobenzene	1,969	6,042	0.326
Nitrobenzene	59	618	0.0955
4-Br-Nitrobenzene	914	3,477	0.263
Aniline	46	69	0.667
m-Toluidine	159	230	0.691
Carbaryl	23,045	1,825	12.6
Captan	31	3,028	0.0102
Ethyl-N-phenylcarbamate	2,269	1,589	1.43
n-Propyl-N-phenylcarbamate	7,279	5,510	1.32
(Experimental partition coefficients from	om Chiou et al. (1983) and	Briggs (1981))	

Some trends are apparent in the results of Table 5. The predictions for the alkylbenzenes are very good. This is expected for these simple, non-polar compounds. The error for naphthalene, however, indicates that some effect of two aromatic rings is not accounted

for. Halogenated solutes, in particular chlorinated compounds, are a problem. Chlorobenzene, 1,2,4-trichlorobenzene, and hexachlorobenzene show a trend of increasing error with increasing number of chlorine atoms. Polarity itself does not seem to be a problem as predictions are good for aniline and m-toluidine. Good results are also achieved for the phenylcarbamate pesticides which are large molecules.

The results are similar for predicted SOM-water partition coefficients. Calculations were made using the Stevenson SOM model, and molar group volumes of both Bondi (1968) and Gmehling (1993). The results, experimental data and predicted-experimental ratios are shown in Table 6. Averaged values were used when multiple experimental data was available.

**Table 6:** Predicted and experimental SOM-water partition coefficients, mole fraction basis.

Solute	Predicted (Bondi)	Predicted (Gmehling)	Experimental	Ratio (Bondi)	Ratio (Gmehling)	
мтве	166	124	N/A	N/A	N/A	
Benzene	1,984	1,222	1,570	1.26	0.778	
Ethylbenzene	6,077	3,816	8,242	0.737	0.463	
Propylbenzene	10,737	6,911	18,830	0.570	0.367	
Naphthalene	58,305	9,006	20,702	2.82	0.435	
1,2,4-Trichlorobenzene	13,733	6,866	43,253	0.318	0.159	
Hexachlorobenzene	258,445	129,222	1,534,660	0.168	0.0842	
2-Chloro-biphenyl	9,420,336	6,453,188	146,600	64.3	44.0	
Phenol	344	225	2,606	0.132	0.0863	
Chlorobenzene	353	242	4,131	0.0855	0.0586	
Nitrobenzene	874	451	4,325	0.202	0.104	
4-Br-Nitrobenzene	44,667	22,488	13,062	3.42	1.72	
Aniline	813	521	1,276	0.637	0.408	
m-Toluidine	1,558	982	2,218	0.702	0.443	
Carbaryl	22,955	15,427	5,200	4.41	2.97	
Captan	5,254	5,112	9,909	0.530	0.516	
Ethyl-N-phenylcarbamate	17,901	12,483	3,281	5.56	3.80	
n-Propyl-N-phenylcarbamate	30,478	21,423	5,702	5.35	3.76	
(Experimental partition coefficients from Chiou et al. (1983) and Briggs (1981))						

Trends seen with octanol-water predictions are seen in the SOM-water predictions. The simple alkylbenzenes are again the most accurate predictions. Halogenated compounds are a problem, but relative errors are lower than the octanol-water case for 1,2,4-trichlorobenzene, hexachlorobenzene, and nitrobenzene (Bondi values). The carbaryl and captan predictions are better, but the phenylcarbamate predictions are worse. Of particular interest is the comparison predictions made with the Bondi versus Gmehling group molar volume parameters. Neither approach has a clear advantage over the other. The Bondi values are generally better for the alkylbenzenes and chlorinated compounds as well as aniline and toluidine. The Gmehling values are somewhat better for the four pesticides. Molar group volume parameters may be best selected based on the solute(s) of interest.

Despite a high variation in relative error, the modified ELBRO-FV predictions are an improvement over the UNIFAC (Sandler, 1989) predictions. Kontogeorgis et al. (1993) states that the original UNIFAC model generally leads to an underestimation of solvent activities as free volume differences are neglected. This would result in a overestimation of the SOM-water partition coefficient which is seen in the preliminary results presented in this work. Table 7 provides a comparison of UNIFAC (Sandler, 1989) predictions to the modified ELBRO-FV predictions using the Bondi molar group volumes. Table 7 includes all of the solutes for which predictions have been made by both methods (excepting MTBE as no experimental data was available). The modified ELBRO-FV predictions compare favorably excepting propylbenzene. Additionally, the error in the modified ELBRO-FV predictions is fairly uniform, while the UNIFAC error is unpredictable as exemplified by hexachlorobenzene.

**Table 7:** UNIFAC vs. modified ELBRO-FV partition coefficient predictions for Stevenson SOM model, mole fraction basis.

Solute	Predicted (UNIFAC)	Predicted (this work)	Experimental	Ratio (UNIFAC)	Ratio (this work)
Benzene	3,900	1,980	1,570	2.48	1.26
Ethylbenzene	12,400	6,080	8,240	1.50	0.738
Propylbenzene	20,900	10,700	18,800	1.11	0.569
Hexachlorobenzene	1,730,000,000	258,000	1,530,000	1,130	0.169
(Experimental partition coefficients from Chiou et al. (1983) and Briggs (1981))					

### 2.3.3 Partition Coefficients using literature activity coefficients

The accuracy of predictions of SOM-water partition coefficients varies with the solutes examined. As described previously, the partition coefficient is a function of two variables, the solute activity coefficients in each phase. Large errors in a partition coefficient could be due to either activity coefficient or both. Comparison of predicted to experimental activity coefficients allows the source of error in predicted partition coefficients to be determined. Water phase activity coefficients from the literature were found for some of the solutes examined and are shown in Table 8 along with predicted values. The predicted-experimental ratios also vary greatly with solute. More importantly however, the errors in the activity coefficient predictions strongly parallel the partition coefficient errors. This suggests that error in partition coefficient predictions is primarily due to error in water phase activity coefficient predictions. If the water phase predictions are erroneous, then experimental values (when available) should allow for improved partition coefficient predictions.

**Table 8:** Predicted vs. literature solute activity coefficients in water.

Solute	Predicted	Literature	Ratio			
МТВЕ	167	82.1	2.03			
Benzene	2,320	2,430	0.955			
Ethylbenzene	28,700	36,900	0.778			
Naphthalene	172,000	63,000	173			
2-Chloro biphenyl	88,600,000	1,550,000	57.2			
Chlorobenzene	3,316	13,900	0.239			
Nitrobenzene	461	3,540	0.130			
Aniline	137	118	1.16			
(Literature activity coefficients from Hwang et al. (1992))						

SOM-water partition coefficients can in fact be improved by using literature water phase activity coefficients in place of predicted ones. While this approach is no longer purely predictive as it requires experimental data, it is still of utility. While no data are currently available for solute activity coefficients in soil organic matter, activity coefficient data are available for water. Partition coefficients can be predicted therefore using: (i) SOM phase activity coefficients predicted with the modified ELBRO-FV model, and (ii) experimental water phase activity coefficients. Water phase infinite dilution activity coefficients are taken from Hwang et al. (1992). The benefit of using experimental activity coefficients is shown in Table 9 for octanol-water partition predictions as a reference.

SOM-water partition predictions are also improved with the use of experimental water phase activity coefficients. The results are shown for Bondi molar group volume predictions in Table 10, and for Gmehling molar group volumes in Table 11. Results are shown for all solutes where activity coefficients in water were available. Clearly, solutes which have the poorest partition predictions gain the most from use of activity coefficient

**Table 9:** Predicted octanol-water partition coefficients using activity data, mole fraction basis.

Solute	Predicted	Experimental	Ratio	Predicted w/ activity data	Ratio w/ activity data
мтве	113	N/A	N/A	55	N/A
Benzene	1,185	1,178	1.01	1,240	1.05
Ethylbenzene	12,420	12,336	1.01	15,974	1.29
Naphthalene	46,399	20,006	2.32	16,995	0.849
2-Chloro-biphenyl	15,278,592	302,807	50.5	267,380	0.883
Chlorobenzene	1,969	6,042	0.326	8,254	1.37
Nitrobenzene	59	618	0.0955	449	0.727
Aniline	46	69	0.667	39	0.565
(Experimental partition coefficients from Chiou et al. (1983) and Briggs (1981))					

data. The results for naphthalene and 2-chloro-biphenyl in particular demonstrate that large errors in partition coefficients are due to errors in the water phase predictions. All three of the halogenated solutes show significant improvement. The difficulty with predictions of halogenated compounds also apparently lies in the water phase not the organic phase. Unfortunately, predictions for some compounds can actually be compromised by using experimental activity coefficients. In these cases, errors in water phase activity coefficient predictions were off-set by errors in the SOM phase activity coefficient predictions. The result is better partition coefficients before any adjustment. Benzene and ethylbenzene predictions are very good as a large number of systems with these compounds were probably available for parameter fitting. Any adjustments to the already near perfect predictions results in decreased accuracy. Aniline shows what can be expected of an intermediate case where the original prediction was moderately good. The accuracy is reduced, but only by a small amount. The benefit of using experimental activity coefficients is more uniform and predictable error. The predictions can be used as

an engineering estimate when data is not available. The trade-off is decreased accuracy for some solutes.

**Table 10:** SOM-water partition coefficients for Bondi molar group volumes, mole fraction basis.

Solute	Predicted	Experimental	Ratio	Predicted w/ activity data	Ratio w/ activity data	
Benzene	1,984	1,570	1.26	2,075	1.32	
Ethylbenzene	6,077	8,242	0.737	7,816	0.948	
Naphthalene	58,305	20,702	2.82	21,356	1.03	
2-Chloro-biphenyl	9,420,336	146,600	64.3	164,859	1.12	
Chlorobenzene	353	4,131	0.0855	1,478	0.358	
Nitrobenzene	874	4,325	0.202	6,705	1.55	
Aniline	813	1,276	0.637	698	0.547	
(Experimental partition	(Experimental partition coefficients from Chiou et al. (1983) and Briggs (1981))					

Table 11: SOM-water partition coefficients for Gmehling molar group volumes, mole fraction basis.

Solute	Predicted	Experimental	Ratio	Predicted w/ activity data	Ratio w/ activity data
Benzene	1,222	1,570	0.778	1,278	0.814
Ethylbenzene	3,816	8,242	0.463	4,908	0.595
Naphthalene	9,006	20,702	0.435	3,299	0.159
2-Chloro-biphenyl	6,453,188	146,600	44.0	112,933	0.770
Chlorobenzene	242	4,131	0.0586	1,013	0.245
Nitrobenzene	451	4,325	0.104	3,457	0.799
Aniline	521	1,276	0.408	447	0.350
(Experimental partition coefficients from Chiou et al. (1983) and Briggs (1981))					

The results are similar to that of octanol-water partition results. 2-Chloro-biphenyl once again show great improvement from previously poor results. Naphthalene improved an amazing 182 to 3 percent error for Bondi predictions, although accuracy decreased for Gmehling predictions. All three halogenated solutes show significant improvement in both the Bondi and Gmehling cases. Notable is an error decrease of 90 to 20 percent for nitrobenzene with Gmehling parameters. These results again indicate that large errors in partition predictions are due to water phase error. While the benzene prediction decreases in accuracy for the Bondi case, it improves slightly for the Gmehling case. Ethylbenzene improves for both cases, from 26 to 5 percent for the Bondi case. The benzene and ethylbenzene results compare very favorably to octanol-water results where both solute predictions were worse with the use of activity coefficient data. Aniline again decreases in accuracy by a small amount. In summary, the use of water phase activity coefficient data significantly improves SOM-water partition coefficient predictions by removing large errors when present, and improving some of the moderate predictions. Apparently only minimal decrease in accuracy results for some solutes with good predictions.

### 2.4 Conclusions

The results presented here are significant as the feasibility of using a group contribution activity coefficient method for predicting soil organic matter-water partition coefficients is demonstrated. A modified version of ELBRO-FV (Kontogeorgis et al., 1993) is used to predict equilibria. The method used here is suitable for SOM as: (i) ELBRO-FV was developed for polymer solutions were molecules vary greatly in size, and (ii) the interaction parameters have been updated with the most recent, broad-based set available. Predictions are varied in accuracy when compared to literature data, but compare favorable to UNIFAC for the limited number of compounds tested. In general, the predictive capabilities are good when considering the heterogeneous nature of soil.

Large errors in partition coefficient predictions were a result of poor activity coefficient predictions for the water phase, as opposed to soil organic matter. The use of experimental water phase activity coefficients greatly improved equilibria predictions where results were originally poor. Halogenated compounds in particular were a problem, but predictions benefited greatly from using experimental water phase activity coefficients.

The Stevenson (1982) humic acid model molecule yielded better results than the Aiken (1985) molecule when compared to literature data. The results indicate that the Stevenson molecule may be more representative of soil organic matter. The primary difference is higher aromaticity in the Stevenson molecule. Further work should include the attempt to correlate SOM chemistry with differences in partition data. Elemental analysis and percent carbon aromaticity could be used to modify the Stevenson molecule and represent a variety of SOM samples. Modified ELBRO-FV predictions could then be compared to experimental partition data for the samples. Successful correlation would demonstrate new understanding of soil organic matter as well as a new predictive method for equilibria. Equally important however is improvement in water phase calculations. More data sets which include water are probably needed in the equilibrium data base used to fit interaction parameters.

### **CHAPTER 3: DESORPTION KINETICS**

#### 3.1 Introduction

The kinetics of nonionic organic solute desorption from water saturated soil is the second of two issues (thermodynamic equilibrium being the first) which must be addressed when considering a bioremediation process. Understanding of the system kinetics allows predictions of solute concentrations as well removal rates for batch or continuous processes. Soil concentrations as a function of time are needed to determine processing times and equipment design which will meet clean-up criteria. Aqueous phase concentrations are needed to determine whether the substrate concentration is sufficient for degradation, but not so high that substrate toxicity is a problem.

A rigorous mass transport model is needed to describe solute desorption from soil into an aqueous phase. As summarized in the literature review, many models have been proposed for desorption kinetics. At best, researchers have modeled the soil as spherical particles and determined an effective diffusion coefficient with a average sieve tray diameter. The limited approaches have resulted in disagreement about sorption mechanism, effective diffusion coefficients, and equilibration times. A rigorous model requires knowledge of the soil morphology. In particular, the morphology of soil organic matter is needed. The location with respect to mineral matter, shape, and pore structure of soil organic matter serve as inputs to a good model.

The understanding of soil morphology can be converged upon from two angles. First, techniques such as scanning electron microscopy, x-ray fluorescence spectroscopy, and mercury porosimetry can be used to physically probe the soil. This approach parallels the characterization of a catalyst, allowing visualization of structure. Second, desorption kinetics can help elucidate morphology with the use of structured soil models. By hypothesizing several physical models for the soil morphology, the model predictions can

be compared to experimental results. Some models will predict the data while others will not. The two approaches are used in an attempt to converge on one or more morphologies which allows for rigorous desorption predictions.

A batch stripping experiment, commonly known in the literature as a gas purge system, is used to obtain kinetic data. While the apparatus has been used previously for kinetic data (Benzing, 1993), the system is re-evaluated as a tool for probing soil morphology. Issues addressed include: (i) the need for a mass transfer coefficient due to rate limited gas-liquid mass transfer, and (ii) the limits of the experiment in regards to discerning between soil particles of different sizes or effective diffusion coefficients. Once the experimental system is properly modeled, soil samples can be evaluated. Kinetic data for soil samples of various sieve tray sizes, as well as ground samples can the be used to evaluated hypothesized soil models. Steam explosion, as a pre-remediation treatment to increase desorption rates, is evaluated. The applicability of an spherical geometry, Fickian diffusion model is examined by estimating effective diffusion coefficients.

### 3.2 Materials and methods

### 3.2.1 Gas purge system

A gas purge system is used to conduct batch stripping experiments. Propylbenzene was chosen as a solute for the studies. Propylbenzene represents a wide class of nonionic organic compounds and has a strong preference for soil organic matter over water as well as a large Henry's law coefficient. These properties allow use of smaller soil sample sizes and make for shorter stripping times respectively.

## **3.2.1.1 Apparatus**

The gas purge apparatus used in this work was the MSU Gas Purge System of the MSU Department of Crop and Soil Science. This system is described in detail by Benzing

(1993), and only a brief description will be included here. The experimental system is depicted in Figure 7.

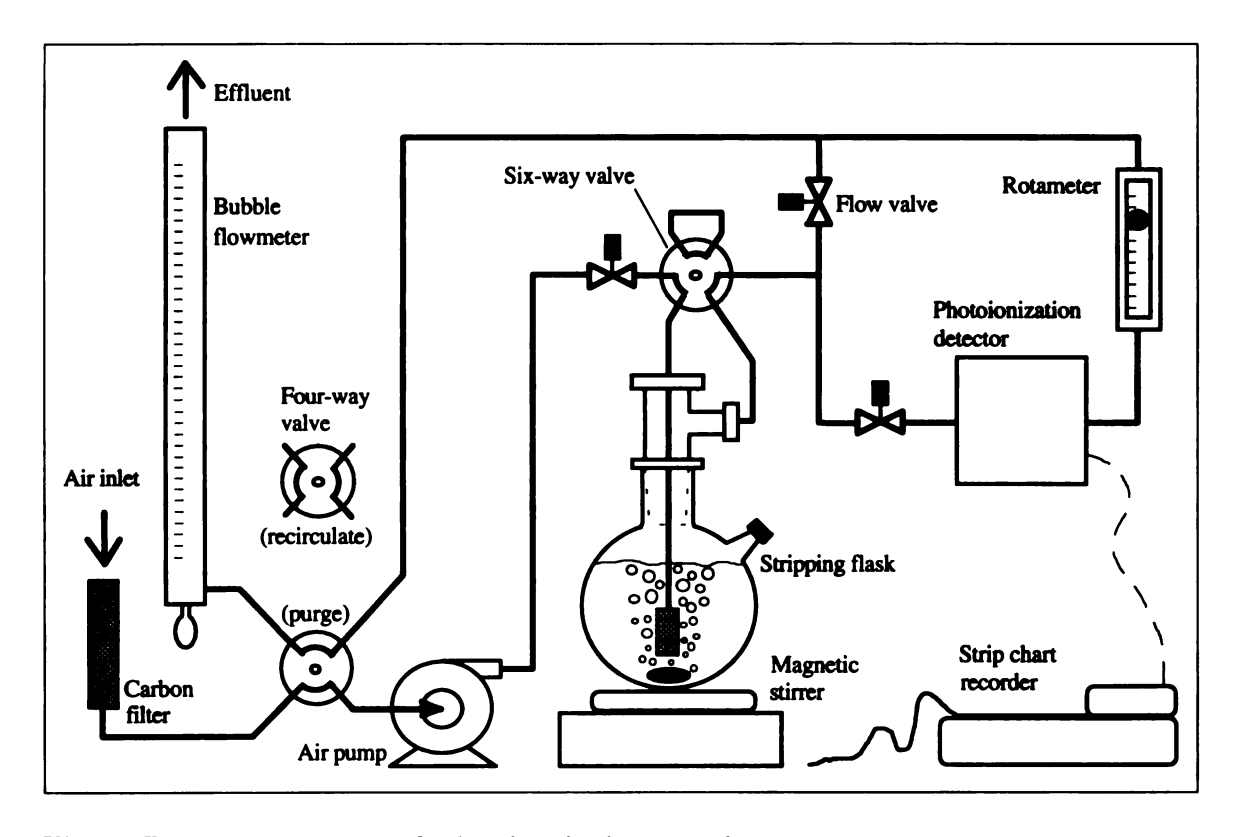


Figure 7: Gas purge system for batch stripping experiments.

The stripping gas (air) flow is as follows when operated in a open system mode. Air is drawn in through a activated charcoal filter by the air pump. Coarse flow rate control is made with a needle valve at the pump exit. The air is routed to either the stripping flask or a bypass loop. Air enters the flask near the bottom via a cylindrical sparger, just above a magnetic stir bar. The air passes through the liquid phase (stripping the solute) and leaves the flask. The air is then split into a stream which passes through the photoionization detector and a detector bypass stream. A needle valve on each stream is used to adjust the flow rate through the detector. The detector stream flow rate is measured with a rotameter at the detector outlet. Finally, the air flows through a bubble flow meter before exiting the system to a fume vent. The bubble flow meter is used to

measure the total air flow rate. The system can also be run in a recirculation mode where the loop is closed between the detector and the air pump.

## 3.2.1.2 Experimental procedure

## 3.2.1.2.1 Solute-soil equilibration

The experimental procedures, with some modification, were developed by Benzing (1993) but are included here for clarity. The first of two procedures for the gas purge experiments is sample preparation. Sample preparation consists of adding a soil sample, solute, and liquid phase to the stripping flask, followed by equilibration of the system. 250 mL round bottom flasks with a side arm were used for the stripping flasks. The side arms were sealed with a silicon-teflon septa. The dry flask with magnetic stir bar was weighed, followed by addition of the soil sample and re-weighing. Soil sample sizes ranged from 1.0 to 2.5 grams depending on the type of sample. The liquid phase in the experiments consisted of Millipore water with 0.01 N calcium chloride and 0.5% by weight mercuric chloride. Calcium chloride is added to mimic groundwater while mercuric chloride prevents biodegradation of the solute. The stripping flask was then sealed with a glass stopper and wrapped with parafilm at the flask-stopper junction.

Propylbenzene was added to the stripping flask in the form of propylbenzene saturated aqueous solution. The use of a aqueous solution insured a pure solute phase did not form in the stripping flask. Millipore water and a layer of propylbenzene were equilibrated in 1 L amber glass bottles. A 10 mL gas-tight syringe was used to withdraw 10 mL of the aqueous phase. The syringe contents were injected through the side arm septum into the flask liquid. The septum and septum cap-side arm junction were wrapped with several layers of parafilm. The flask was then placed on a rotary shaker for 2 to 5 days in order to achieve system equilibrium. Typically, two flasks with soil samples would

be prepared at time as well as a third control flask. The control flask preparation was identical to the sample flasks excepting the addition of soil to the flask.

## 3.2.1.2.2 Batch stripping of soil sample

The second phase of experimentation is batch stripping of the sample. Typically, three flasks were stripped on a day, each flask referred to as a run. At the beginning of the day, the air pump was powered up and allowed to run for about one hour in order to reach a steady temperature. During this time fresh anhydrous CaSO<sub>4</sub> (Drierite) and granular activated carbon were loaded in their respective tubes at the inlet of the gas purge system. During set-up, air was drawn through the Drierite and routed through the flask by-pass loop. The photoionization detector temperature was regulated by a Hewlett Packard 5890 Gas Chromatograph. The cartridge heater and ceramic temperature probe were connected to a proportional control circuit for an unused injector port. After one hour, the photoionization detector lamp was turned on at a power setting of 8. A blank stripping flask was prepared consisting of 200 mL Millipore water and connected in the flask loop of the gas purge system. The air flow was then switched from Drierite to carbon and from by-pass to stripping flask. At this time the system flow rates were set. The coarse setting valve was used to adjust the total flow to roughly 100 mL/min or set at full open for 600 mL/min runs. The detector and detector by-pass needle valves were used to adjust the detector flow rate between 45 and 60 mL/min which is the linear range of the detector (Benzing, 1993). Baseline readings were taken on the recorder for ranges of 1 V, 100 mV, and 10 mV. Flow was switched back to the flask by-pass and the blank flask was disconnected. The gas purge system was switched to recirculating mode. A sample or control flask was then prepared by quickly replacing the glass stopper with the two-way purging stopper assembly. The flask was connected and flow was directed through the flask. After an initial signal spike, a steady signal was reached in 2 to 5 minutes. At this time the system was switched back to open mode. Initial temperature and total flow rate measurements were taken and repeated during the experiment. Temperatures were 23 to 25 degrees Celsius excepting the heated re-stripping experiment. The recorder chart speed was set initially at 3 cm/min as the signal changes rapidly. The chart speed was slowed through the experiment as signal slope decreased to conserve paper. The initial recorder range was 1 V. The 100 and then 10 mV settings were selected once the signal was on chart for the respective setting.

A run was stopped once the signal was deemed constant. The flow was switched back to the flask by-pass, and the flask was disconnected. The blank flask was reconnected and baseline readings were taken again. Once finished, the blank flask was disconnected and the system was dried for 30 minutes. The inlet flow was switched to Drierite and routed through the flask by-pass loop. A laboratory air line was attached to the stripping flask loop. Once drying was completed the system was ready for the next run, or to be powered down for the day.

### 3.2.1.2.3 Heated re-stripping

Experiments were conducted to determine if all the propylbenzene was removed from the soil (250-500 micron enriched Colwood A) during a stripping experiment. A purge experiment was conducted in the manner described above with a total flow rate of 600 mL/min. When the signal was nearly level the system was switched to flask by-pass and recirculation mode. A water bath was placed around the flask. The bath was heated with a heating plate and stirred frequently with a spatula. To avoid soil sample pulverization, flask stirring was done for 15 seconds every 5 minutes during the heating period. Once the bath had reached 75 degrees Celsius, the system was switched from recirculate to open followed by switching from flask by-pass to stripping flask. The run was continued until the signal again appeared constant.

## 3.2.2 Soil sample preparation

Due to the heterogeneity of soil, a balance must be struck between a morphologically uniform, easy to model sample, versus one which is representative of nature. Having identified the importance of soil organic matter, a high organic carbon soil was chosen for study, and modified in order increase organic carbon content with minimal alteration to the natural morphology.

Colwood A horizon was chosen for its organic carbon content of 5.36% (Benzing, 1993) and availability from the Michigan State University Department of Crop and Soil Science. Organic fractionated samples, prepared in the following manner (Benzing, 1993) were also obtained from the Department of Crop and Soil Science.

Air-dried Colwood A horizon (200 g) was added to a sealable 1 L polypropylene bottle. The bottle was filled with 5% sodium hexametaphosphate solution (Millipore MilliQ water), sealed and placed on a rotary shaker for 24 hours. After shaking, the mixture was transferred to a continuous flow separation system. A density separation was made the liquid vortex in the column. The lightest material passed through the column into a series of sieves. Sieve tray sizes were 500, 250, 125, and 53 micron mesh diameter. The size fractions were centrifuged to remove excess solution, freeze dried, and stored in polypropylene bottles. The organic carbon content for the samples was determined by combustion (Benzing, 1993) and is listed in Table 12.

**Table 12:** Organic carbon content of soil samples.

Sample	Organic carbon (%), measured
Colwood A horizon	$5.19 \pm 0.13$
53-125 micron	23.30±0.57
125-250 micron	24.80±0.97
250-500 micron	26.09±0.95
(Source: Benzing, 1993)	

In order to evaluate an appropriate scale for a diffusion path length, crushed samples were also prepared. Approximately 2 grams of the 250-500 micron size fraction was crushed to a powder with a mortar and pestle. The sample was ground for approximately 10 minutes.

Steam exploded samples were prepared in order to effect the sample morphology in a way detectable by gas-purge analysis and/or scanning electron microscopy. In brief, soil slurries were heated in a closed vessel, elevating the pressure, followed by a rapid pressure drop to ambient conditions. The instantaneous vaporization of water in pores is intended to disrupt soil organic matter. A full description of sample preparation is included in Chapter 4.

## 3.2.3 Model development and implementation

A mathematical model was developed for the gas purge experiment in order to interpret kinetic data. Model criteria include the ability to: (i) discern gas-liquid phase mass transfer from solid phase (soil) mass transfer, and (ii) account for multiple solid phase (soil) morphologies such as size, shape, and soil organic matter distribution. The prior is accomplished by including rate limited gas-liquid mass transfer. The latter is achieved by choice of several solid phase mass balances which if needed, can be implemented simultaneously. The model consists of a mass balance for each of the three phases, with the following assumptions:

- (a) Both the gas (sparging bubbles) and liquid phases are well mixed.
- (b) Mass transfer resistances between the liquid and solid phases is negligible.
- (c) Gas-liquid equilibrium obeys Henry's law.
- (d) The liquid phase volume is constant as verified by Benzing (1993).

The model is given by Equation 7 through Equation 10 and is described in the following sections.

## **3.2.3.1 Head space**

The head space is the volume of gas between the liquid phase and the stainless steel tubing leading to the photoionization detector. As the head space is irregularily shaped (varying cross-sectional area), the total volume and height were used to calculate an average cross-sectional area. The volumetric gas flow rate divided by the cross-sectional area gives the linear gas flow rate  $(v_h)$  which is required for the model described in Equation 7.

$$\frac{\partial C_h}{\partial t} = D_{disp} \cdot \frac{\partial^2 C_h}{\partial z^2} - v_h \cdot \frac{\partial C_h}{\partial z} \tag{7}$$

Equation 7 represents a plug flow reactor with axial dispersion.  $(C_h)$  is the head space concentration as a function of space and time,  $(D_{disp})$  is a diffusion coefficient, and (z) is the length of the head space. This representation was chosen as experimental behavior was indicative of neither a CSTR or PFR. As stripping experiments were started at equilibrium, the detector signal remained constant after stripping was started due to plug flow behavior of the tubing to the detector and the head space. Ideal versus actual breakthrough times are compared in Table 13.

**Table 13:** Ideal vs. actual head space break-through times in seconds.

Flow rate (mL/min)	Ideal PFR	Experimental	Ideal CSTR
100	49	30	6
600	8	5	1

The ideal CSTR times are non-zero as they represent the breakthrough times of the tubing to the detector modeled as a PFR. The PFR with axial dispersion model was chosen as:

(i) the break-through times are close to that of a PFR, and (ii) a laminar flow model

requires two spacial variables which is not accommodated by an IMSL routine. Additionally, Fogler (1986) notes that the PFR with dispersion model can compensate not only for problems caused by axial mixing, but also for those caused by radial mixing and nonflat velocity profiles. As the tubing residence times were on the order of experimental error in strip chart measurements, a separate equation for the length of tubing to the detector was not included in the model.

## **3.2.3.2** Gas phase

The gas phase is the volume of gas which is in contact with the liquid phase, i.e. the sparging bubbles. The mass balance consists of convective terms and mass-transfer with the liquid phase as given by Equation 8.

$$\frac{dC_g}{dt}V_g = F(C_{g,in} - C_g) - k_L a(C_g - H \cdot C_l)V_l \tag{8}$$

 $(C_g)$  is the concentration in the gas bubbles as a function of time,  $(V_g)$  is the gas volume, (F) is the gas volumetric flow rate,  $(C_{g,in})$  is the inlet concentration,  $(k_La)$  is the gasliquid mass transfer coefficient, (H) is a Henry's law coefficient,  $(C_l)$  is the liquid phase concentration, and  $(V_l)$  is the liquid phase volume.

## 3.2.3.3 Liquid phase

The liquid phase mass balance consists of mass-transfer with the gas phase as well as the solid phase as given by Equation 9. The solid phase term is the diffusion flux in or out of the soil at the solid surface multiplied by total area over which the flux occurs.

$$\frac{dC_l}{dt}V_l = k_L a \left(C_g - H \cdot C_l\right) V_l - D_{eff} \cdot \frac{\partial C_s}{\partial r} \bigg|_{r=R} \cdot A_s \tag{9}$$

 $(D_{e\!f\!f})$  is the soil effective diffusion coefficient, (R) is the soil particle radius, and  $(A_s)$  is the total surface area of the soil particles.

# 3.2.3.4 Solid phase

The solid phase mass balance consists of Fickian diffusion inside soil particles. As previously indicated the mass balance is adjustable. Several morphologies have been hypothesized and are listed in Table 14. The use of different structured soil models allows for testing of hypothesized morphologies.

Table 14: Hypothetical morphologies of soil organic matter and respective material balance equations.

Visualization of SOM	Description	Equation
Solid Particles		
	Diffusion into a solid sphere of SOM	$\frac{\partial \mathbf{C}}{\partial \mathbf{t}} = D_{SOM} \left( \frac{\partial^2 \mathbf{C}}{\partial \mathbf{r}^2} + \frac{2}{\mathbf{r}} \frac{\partial \mathbf{C}}{\partial \mathbf{r}} \right)$
1/2	Diffusion into a solid cylinder of SOM	$\frac{\partial \mathbf{C}}{\partial \mathbf{t}} = D_{SOM} \left( \frac{\partial^2 \mathbf{C}}{\partial \mathbf{r}^2} + \frac{1}{\mathbf{r}} \frac{\partial \mathbf{C}}{\partial \mathbf{r}} + \frac{\partial^2 \mathbf{C}}{\partial \mathbf{z}^2} \right)$
Coatings		
T or x	Diffusion into spherical coating of SOM, or approximate with an infinite plane	same as sphere above with annular boundary conditions, or for a plane: $\frac{\partial \mathbf{C}}{\partial \mathbf{t}} = D_{SOM} \left( \frac{\partial^2 \mathbf{C}}{\partial \mathbf{x}^2} \right)$
r or x	Diffusion into cylindrical coating of SOM, or approximate with an infinite plane	same as cylinder above with annular boundary conditions, or for a plane: $\frac{\partial \mathbf{C}}{\partial \mathbf{t}} = D_{SOM} \left( \frac{\partial^2 \mathbf{C}}{\partial \mathbf{x}^2} \right)$
Aggregates		
	Diffusion into non-mineral space of spherical aggregate coupled with diffusion into solid spheres of SOM	$\frac{\partial C_{agg}}{\partial t} = D_{agg} \left( \frac{\partial^2 C_{agg}}{\partial r^2} + \frac{2}{r} \frac{\partial C_{agg}}{\partial r} \right)$ $\frac{\partial C}{\partial t} = D_{SOM} \left( \frac{\partial^2 C}{\partial r'^2} + \frac{2}{r'} \frac{\partial C}{\partial r'} \right)$
	Diffusion into continuous sphere of SOM disrupted by "void" spaces of mineral matter, SOM viewed as "mortar in concrete"	$\frac{\partial \mathbf{C}}{\partial \mathbf{t}} = D_{eff} \left( \frac{\partial^2 \mathbf{C}}{\partial \mathbf{r}^2} + \frac{2}{\mathbf{r}} \frac{\partial \mathbf{C}}{\partial \mathbf{r}} \right)$ with diffusion coefficient reflecting "void" spaces of mineral matter

## 3.2.3.5 Multiple solid phases

In order to accommodate multiple soil particle sizes with a single spacial variable the spacial variable must be made dimensionless. In the present work, however, only the simple case of diffusion into a sphere was considered as given by Equation 10.

$$\frac{\partial C_s}{\partial t} = D_{eff} \left( \frac{\partial^2 C_s}{\partial r^2} + \frac{2}{r} \frac{\partial C_s}{\partial r} \right) \tag{10}$$

 $(D_{eff})$  is an effective diffusion coefficient which is dependent on the morphology of the spherical particle. The spacial variable (radial position) was nondimensionalized with the inner  $(R_i)$  and outer  $(R_o)$  particle radii with Equation 11.

$$\overline{r} = \frac{r - R_i}{R_o - R_i} \tag{11}$$

Annular geometries such as coatings can be accommodated by using both an outer and an inner radius for the nondimensionalization. The substitution yields the following two equations for the liquid and solid phase mass balances.

$$\frac{dC_l}{dt}V_l = k_L a \left(C_g - H \cdot C_l\right) V_g - \frac{3 \cdot D_{eff} \cdot V_s}{\left(R_o - R_l\right) R_o} \frac{\partial C_s}{\partial \overline{r}} \bigg|_{r=1}$$
(12)

$$\frac{\partial C_s}{\partial t} = \frac{D_{eff}}{\left(R_o - R_i\right)^2} \left(\frac{\partial^2 C_s}{\partial \bar{r}^2} + \frac{2}{\bar{r}} \frac{\partial C_s}{\partial \bar{r}}\right) \tag{13}$$

The dimensionless spacial variable now ranges from zero at the center of the sphere to unity at the outer surface. Additional soil particle types are handled by (i) adding additional equations of the form of Equation 13 for each particle, and (ii) adding additional

soil flux terms onto Equation 12. Thus for each solid phase particle type the outer radius, inner radius, effective diffusion coefficient, and total volume is specified. While not developed further here, the model could be expanded to include not only spheres but various combinations of morphologies listed in Table 14. This provides flexibility for modeling morphologies as visualized by techniques such as scanning electron microscopy.

# 3.2.3.6 IMSL solution of differential equations

The base-case model (for only one soil particle type) consists of two ordinary differential equations and two partial differential equations. More advanced models may include multiple differential equations for multiple soil particles. The IMSL v. 10.0 routine MOLCH was chosen to solve the model equations. The routine solves a system of partial differential equations of the form  $u_t = f(x, t, u, u_x, u_{xx})$  using the method of lines. The solution is represented with cubic Hermite polynomials. A FORTRAN program was written to utilize MOLCH and output numerical results. The program is listed in Appendix C. Text output file results were imported into Microsoft Excel spreadsheets for interpretation and graphic representation.

The solution of the two ordinary differential equations and two second-order partial differential equation requires four initial conditions and four boundary conditions.

The boundary conditions for the soil phase are given by Equation 14 and Equation 15.

$$\left. \frac{\partial C_s}{\partial \overline{r}} \right|_{\overline{r}=0} = 0 \qquad (14) \qquad C_s \big|_{\overline{r}=1} = K_d \cdot C_l \qquad (15)$$

Equation 14 describes spherical symmetry. Equation 15 describes equilibrium between the liquid phase and the outer surface of the solid phase using the solute partition coefficient (K<sub>d</sub>). The boundary conditions for the head space are given by Equation 16 and Equation 17.

$$C_h \Big|_{z=0} = C_g - D_{disp} \cdot \frac{\partial C_h}{\partial z} \Big|_{z=0}$$
 (16)  $\frac{\partial C_h}{\partial z} \Big|_{z=L} = 0$  (17)

These are the Danckwerts boundary conditions (Danckwerts, 1953). The first boundary condition describes the step change in concentration due to diffusion (dispersion) at the entrance of the vessel.

The initial conditions are specifications for initial concentrations in the gas, liquid, and solid phase. The initial conditions are calculated by Equation 18 through Equation 20.

$$C_{lg} \cdot V_{lg} + C_l \cdot V_l + C_s^m \cdot M_s = m_T \tag{18}$$

$$C_{s} = K_{d} \cdot C_{l} \tag{19}$$

$$C_{lg} = H \cdot C_l \tag{20}$$

Equation 18 is a total mass balance where  $(m_T)$  is the known amount of solute injected into the system. The subscript  $(_{tg})$  represent 'total gas' including sparging bubbles, head space, tubing to the detector, and recycle tubing.  $(C_s^m)$  is a mass fraction and  $(M_s)$  is the mass of soil. Equation 19 and Equation 20 are equilibrium relationships where (H) is a Henry's law coefficient and  $(K_d)$  is the propylbenzene soil-water partition coefficient. The initial head space and gas phase concentrations are simply  $(C_{tg})$ . Calculations for initial concentrations are included in Appendix D.

The model parameters used for initial condition calculations and batch stripping predictions are listed in Table 15. Parameters which are dependent on gas flow rate are listed with the value for each flow rate.

**Table 15:** Batch stripping model parameters.

Parameter	Value
Head space volume	72 cm <sup>3</sup>
Head space length	12 cm
Head space cross-sectional area	6.0 cm <sup>2</sup>
Head space dispersion coefficient	(fitted) cm <sup>2</sup> /min
Stripping gas flow rate	97.2 or 599 cm <sup>3</sup> /min
Gas phase volume	1 or 5 mL
Gas-liquid mass transfer coefficient	(fitted) 1/min
Henry's law coefficient	0.387 (g per mL / g per mL)
Liquid phase volume	210 mL

The values for the stripping gas flow rates are average values for experimental runs. The Henry's law coefficient for propylbenzene was calculated using the Modified UNIFAC model of Gmehling et al. (1993). A value of 0.29 to 0.30 (depending on temperature) was calculated from solubility and vapor pressure data. However, experiments show propylbenzene is removed from the water phase significantly faster than is theoretically possible for Henry's law-equilibrium stripping using these values. Additionally, the trend in Henry's law coefficients for alkylbenzenes shown in Table 16 indicates a value of 0.30 is erroneous. The value predicted with Modified UNIFAC (Gmehling et al., 1993) fits the increasing trend for alkylbenzenes shown in Table 16.

### 3.2.3.7 Data analysis

Each experimental run yielded data in the form of a continuous detector response versus time. Discrete response values versus time were manually recorded from the strip charts and entered into a Microsoft Excel spread sheet as raw data. Baseline detector responses before and after the run were also entered and averaged. Subtracting the

average baseline and correcting for recorder range setting (1 V, 100 mV, 10 mV) yielded a detector response curve. The data could then be analyzed in a differential (concentration) or integral (mass removed from system) manner.

Table 16: Henry's law coefficients for alkylbenzenes.

Compound	Henry's law coefficient
benzene	0.2208
toluene	0.3018
ethylbenzene	0.3460
propylbenzene	N/A
isopropylbenzene	0.5889
(Source: Hwang et al., 1992b)	

Examining the experimental data on a differential or concentration basis is useful for comparison to model predictions. Additionally, only the initial condition assumptions are involved excepting that of detector response linearity. Concentration data was either examined directly as arbitrary concentrations versus time or normalized to the initial gas phase concentration calculated for the experimental run.

Integrating the concentration data yields the solute mass removed from the system. Of interest is the percent of total mass removed versus time curve. This curve can be generated in one of two ways. First, the integral data curve is normalized with the total area under the detector response curve. The normalization assumes that all of the solute has been removed from the system at the end of the experiment. Second, the differential data which has been normalized to initial concentrations is integrated yielding (mass)(time)/(volume). Multiplying by the average gas flow rate gives the total mass removed at a given time. Dividing by the total mass of solute added to the system yields percent of total mass removed.

## 3.3 Results and Discussion

## 3.3.1 Apparatus analysis

The batch stripping apparatus itself must be correctly modeled before any soil analysis can be done. The two fitable parameters, (k<sub>L</sub>a) and (D<sub>disp</sub>), were determined and the model was verified as able to represent experimental data. The analysis was done for both 100 mL/min and 600 mL/min flow rates as stripping characteristics are quite different.

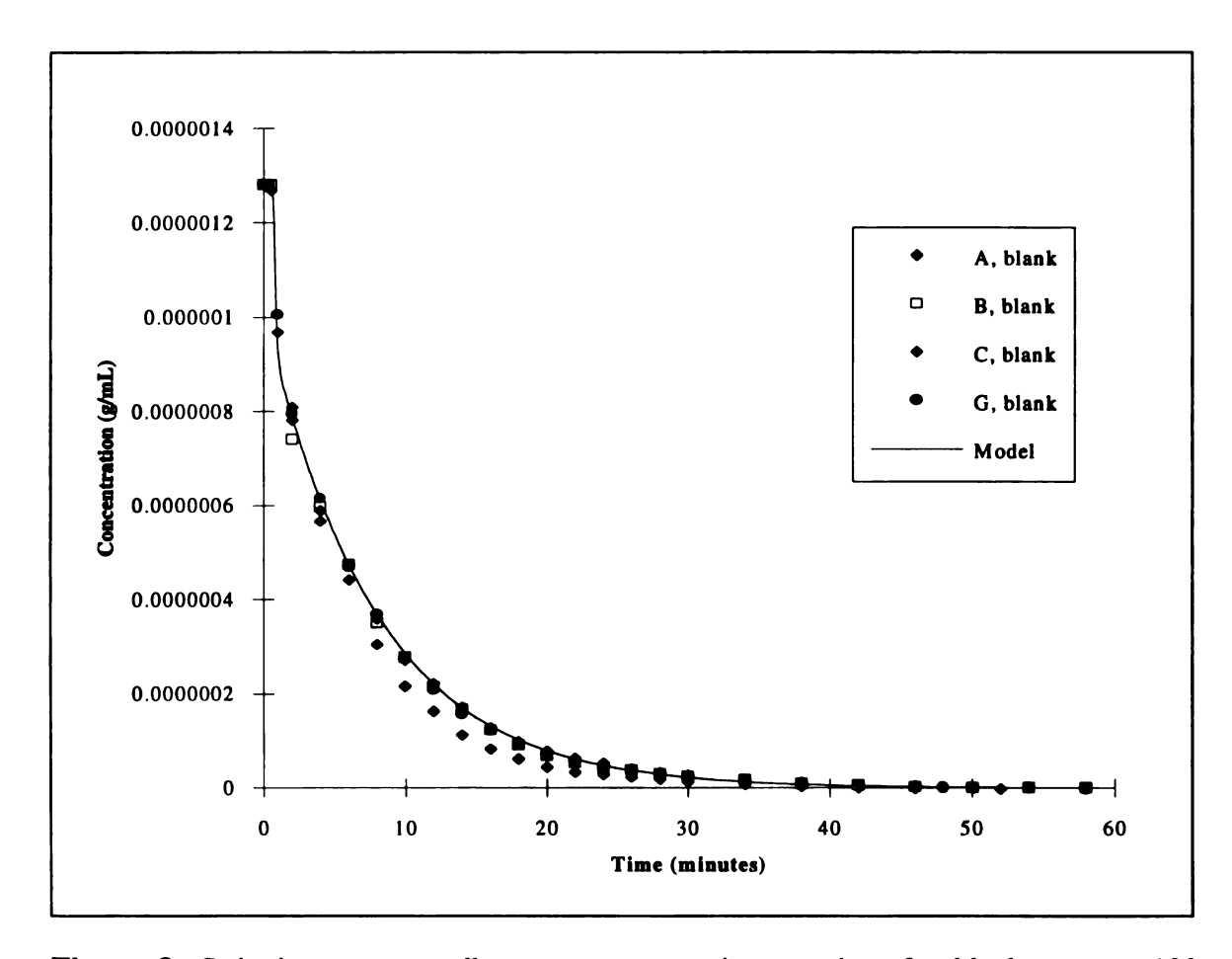


Figure 8: Stripping gas propylbenzene concentration vs. time for blank runs at 100 mL/min flow rate.

Calculated initial concentrations for the head space (measured variable) were used to normalize experimental data. The results are desorption curves in the form of concentration versus time. The curves for 100 mL/min and 600 mL/min flow rate are shown in Figure 8 and Figure 9 respectively. Good model fits were obtained at both flow rates although the 600 mL/min flow rate data is more sporadic than the 100 mL/min data. Mass transfer coefficients and head space dispersion coefficients were fit by a trial and error method. The model fitted model parameters are listed in Table 17. The values found to be optimal are listed with a range. Values outside the range are unable to provide a good model fit regardless of the value of the other parameter.

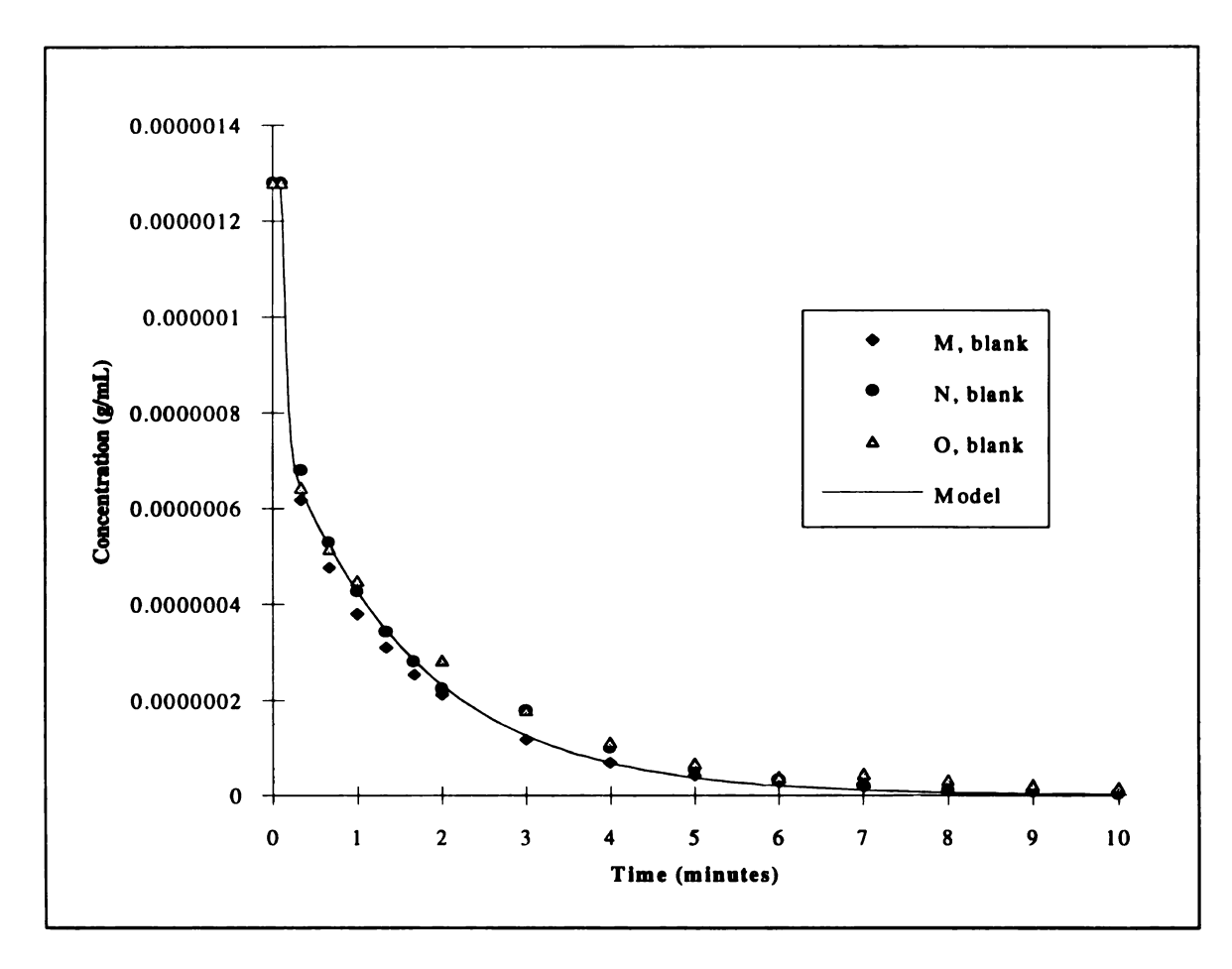


Figure 9: Stripping gas propylbenzene concentration vs. time for blank runs at 600 mL/min flow rate.

**Table 17:** Fitted model parameters for batch stripping experiment.

Parameter	100 mL/min	600 mL/min	
k <sub>L</sub> a (1/hr)	69 ± 6	$210 \pm 30$	
D <sub>disp</sub> (cm <sup>2</sup> /min)	$0.033 \pm 0.033$	$0.50 \pm 0.33$	

The values determined for the mass-transfer coefficient are indicative of rate limited mass transport. As seen in the desorption curves, the stripping gas concentration drops rapidly as the gas phase (bubbles) are rapidly depleted of propylbenzene by convection, while mass transfer from the liquid phase is slower. This finding contrasts the assumption of liquid-gas equilibrium made by Benzing (1993) for the 100 mL/min flow rate. If the gas and liquid were in equilibrium a more shallow curve would result, as discussed further in the section on parameter sensitivity. The 600 mL/min flow rate (k<sub>r</sub> a) is roughly three times greater than the 100 mL/min flow rate (k<sub>1</sub> a). However, the 600 mL/min gas volume (bubbles) is estimated at five times greater than the 100 mL/min volume. As (a) is defined as the surface area per volume of liquid, it should be 2.9 times greater for the 600 mL/min case assuming a constant bubble radius. This indicates that (k<sub>I</sub>) is roughly the same at both flow rates. Comparison of the mass transfer coefficient values to literature values should be made with some caution. The fitted values are dependent on the values used for the gas phase volume which were estimated from the very small rise in liquid level during sparging. Dispersion in the PFR results not only in an earlier breakthrough time, but also in a smoothing out of the rate limited portion of the desorption curve. The dispersion coefficient magnitude of effect is much less than the mass transfer coefficient. The 600 mL/min dispersion coefficient is significantly greater than for 100 mL/min. This is interpreted as a result of increased head space turbulent mixing at the higher flow rate.

## 3.3.2 Soil sample analysis

Knowing the values of model parameters related to the experimental apparatus, the desorption of soil samples can be analyzed. The assumption is made that parameters determined without soil remain constant for experiments with soil. Differences between desorption curves of soil and no-soil samples as well as different soil samples can then be examined and interpreted with a chosen model for the soil phase. In this work, the soil phase was modeled as spheres in which Fickian diffusion occurs, dependent on a single effective diffusion coefficient.

## 3.3.2.1 Virgin and steam exploded Colwood A

Both virgin (untreated) and steam exploded samples were batch stripped at the 100 mL/min flow rate. The objectives were to: (i) determine if the desorption kinetics had been effected by steam explosion, and (ii) determine if the simple soil model could describe the desorption curves of the samples. The results are shown in Figure 10. For clarity, the steam exploded runs are shown with dark data points, while virgin runs are white. A difference is seen in the virgin versus steam exploded runs indicating steam explosion has effected the sorption/desorption kinetics. The virgin Colwood runs are fit very well using an average particle radius of 280 microns and an effective diffusivity of 1 E-6 cm<sup>2</sup>/min (1.67 E-8 cm<sup>2</sup>/sec).

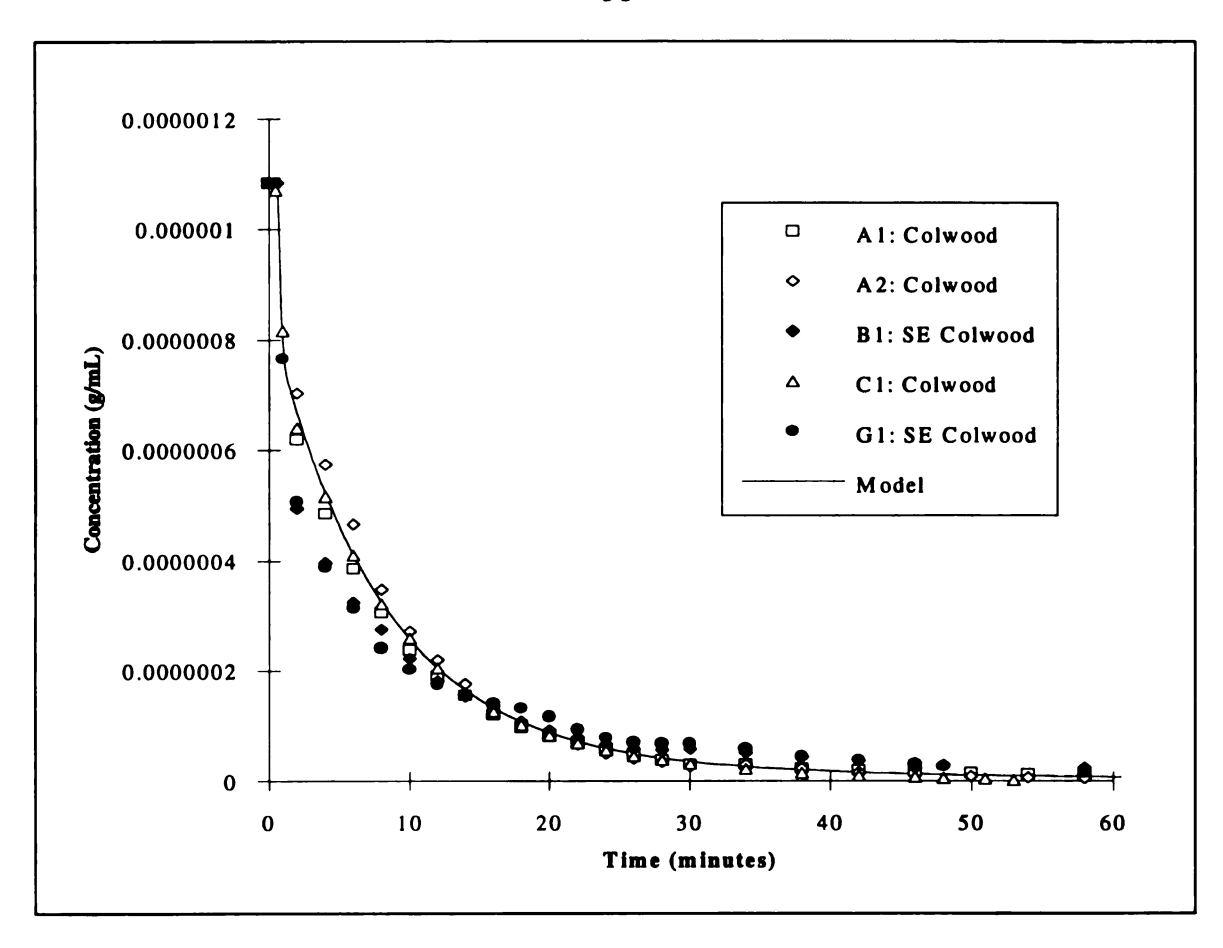


Figure 10: Stripping gas propylbenzene concentration vs. time for virgin and steam exploded Colwood A at 100 mL/min flow rate.

No model curve is included for the steam exploded runs as a reasonable fit could not be obtained. It was hypothesized that the addition of soil, in particular the small particles of a steam exploded sample, may have effected the gas-liquid mass transfer coefficient. Mass transfer coefficients are known to change upon addition of solids (Atkinson and Mavituna, 1983). Supporting this, the steam exploded desorption curves are indicative of decreased mass transfer as the initial concentration drop is steeper than that of virgin runs. Potential mechanisms may include solids coating of bubble interfaces and viscosity effects. Despite this, the steam exploded runs could not be fit even by lowering the gas-liquid mass transfer coefficient. While the mass transfer coefficient is

probably effected by the addition of soil, the effects of steam explosion cannot be modeled by the simple spherical, Fickian diffusion soil model.

## 3.3.2.2 Size fractions of organic enriched Colwood A

Samples of different particle size were batch stripped at the 600 mL/min flow rate. Two sieve fractions (53-125 and 250-500 micron) of organic enriched Colwood A as well as a ground 250-500 micron sample were examined. Similar to the previous section, the objectives were to: (i) determine the effect of particle size (if any) on desorption curves, and (ii) determine if the simple soil model could describe the desorption curves. The results are shown in Figure 11. The graph indicates that the particle size has an effect on the desorption kinetics. Apparently, rate limiting diffusion is occurring over a diffusion path length on the order of magnitude of the particle radius. In particular, the ground 250-500 micron sample has higher gas phase concentration than the 250-500 micron past 1.5 minutes. The ground sample is expected to contribute propylbenzene to the gas phase at a higher rate. At early times however, the results are the opposite. The model fits therefore are not as good as with the whole Colwood samples. In each case, the model curve is fit somewhat poorly at early times to get a good fit in the 2 to 10 minute range. It should be noted that the data points do not form smooth curves, making curve fitting over the entire time-scale difficult. Variation among replicate 600 mL/min no-soil runs was also higher than with the 100 mL/min no-soil runs. The apparent correlation between desorption curves and radius should be viewed with caution as variation in no-soil runs is on the order of magnitude with variation in the soil runs. Additional experiments are required to verify the differences in desorption curves are not merely experimental error.

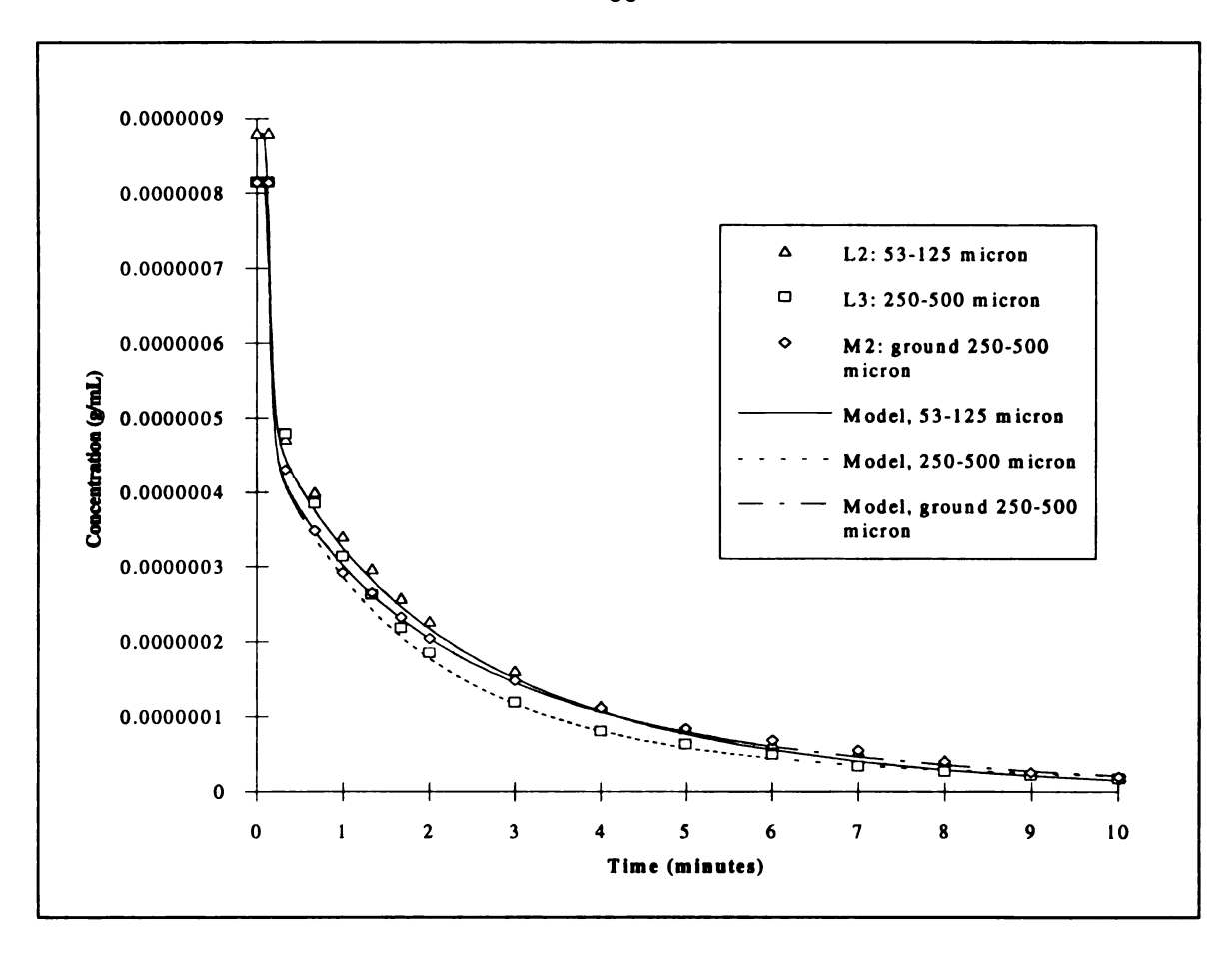


Figure 11: Stripping gas propylbenzene concentration vs. time for three soil sample particle sizes at 600 mL/min flow rate.

At this point, speculation can be made about soil organic matter morphology. Several model morphologies were listed in Table 14 for SOM. Assuming the diffusion path length is the particle radius, then SOM would be expected mainly in the form of solid particles or aggregates. Solid SOM particles would obviously be expected to have different desorption rates for different particle sizes. Aggregate desorption rates would also depend on aggregate radii as long as the aggregate or pore diffusion was significantly rate limiting compared to intraorganic matter diffusion. Diffusion rates for SOM coating morphologies would be expected to show very little or no dependence on particle size, as the diffusion path length would be the coating thickness.

Effective diffusion coefficients were fit to the nearest half-order of magnitude in order to obtain model curves. Values for 53-125 and 250-500 micron were 5 E-6 and 1 E-5 cm<sup>2</sup>/min respectively using average radii of 89 and 375 microns. An average radius for the ground sample was not determined, but an estimated value of 50 microns yielded a diffusion coefficient of 1 E-6 cm<sup>2</sup>/min. The similarity of fitted diffusion coefficients for 53-125 and 250-500 micron samples is again indicative of a diffusion path-length on the order of magnitude of the particle radius.

# 3.3.2.3 Heated re-stripping analysis

The entirety of the solute may not be removed from the soil as commonly assumed in gas purge experiments. The heated re-stripping described in the materials and methods section was used to determine if all of the propylbenzene had been removed from the soil for the 600 mL/min experiments. The results of the initial stripping are shown in Figure 12, while the re-stripping portion is shown in Figure 13.

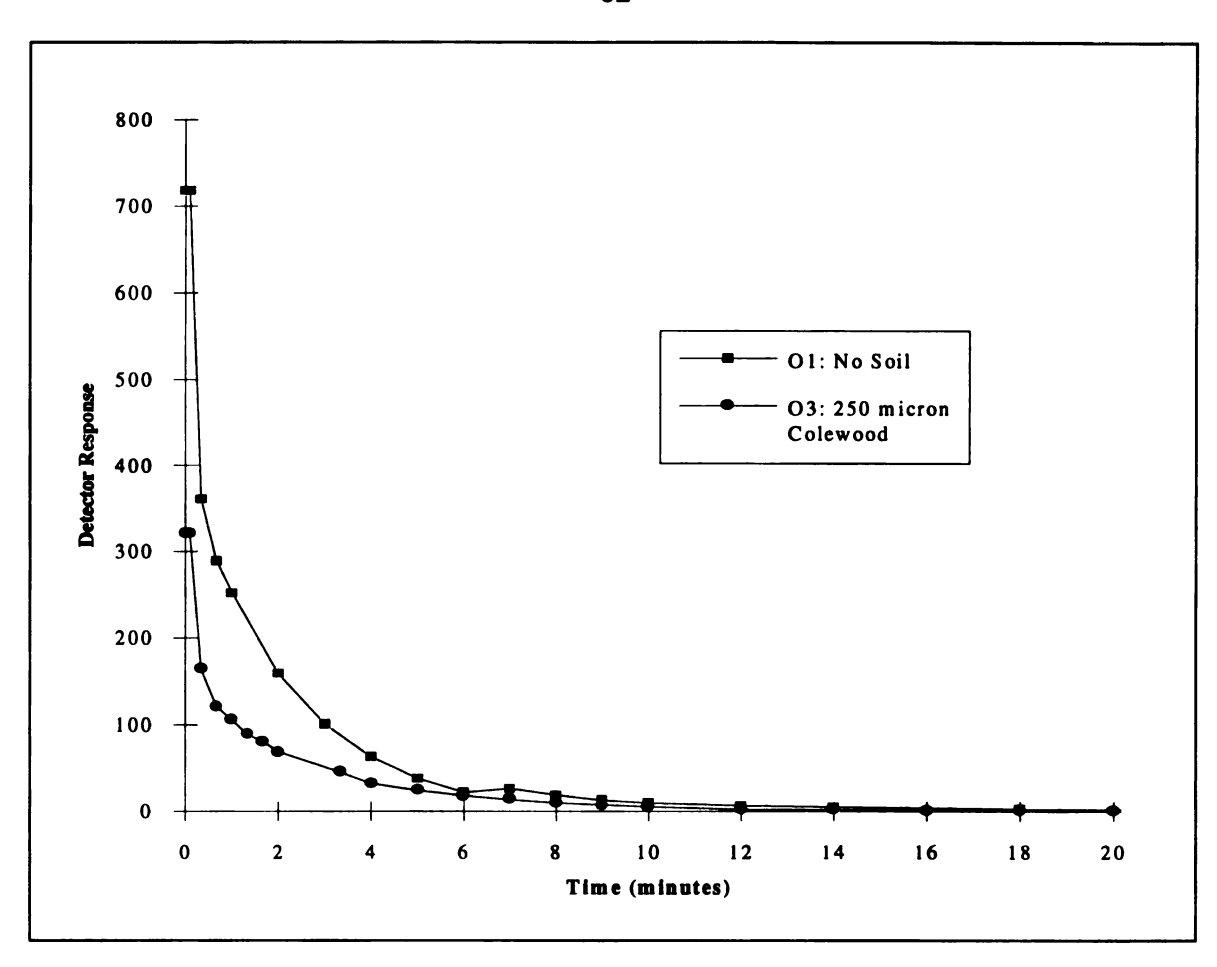


Figure 12: Stripping gas propylbenzene concentration vs. time for initial stripping at 600 mL/min flow rate, 25 degrees Celsius.

The results demonstrate that all the propylbenzene may not be removed from the soil. As seen in Figure 12, the initial stripping was continued until the detection limit was reached, and past that point to 30 minutes. Despite this, upon heating the system and resuming stripping, additional propylbenzene was removed from the system. Surprisingly however, additional propylbenzene was also removed from the no-soil sample. The data indicates that more solute was removed from the soil sample as would be expected.

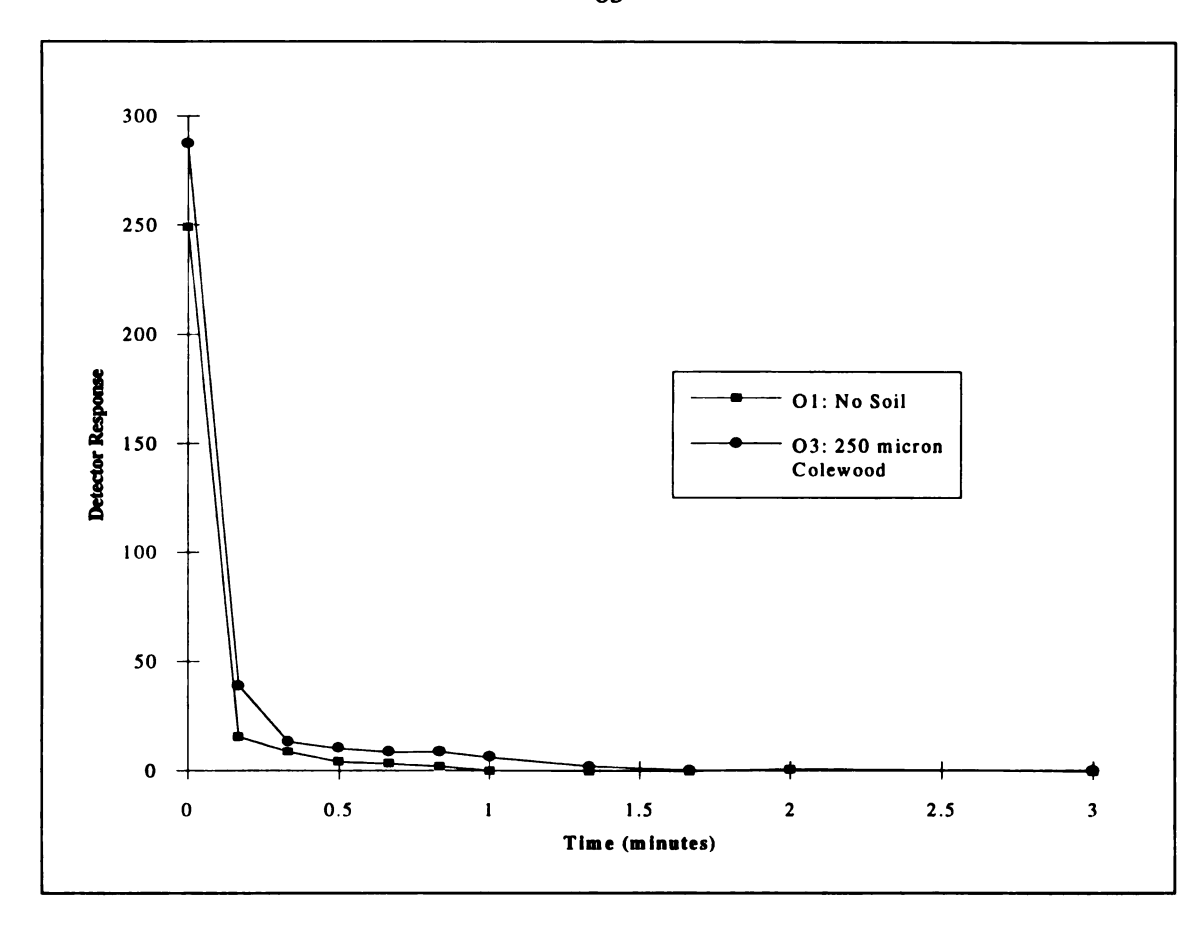


Figure 13: Stripping gas propylbenzene concentration vs. time for heated re-stripping at 600 mL/min flow rate, 75 degrees Celsius.

The additional solute removal in both samples is most likely related to the detection limit of the experiment. The detection limit of the experiment is not zero. Therefore, once the detection limit is reached, any solute which is removed is not detected and not accounted for. The results above could be explained in two ways. The first relates to the rate limited gas-liquid mass transfer. Once the stripping flow is stopped and the system is closed, gas-liquid equilibrium can be achieved, resulting in a re-saturating of the gas phase. When stripping is resumed, the gas phase concentration is detectable, although quickly drops back under the detection limit. The second explanation relates to the heating of the system. Heating of the closed system should drive the solute into the gas phase. The result would again be a detectable gas phase concentration which quickly

drops below the detection limit upon resuming stripping. Both of these mechanisms are probably responsible for the additional solute removal in both samples. However, the data also indicates that more solute was removed from the system containing soil.

#### 3.3.2.4 Total mass removed

While the detection limit issue does not pose a problem for modeling based on concentration data, it is a problem when determining percent of total mass removed. Gas purge data is typically integrated and expressed in the form of percent of total mass removed versus time. Without initial and final concentration measurements, all the solute is assumed to be removed from the system once the detection limit is reached. This would obviously be in error if the detection limit was significantly above zero. complicating matters, the detector signal did not usually return to baselines for the most sensitive (10 mV) setting which were measured before and after the run. Thus a steady signal just above the baseline could be a detectable concentration or noise. These issues make the batch stripping experiment incapable of closing a mass balance on the system without initial and final concentration measurements by a method such as gas chromatography or high performance liquid chromatography. Percent of total mass removed values were calculated by integrating normalized concentrations curves and multiplying by average flow rates. The degree of variation is illustrated in Table 18. The results would seemingly indicate that roughly all the solute is removed from soil samples during the stripping experiment. However, as mentioned above the proper time to stop the experiment is not known. Continuing concentration readings for long times may integrate signal noise into the mass removed. This may have contributed to the erroneous results of runs L and O. Additionally, all the results may still be overestimations of the mass removed as concentration curves were normalized to calculated, not measured values.

**Table 18:** Percent of total propylbenzene removed for batch stripping runs.

No-soil samples	% Mass removed	Soil samples	% Mass removed
A	83	A1	90
В	94	A2	98
С	97	B1	110
L	190	C1	91
М	100	G1	100
N	120	L2	110
О	150	L3	96
		M2	100
		О3	92

# 3.3.2.5 Parameter sensitivity

Model sensitivity to adjustable parameters is important not only for understanding model predictions, but also for interpretation of data. Understanding the effect of varying a parameter may give insight to the nature of a physical mechanism, or demonstrate the limits of application of an experiment. The gas-liquid mass transport coefficient ( $k_L$ a) and the soil effective diffusion coefficient ( $D_{eff}$ ) are examined in terms of model sensitivity and physical significance.

#### 3.3.2.5.1 Mass transfer coefficient

The gas-liquid mass transfer coefficient describes the rate of solute transfer from the liquid to the gas phase. At infinite values of  $(k_L a)$ , the gas and liquid phases will be at equilibrium as described by the Henry's law coefficient. At finite values, mass transfer to the gas phase will be rate-limited, and the gas phase concentration will be lower than that of the equilibrium case. At very low values mass transfer may be so poor that it limits the

overall rate of solute removal from the system instead of the mechanism of interest, soil desorption. The batch stripping model was used to: (i) evaluate how close the experiments were to gas-liquid equilibrium, and (ii) compare experimental values to that which may be expected from a system designed for good mass transfer. A value of 1000 1/hr was used as an obtainable value for a standard design stirred bubble fermenter (Atkinson and Mavituna, 1983). The results for the 100 mL/min and 600 mL/min cases are shown in Figure 14 and Figure 15 respectively.

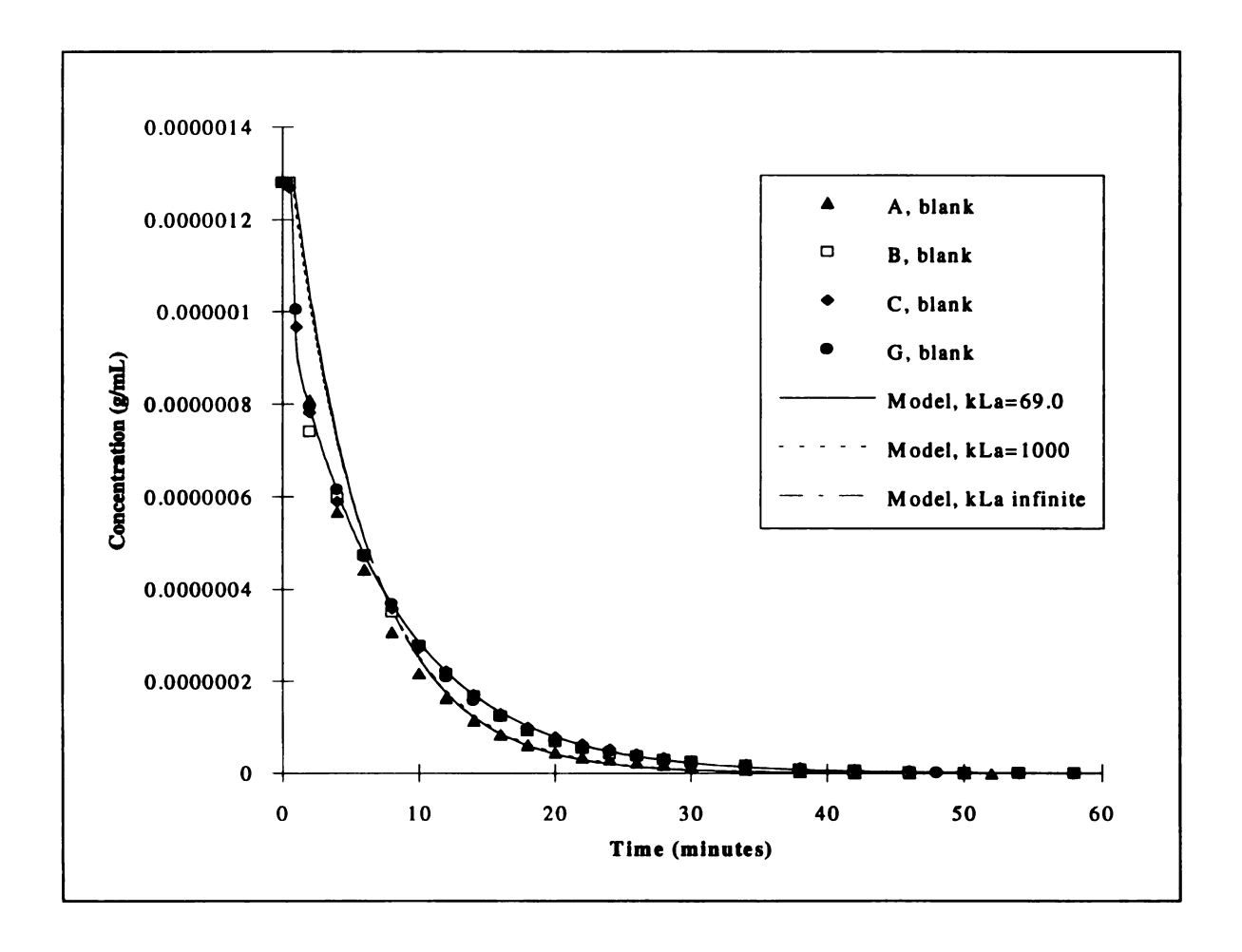


Figure 14: Stripping curve dependence on mass-transfer coefficient for no-soil runs at 100 mL/min flow rate.

The batch stripping experiments, as mentioned earlier in the results section, are not at equilibrium. The above curves show that the experimental curves are far from infinite

mass-transfer coefficient curves. Additionally, the curves for a (k<sub>L</sub>a) of 1000 1/hr indicate that proper experimental design would allow for essentially equilibrium operation at 100 mL/min and near equilibrium operation at 600 mL/min. Experimental design modifications should include: a cylindrical vessel, baffles, a bottom sparger, and a motor driven impeller. Such a stripping vessel may allow for the use of a simplified model which does not include a gas-liquid mass transfer coefficient, at the 100 mL/min flow rate. The potential benefits of an improved stripping vessel include: simpler modeling, shorter experiment times, and improved ability to discern different soil diffusion coefficients or particle sizes. The later is discussed in the following section on diffusion coefficient sensitivity.

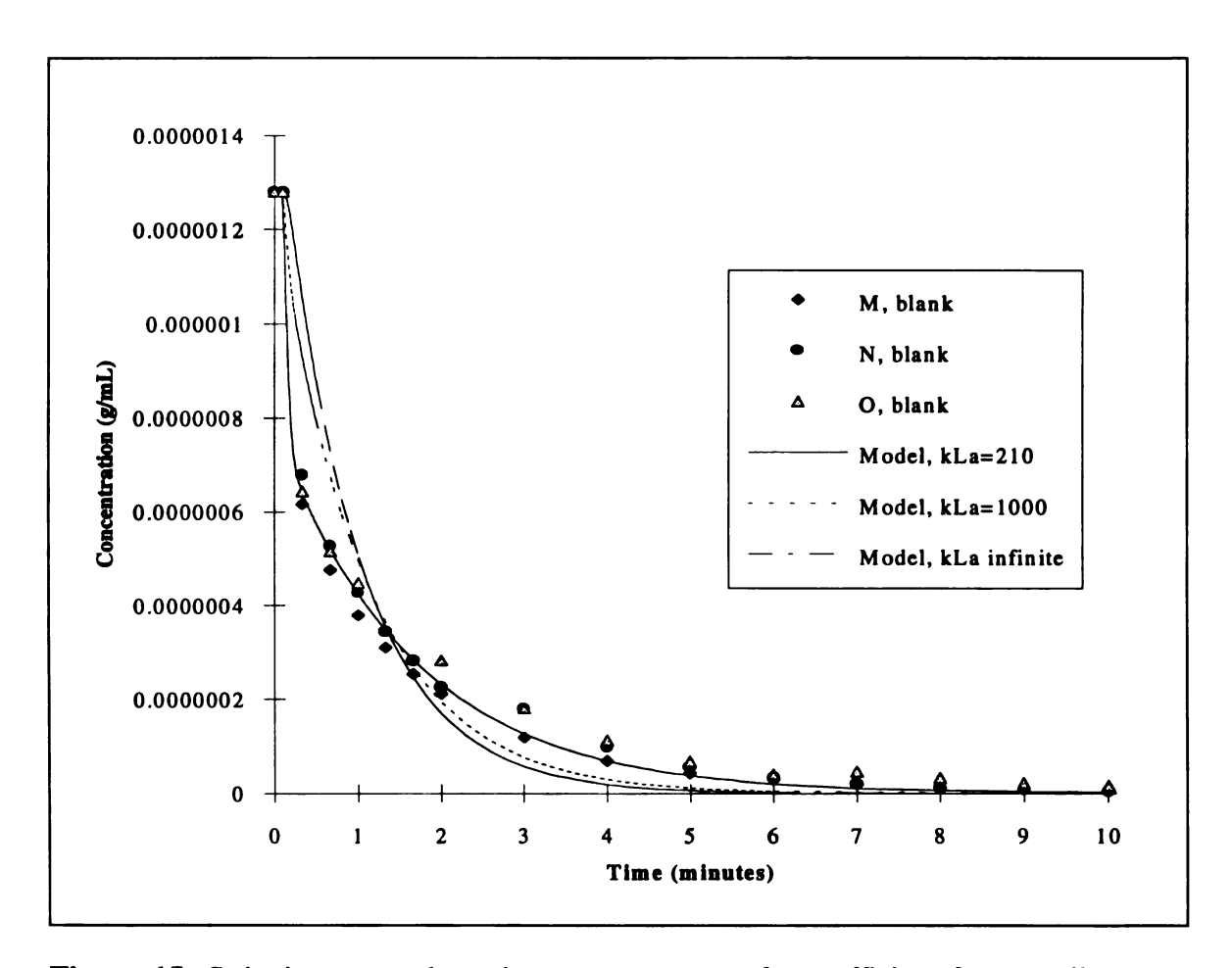


Figure 15: Stripping curve dependence on mass-transfer coefficient for no-soil runs at 600 mL/min flow rate.

#### 3.3.2.5.2 Effective diffusion coefficient

The effective diffusion coefficient describes the rate of solute transfer within the soil particle as modeled. Ultimately, it describes the rate of solute transfer from the soil to the liquid for the model chosen in this work. Since it is the only variable parameter for the soil, its value can be determined within reason from the batch stripping curves. This method is limited however to a range of diffusion coefficient values for a given particle radius. As the diffusion coefficients become very small, the rate of solute transfer from the soil to the liquid becomes insignificant. Therefore, the curves approach that of the no-soil case. This is a problem of time-scale, as the time-scale of the experiment is much shorter than that of the diffusion process. A second limitation occurs as the diffusion coefficients become large. Mass transfer may be limited at the gas-liquid interface. The time-scale of the diffusion would be faster than that of the experiment. For a particle radius of 280 microns and an average enriched Colwood partition coefficient, several stripping curves were generated as a function of effective diffusion coefficient. The range of curves for which good separation is obtained are shown in Figure 16 and Figure 17 for the 100 mL/min and 600 mL/min cases respectively.

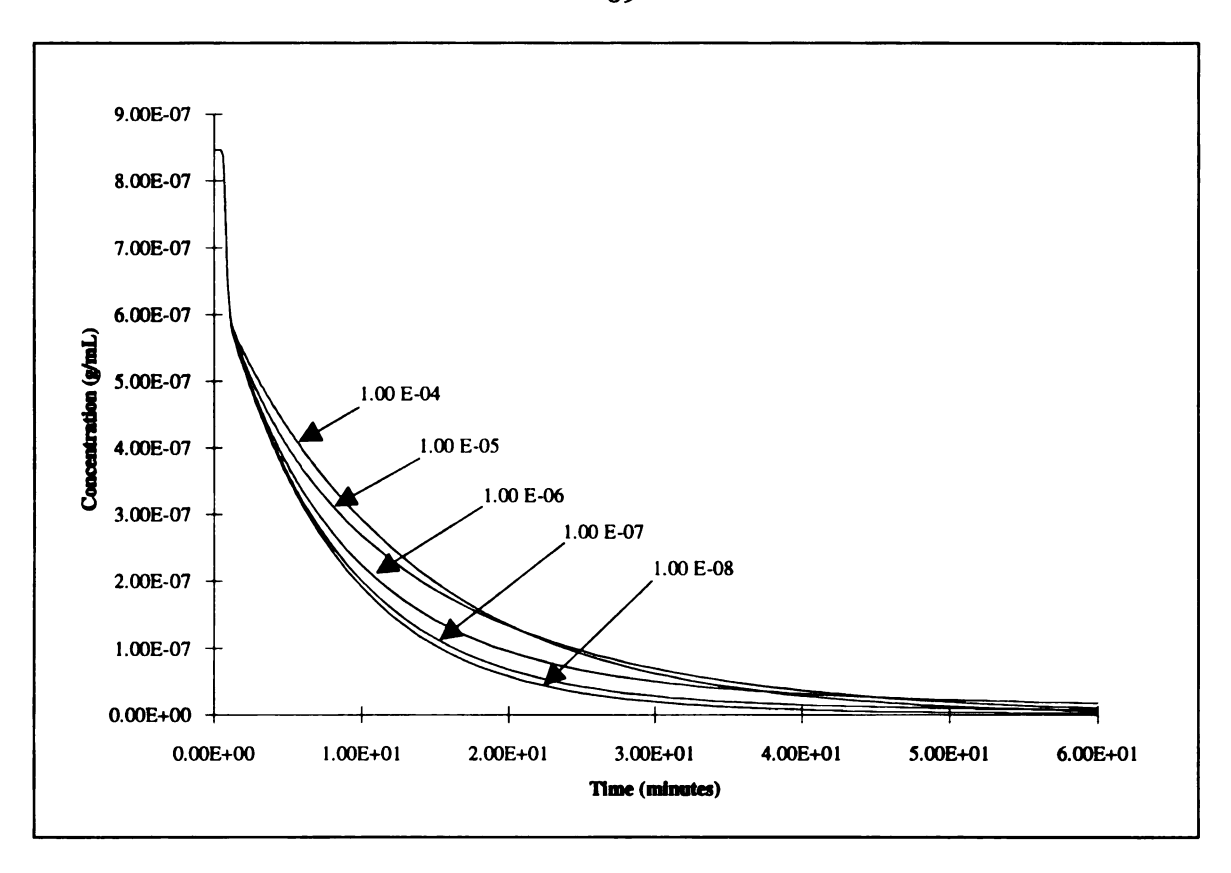


Figure 16: Stripping curve dependence on effective diffusion coefficient (cm $^2$ /min) for 280 micron spheres at 100 mL/min flow rate and  $k_L = 69 \text{ 1/hr}$ .

As expected, the stripping curves become indistinguishable at small and large values of the diffusion coefficient. Comparing the two flow rates, the difference in experimental time-scale can be seen. The shorter time-scale of the 600 mL/min case distinguishes high-end diffusion coefficients better than the 100 mL/case. These results indicate that the stripping gas flow rate can be used to adapt the batch stripping system to the desired time-scale of diffusion.

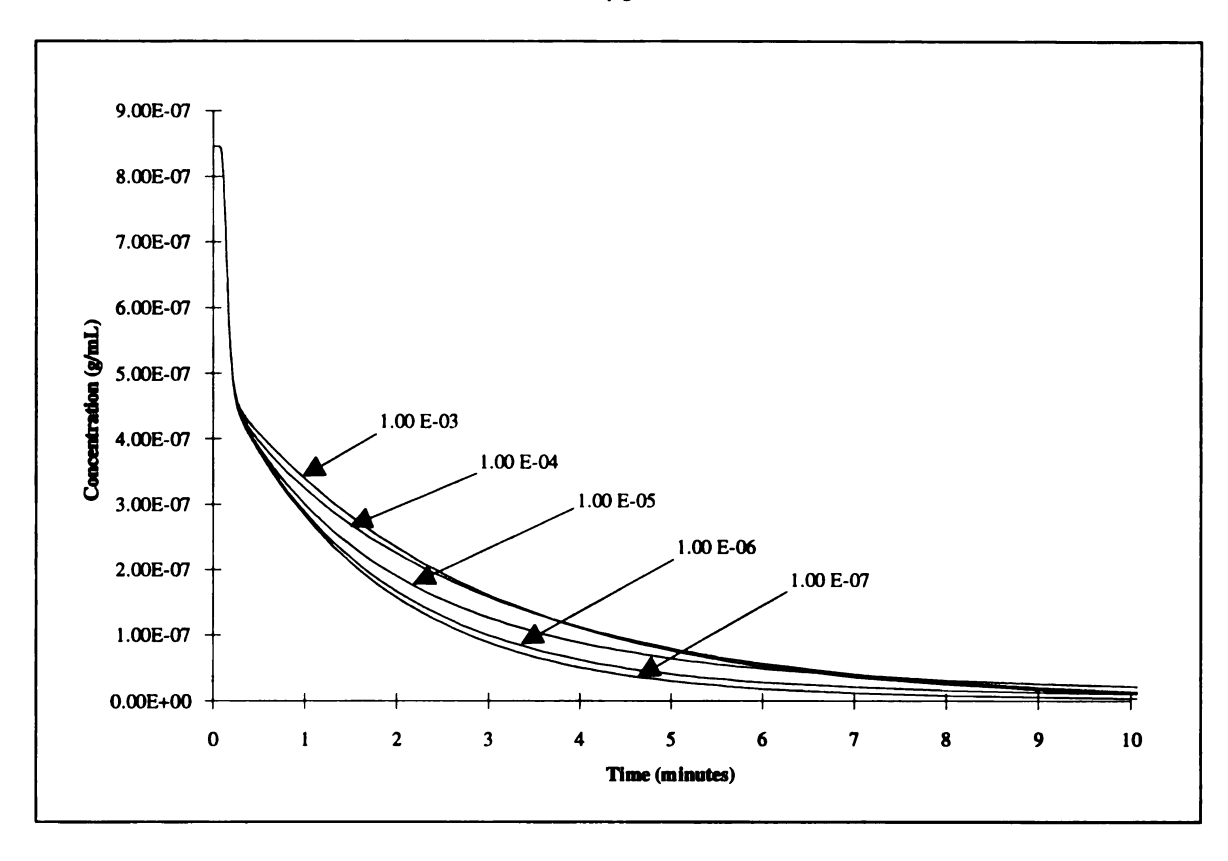


Figure 17: Stripping curve dependence on effective diffusion coefficient (cm $^2$ /min) for 280 micron spheres at 600 mL/min flow rate and  $k_L$  a=69 1/hr.

The results also show that the batch stripping system, at either flow rate, is applicable for fitting (D<sub>eff</sub>) for the soil samples being studied with some caution. The fitted effective diffusion coefficients were in the range of 1 E-5 to 1 E-6 cm<sup>2</sup>/min. The curve separation in this range is good at both flow rates. It should be noted however, that the important parameter is actually the effective diffusion coefficient divided by the square of the particle radius. Thus, if the maximum discernible diffusion coefficient was 1 E-4 cm<sup>2</sup>/min for 280 micron particles, the maximum discernible diffusion coefficient for 53 micron particles would be 3.6 E-6 cm<sup>2</sup>/min. Depending on the diffusion coefficient, the batch stripping experiment may not be appropriate for small particle samples such a ground or steam exploded soil even at high gas flow rates. The maximum (D<sub>eff</sub>/R<sup>2</sup>) appears to be roughly 0.06 1/min for 100 mL/min and 0.6 1/min for 600 mL/min.

Assuming an effective diffusion coefficient of 1 E-5 cm<sup>2</sup>/min, the minimum particle size would be approximately 130 and 40 microns for 100 mL/min and 600 mL/min respectively. In other words, no difference in the desorption curve would be expected for smaller particles. This implies the 600 mL/min flow rate would be sufficient for the 53-125 micron size fraction. The 53 and 125 micron sieve trays are estimated as good bottom limits for the 600 and 100 mL/min flow rates respectively. Furthermore, if whole soil is to be used, the particle size distribution should be determined by use of sieve trays.

A final consideration related to diffusion coefficient sensitivity is that of the benefit in increasing the gas-liquid mass transfer coefficient. A small improvement in ability to fit effective diffusion coefficients may be gained with an improved batch stripping vessel. Regardless of the effective diffusion coefficient, the initial gas-liquid rate limited drop in gas concentration is the same. If the mass transfer coefficient ( $k_L$ a) is increased, then diffusion coefficient ( $D_{eff}$ ) effects are evident sooner for a ( $k_L$ a) of 1000 1/hr. A larger time range (and data points) would then be available for fitting of the diffusion coefficient. This may be of value if a mathematical fitting routine was employed. It was expected that the gas-liquid mass transfer coefficient might be overall rate limiting for large diffusion coefficients. However, increasing the ( $k_L$ a) only produced a small difference in separation is seen in the 20 to 30 minute range.

#### 3.4 Conclusions

The gas purge apparatus is a useful system for obtaining batch desorption data. Important aspects of the system have been examined in this work. The gas and liquid phases are not in equilibrium, and proper modeling requires the use of a mass transfer coefficient (k<sub>L</sub>a). With improved vessel design, (k<sub>L</sub>a) can be increased, possibly approaching gas-liquid equilibrium for the slower 100 mL/min gas flow rate. The mass transfer coefficient may change upon the addition of soil to the liquid phase.

Batch stripping results indicate that desorption rates are dependent on particle size. Additional experiments are needed to confirm this preliminary result. Dependence on particle size supports a hypothesis of SOM as solid chunks or aggregates, but not coatings. The use of a single effective diffusion coefficient was able to fit whole Colwood A desorption curves well, and enriched Colwood sieve fractions within reason.

The batch stripping experiment has a limit of resolution with respect to desorption rate. For a given effective diffusion coefficient, all particles smaller than a critical size will yield the same desorption curve, rate-limited by the experimental apparatus. Only sieved samples should be used as whole soil contains fines. The 53 and 125 micron sieve trays are estimated minimum size limits for the 600 and 100 mL/min gas flow rates respectively.

Batch stripping utility is currently limited by the uncertainty in: (i) pre-stripping solute equilibria between soil and water, and (ii) removal of the entirety of the solute from the soil during stripping. This information can only be provided by measurement of solute concentrations in the various phases before and after stripping. Initial concentration measurements would verify the attainment of equilibria and provide model initial conditions in place of calculated values. Final concentrations would close the system mass balance.

Steam explosion also effects desorption characteristics, although results are not fit with the spherical geometry, Fickian diffusion model. Differences in desorption curves of steam exploded and virgin samples may be to a change in soil organic matter morphology or mass transfer effects. The utility of steam explosion as a pre-remediation treatment can only be determined once any existing mass transfer effects are sorted out.

#### **CHAPTER 4: SOIL MORPHOLOGY**

## 4.1 Introduction

Knowledge of morphology is required for development of a fundamental mass transport model for soil. Several such models were hypothesized in Chapter 3. Along with kinetic data, physical probing of soil samples is used to understand soil morphology. Visualization of the soil system is achieved with scanning electron microscopy. The effort to distinguish between organic and mineral matter is made with x-ray fluorescence spectroscopy. Finally, steam explosion of soil is identified as a tool for altering morphology. Comparison of changes in measurable quantities such as pore size and desorption kinetics may yield insight to soil organic matter morphology.

#### 4.2 Materials and Methods

## 4.2.1 Sample preparation

Whole Colwood A horizon soil as well as the 53-125, 125-250, and 250-500 micron size fractions of organic matter enriched Colwood A were used in morphological studies. These samples were prepared as described in Chapter 3. Cryogenic grinding was also used to prepare samples. The 125-250 micron size fraction of organic matter enriched Colwood A was placed in a sealable 500 mL polypropylene bottle. Six half-inch diameter steel ball bearings were also placed in the bottle. Liquid nitrogen was added until the liquid nitrogen no longer boiled when added to the bottle. The bottle was sealed and shaken by hand in both axial and circular motions for about five minutes. The sample was then removed and stored in a sealed polypropylene vial.

Scanning electron microscopy was also used to determine the amount of particle size reduction occurring in batch stripping experiments. Particle shearing due to stirring was suspected. Samples which had been used in batch stripping experiments as described

in Chapter 3 were compared to a fresh sample. After batch stripping was completed, the solids were allowed to settle in the stripping flask for a few days. The supernatant liquid was then withdrawn using a pipette. The remaining wet cake was frozen in an acetone-dry ice bath and freeze dried.

## 4.2.2 Scanning electron microscopy

Soil samples were mounted on microscope stubs with the aid of an adhesive. Press-on glue tabs were used to apply adhesive to the stubs. Soil samples were placed and even distributed on the stubs with a metal spatula. The stubs were turned on their side and tapped on the lab bench in order to achieve a thin coating of soil sample. The loaded stubs were inserted into a mounting stage. The complete assembly was coated with gold for approximately five minutes in a Polaron SEM Coating System at 25 milliamps and 2.5 kV. The long coating time provided a thick gold coating required to minimize sample charging. Soil samples are non-conductive and will build a charge without the conduction to the stub provided by the gold coating. Charged samples will occasionally discharge resulting in lines on SEM photographs. Scanning electron microscopy (SEM) was performed with a JEOL JSM-T330. A beam energy of 10,000 eV was used for all samples. Magnifications of 35 to 15,000 X were used.

# 4.2.3 X-ray fluorescence spectroscopy

X-ray fluorescence spectroscopy (XRF) was used to obtain elemental dot maps which corresponded to scanning electron microscope photographs. Bombardment with an electron beam results in the ejection of a X-ray photon which carries elemental information. By rastering over a sample frame, elemental dot maps can be obtained for a SEM picture of the same sample frame.

The 53-125 micron size fraction of organic matter enriched Colwood A was used for the XRF studies. The sample was prepared for coating as described for SEM. A

carbon coating was applied to the sample for conductivity. SEM photographs and XRF dot maps were done with a with a beam energy of 20,000 or 15,000 eV using a integrated SEM/XRF system. The SEM was a JEOL JSM-35C and the XRF was a Tracor Northern TN2000. Elemental dot maps examined included silicon, calcium, and aluminum. The desired elemental dot map is carbon, as it would be most useful in finding soil organic matter. Carbon dot maps were not possible however due to the composition of the x-ray collection window.

# 4.2.4 Steam explosion

Steam exploded samples were prepared in order to effect the sample morphology in a way detectable by batch stripping analysis and scanning electron microscopy. In brief, soil slurries were heated in a closed vessel, elevating the pressure, followed by a rapid pressure drop to ambient conditions.

The apparatus consists of a 25 mL stainless steel pressure vessel with an o-ring sealed lid. The lid was fit with (i) a thermocouple probe, and (ii) a 600 psia pressure gauge. The pressure gauge was connected to the vessel by 30 cm of stainless steel tubing to prevent damage from heating. The vessel was fitted with a 90 degree ball valve, allowing for quick pressure release. Heat was applied with a fiberglass coated heating tape. A second thermocouple probe was wrapped in the heating tape. A digital thermocouple thermometer was used to measure internal and external (heating tape) temperatures. A voltage controller was used to manually regulate the heating tape temperature.

The pressure vessel was loaded with 8 to 10 grams of whole Colwood A soil and enough water to completely fill the vessel (18-20 mL). The lid was sealed and the vessel was mounted in a wood stand which was placed in a vacuum hood. The heating tape was wrapped around the vessel and the external thermocouple. Once electrical connections were made, the voltage to the heating tape was set to give a rapid increase in the external

temperature to approximately 200 degrees Celsius in under five minutes. The voltage was then decreased to give a slow increase to an external temperature of 225-250 degrees Celsius. The external temperature was kept in this range for the duration of the experiment by frequent manual adjustments. The vessel pressure was monitored, and upon reaching 220 psia the heating was continued for five more minutes. At the end of five minutes the internal temperature was recorded (186-189 degrees Celsius). The ball valve was then opened resulting in a 2-3 second discharge into a 2 L Nalgene beaker. The processed slurry was distributed into 25 mL test tubes and centrifuged until all solid had apparently settled. The supernatant fluid was decanted and the samples were frozen in a acetone-dry ice bath. The samples were immediately freeze dried and stored in polypropylene vials. Samples were freeze dried as a precaution against capillary forces found in normal drying. Pores which were expanded during steam explosion could be shrunk or collapsed during air drying. Preliminary samples were both air dried and freeze dried after freezer freezing, resulting in caking which required break-up with a spatula.

#### 4.2.5 Mercury porosimetry

Mercury porosimetry was performed in order to determine if steam explosion altered the pore structure of soil samples. Both virgin and steam exploded samples (as described previously) were tested. The instrument used was a Micromeritics Pore Sizer 9310. Both low and high pressure testing was performed covering a range from approximately 1 to 30,000 psia. Low pressure testing (1 to 25 psia) was performed manually, while high pressure testing (25 to 30,000 psia) was computer (a PC) controlled. All data was automatically recorded by the PC. A 5 cc powder penetrometer was used. Operating procedures are described in detail in the Micromeritics Pore Sizer manual.

Results in the form of cumulative intrusion volume and incremental pore volume per gram were calculated by the Pore Sizer 9310 software. Capillary calculations assumed round pores, allowing pore diameters to be determined by Equation 21.

$$D = -\frac{1}{P} \cdot 4 \cdot r \cdot \cos(x) \tag{21}$$

The pore diameter is (D), (P) is the applied pressure, (r) is the surface tension, and (x) is the contact angle. Values of 484 dynes/cm for surface tension and 130 degrees for contact angle were used. The change in penetrometer mercury volume and pore diameter versus pressure yields an incremental pore volume as well as cumulative intrusion volume.

#### 4.3 Results and Discussion

## 4.3.1 Scanning electron microscopy

## 4.3.1.1 Particle morphology

The organic matter enriched size fractions of Colwood A were examined in order to visualize the solid phase in the kinetic model. Four size fractions were initially examined: 53-125, 125-250, 250-500, and > 500 microns. Samples were examined at 100 and 500 times magnification. A notable characteristic of the smallest size fraction is the two distinct particle types. Most particles appear to be either aggregates of smaller sub-particles or solid particles of a single material. This trend is seen in the 125-250 micron fraction, but with less distinction. In the 250-500 micron sample, partially decayed plant material becomes apparent as evidenced by tubular structures in the particles. The evidence of plant matter is quite clear in the largest size fraction. Woody material in this size fraction could be seen with the naked eye.

Preliminary results allowed for speculation on the nature of organic matter in the soil. The aggregate particles seen in the smaller size fractions were hypothesized as a mixture of organic and mineral matter. Organic matter was obviously also found in the form of the partially degraded plant matter, particularly in the larger size fraction samples.

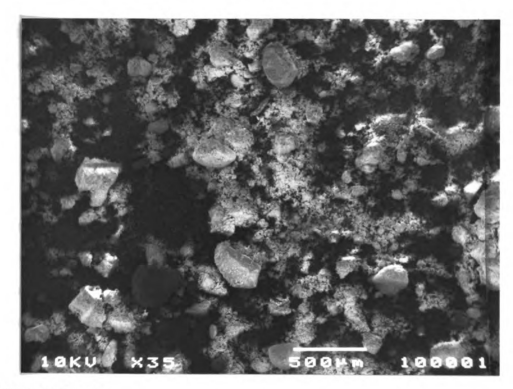
In terms of solid phase modeling, both aggregates and solid chunks shown in Table 14 of Chapter 3 would be appropriate. Aggregate particles could also be modeled with a single effective diffusion coefficient as done in Chapter 3.

Further investigation of the aggregate particles was done to determine the internal morphology. Cryogenically ground 125-250 micron fraction was examined at 1,500, 5,000, and 15,000 times magnification. Cryogenic grinding is done in order to fracture particles into smaller pieces, thereby exposing the inner morphology. Several aggregate particles as small as 10 microns were seen indicating particle fracture had been achieved. The small aggregate particles appeared identical to the large aggregates, indicating a uniform morphology throughout the particles. The results indicate a homogeneous organic-mineral aggregate model may be applicable. Modeling parameters such as pore sizes and sub-particle diameters can be estimated from a 5,000 X photograph. Pores appear to be around 1 micron wide while sub-particles may range from 1 to 10 microns.

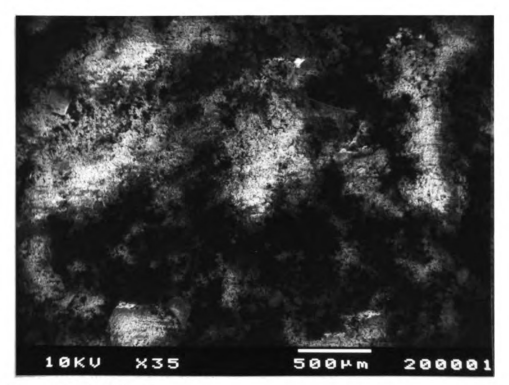
## 4.3.1.2 Steam explosion

Steam explosion of soil samples was investigated for two purposes. Steam explosion would be a valuable soil remediation processing step if desorption rates of organic compounds from soil could be increased. This might occur if water vaporizing to steam expanded or ruptured pores in the soil organic matter. Steam explosion was also examined as tool for manipulating soil morphologies. If the soil or soil organic matter could be manipulated in a known way, resulting changes in desorption kinetics could provide new information about the sorption mechanism. It is in this second capacity that steam exploded samples were examined with scanning electron microscopy.

SEM pictures demonstrated that steam explosion changed the soil morphology. Steam explosion was performed as described in Chapter 3 on whole Colwood A soil. Fresh Colwood A was wetted and freeze dried in a manner identical to steam exploded samples as a control. The results at 35 times magnification are shown in Figure 18.



(a) Virgin Colwood.



(b) Steam exploded Colwood.

Figure 18: Virgin and steam exploded Colwood samples at 35 X magnification.

At 35 times magnification (as well as 100 X), a size reduction of medium to large particles is apparent. The explosion or break-up of 50 to 500 micron particles are termed here as macro-scale effects. Micro-scale effects would be disruption of particles 10 microns or less, expansion of pore systems in aggregates, or expansion of micro-pores in soil organic matter (if viewed as a cross-linked polymer). However, efforts to find these types of effects were not successful. SEM images at 500 and 2,000 times magnification appeared the same for both samples. This is not interpreted as proof against micro-scale effects, as they are not expected to be readily apparent like large particle break-up. The search for micro-scale effects suffers primarily from not knowing what is soil organic matter and what is mineral matter.

These results have implications for steam explosion as a investigative tool for desorption kinetics. Assuming that steam explosion only causes macro-scale effects, a change in desorption kinetics for steam exploded samples would only be expected if the characteristic diffusion path length was the particle radius. If the path length was the radius of 1 to 10 micron sub-particles in an aggregate particle, then the macro-scale morphology changes would have little or no effect on sorption.

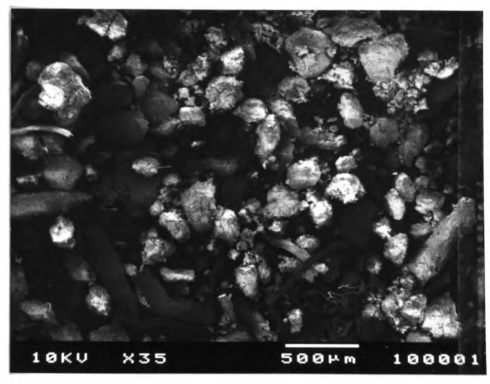
## 4.3.1.3 Particle shearing during batch stripping

SEM qualitatively showed that particle shearing was a problem at long stripping times. Two sets of comparisons were made. Fresh 53-125 micron enriched Colwood A was compared to the same soil which had been stripped for 195 minutes. Fresh 250-500 micron enriched Colwood A was compared to the same soil which had been stripped for (i) 55 minutes, and (ii) 81 minutes. The 53-125 micron sample stripped for 195 minutes had a significant amount of particles with a diameter smaller than the 53 micron cut-off. Particle size reduction is severe at this long stripping time.

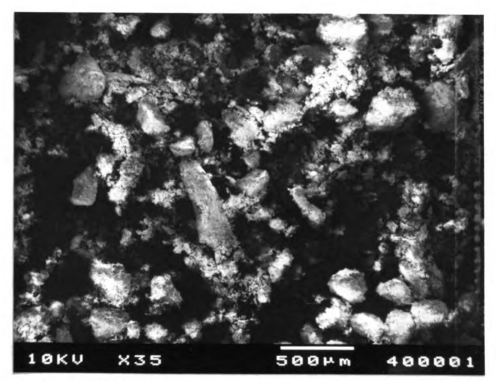
Similar results are found with the 250-500 micron samples. Figure 19 compares a fresh sample with a sample stripped for 55 minutes. Some particle pulverization is

apparent at 55 minutes of stripping. Fewer large particles as well as more fines are present in the stripped sample. The fines were likely generated from shearing of larger particles. Further particle pulverization is apparent at 80 minutes. Most of the large particles seen in the previous samples are not present. While a few particles in the 250-500 micron range remain, most of the soil appears to be particles of 100 microns or less. Comparing the fresh sample to the 80 minute sample, the particle size reduction is extreme.

Particle size reduction during sample stripping has important implications for kinetic data. The characteristic diffusion path-length has many possibilities including the particle radius, the thickness of particle coatings, or the radius of small 'sub-particles' which comprise an aggregate particle. If the diffusion path length were that of the particle radius then shearing would change the path length over the course of an experiment. Results would be worthless. The qualitative information gathered here provides only an estimate of appropriate experimental consideration. Very long stripping times (195 minutes) are clearly not acceptable. Results from 250-500 micron samples are more ambiguous do to heterogeneous nature of the sample, but stripping times of less than 30 minutes are probably needed. This information provides motivation to use faster gas flow rates, such as 600 mL/min in order to prevent particle pulverization. Achievement of higher gas-liquid mass transfer coefficients (k<sub>L</sub>a) may also decrease stripping times as discussed in Chapter 3.



(a) Fresh sample.



(b) 55 minutes stripping time.

Figure 19: Pulverization effects of batch stripping on 250-500 micron Colwood samples.

# 4.3.2 X-ray fluorescence spectroscopy

A viewing field of several particles was examined at 200 times magnification. The particles were fairly uniform ranging in size from roughly 5 to 100 microns (major axis). Exceptions were some ribbon shaped objects thought to be plant or animal matter. The silicon dot map was similarly uniform giving a general outline of the particles. However, the dot density (concentration) was not uniform for all particles. Some particles of 10 microns or less had a particularly high concentration of silicon and were presumably mineral matter.

A particle of lower silicon content was magnified by 1000 times. The particle appeared as a homogenous mixture. The silicon dot map highlighted a few particles of roughly 2 to 10 microns in diameter on the surface of the particle. A calcium dot map was completely uniform, probably due to the soluble calcium in groundwater. Silicon and aluminum dot maps taken at 3900 times magnification were similarly uniform, showing no correlation with visible differences in the particle.

Another particle of interest was examined at 3600 times magnification. The particle appeared to be fairly homogeneous mixture with generally with soft edges. Dispersed in the continuous phase were some very smooth particles appearing to have sharp edges. A dot map showed some areas as higher silicon content, in particular the smooth, sharp edged particles. These results may suggest homogenous mixture of mineral and organic matter.

Similar results were found in another viewing field at 1300 times magnification. Several soft edged, dark particles which appeared to be a single material (opposed to an aggregate) were dispersed in a lighter colored, semi-continuous phase. The dark particles had a particularly high concentration of silicon. The picture again suggests a mixture of mineral and organic matter. An appropriate visualization model may be that of concrete. The mineral matter may be visualized like the stones or gravel, while the organic matter is represented by the cement, binding the gravel together.

Finally, a particle quite different in nature was found while at 2400 times magnification. The particle was approximately 40 by 20 microns, had soft edges, and appeared to be comprised of a single material. A few smaller particles of 1 to 5 microns were attached to the surface. Silicon, as well as heavier elements, were of negligible concentration suggesting a solid chunk of organic matter, or at least a thick coating.

#### 4.3.3 Mercury porosimetry

Steam explosion was found to effect the pore structure of Colwood A soil samples. Changes in pore structure were examined by mercury porosimetry. Results comparing a virgin and steam exploded sample are shown in Figure 20.

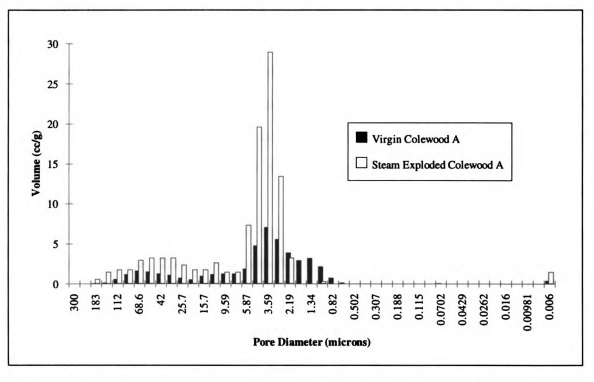


Figure 20: Incremental pore volumes for virgin and steam exploded Colwood samples.

The most significant effects of steam explosion are: (i) a large increase in pore volume for roughly 3 to 6 microns diameter pores, (ii) approximately a doubling of pore volume for

12 to 112 microns diameter pores, and (iii) a near complete loss of pore volume for 0.8 to 1.7 microns diameter pores.

The intended effect of steam explosion is to expand or rupture pores by rapid vaporization of water. The results above would seem to agree with this process. Overall pore volume per gram is increased. Unclear however, is the mechanism of change as well as how much of the pore volume is actually that of soil organic matter. Porosimetry of a sample in which the SOM was removed thermally may elucidate organic versus mineral contributions.

Some speculation can be made on steam explosion mechanism. Steam explosion may simply enlarge pores. A good case for this mechanism is made by the loss of pore volume for 0.8 to 1.7 micron diameter pores, and the large gain in the 3 to 6 microns diameter range. The small pores would of course be lost upon expansion, showing up as larger pores in the exploded sample. Additionally, an increase in pore volume would be expected if the number of pores remained constant. This is certainly seen. A similar although less dramatic increase is seen in roughly the 10 to 100 micron range. New pores appear in the 140 to 180 micron range. Considering the large size, this may represent the break-up of large particles.

An alternative explanation for the loss of pore volume in the 0.8 to 1.7 micron range is pore collapse. The problem with this explanation is two-fold. First, some signs of the collapsed pores may be expected at very small diameters. The increase in volume at 0.006 microns may represent this, or merely experimental error. Second, pore collapse would not explain the large net increase in pore volume.

#### 4.4 Conclusions

Insight to the nature of soil organic matter was gained through scanning electron microscopy and x-ray fluorescence spectroscopy. In general, the morphology appeared to be either aggregates of a mixture of organic and mineral or solid organic matter.

Aggregates are envisioned as concrete with stone and cement representing the mineral and organic matter respectively. An aggregate model including intraorganic matter diffusion as well as pore diffusion (between sub-particles of aggregate) would seem appropriate. A simplified approach is the single effective diffusion coefficient model used in Chapter 3 of this work. Solid organic matter would be modeled similarly, but the diffusion would be that of the organic material. The results are limited as the identification of organic versus mineral matter requires additional probing techniques. Such techniques may include x-ray fluorescence spectroscopy for carbon maps or examination of samples in which the organic matter has been thermally removed.

Steam explosion can be used as a tool to change the soil morphology. The pore structure is effected with an increase in pore volume as shown by mercury porosimetry. The mechanism of change is not understood but is hypothesized as expansion of pores.

Particle pulverization due to stirring during batch stripping is significant at longer stripping times. If diffusion path lengths are that of particle radii, pulverization will invalidate any kinetic results. Experiment times must be kept short (probably less than 30 minutes). The batch stripping vessel should be re-designed to keep particle shearing forces to a minimum.

#### CONCLUSIONS AND RECOMMENDATIONS

The research objectives of this work concern both the equilibria and kinetics of nonionic organic compound sorption to water saturated soil systems. The results are significant as accurate prediction of both equilibrium concentrations as well as desorption kinetics is an integral part of designing successful bioremediation processes. Achievements of this work include: (i) presentation of a method for predicting solute-soilwater equilibrium, (ii) critical evaluation of a batch stripping method for collecting desorption data, and (iii) preliminary development of a mass transport model for soil organic matter based on morphological information.

A group contribution activity coefficient method has been developed from the ELBRO-FV model of Kontogeorgis et al. (1993) and the Modified UNIFAC model of Gmehling et al. (1993). The method has been tested by predicting SOM-water partition coefficients for a limited number of nonionic organic compounds with good results. Large errors were found to be a result of water phase activity coefficient predictions. Marked improvements in predictions therefore were made with the use experimental water phase activity coefficients. UNIFAC predictions were significantly different for Stevenson (1982) and Aiken (1985) model molecules. The Stevenson predictions were closer to literature values indicating the higher aromaticity of the Stevenson molecule may be more representative of actual soil organic matter.

The difference in Stevenson and Aiken predictions as well differences in literature values dependent on soil source, indicates that SOM chemistry may be correlated with partition coefficients. A logical continuation of the current work would be to develop new model SOM molecules which are representative of samples which vary in chemistry. Information from samples such as elemental analysis and percent aromaticity could be used to modify the Stevenson or Aiken models. Hopefully, the partition coefficient predictions made with the method presented in this work would agree with differences seen in experimental values for various samples. Significance of such efforts would

include a better understanding of the implications of SOM chemistry as well as a more accurate, site-specific method for predicting equilibrium pollutant concentrations in soil and water.

The gas purge apparatus of Benzing (1993) was analyzed for collection of batch desorption data. The experiment was found to be rate-limited and was therefore modeled with a gas-liquid mass transfer coefficient. Head space non-idealities were accounted for by a PFR model with dispersion. Accurate modeling of the system was a required precursor to soil desorption studies. The spherical geometry, Fickian diffusion model for soil samples allowed for elucidation of experimental limitations. Appropriate minimum sieve sizes were estimated at 125 and 53 microns for 100 and 600 mL/min gas flow rates respectively. Smaller particles sizes are not expected to yield different desorption curves as the experiment itself will be rate limiting. The experiment is not capable of closing a mass balance without measuring solute concentrations. Future work should minimally include gas or liquid chromatography determination of solute concentrations in the aqueous phase before and after stripping. The gas-liquid mass transfer could be improved with better vessel design, leading to simpler modeling and shorter stripping times. Short stripping times are important as scanning electron microscopy showed significant particle pulverization due to stirring.

The groundwork for a morphological based, mass transport model for soil organic matter has been laid down. Two approaches were taken. First, kinetic data was collected using the gas purge apparatus and analyzed with a mathematical model. A spherical geometry, Fickian diffusion model was able to produce reasonable fits of the data by adjusting the effective diffusion coefficient. Desorption kinetics were found to be dependent on particle size, indicating the particle radius may be an appropriate diffusion path length for the model. Second, scanning electron microscopy and x-ray fluorescence spectroscopy were used to view the soil morphology. Results indicate soil organic matter may be found in organic-mineral aggregates or solid chunks. Either of these morphologies

could accommodate a diffusion path length dependent on particle size as found in desorption studies.

The simple effective diffusion coefficient model can be used for both aggregates and solid chunks. The effective diffusion coefficient may be a function, however, of whether the particle is an aggregate or solid, porosity, tortuosity, and the pure SOM diffusion coefficient. Future work should continue to elucidate the soil morphology with regard to the above aspects. More kinetic data should be collected using soil samples of the narrowest size distributions possible (close sieve tray sizes). Sample pulverization due to stirring must be monitored and minimized. X-ray fluorescence spectroscopy for carbon dot maps should be attempted to discern organic matter from mineral matter. Samples in which organic matter has been thermally removed should be used for kinetic studies and examined by SEM as well as mercury porosimetry. These approaches may also help in discerning mineral matter (and its properties) from organic matter.

Steam explosion was shown to effect soil morphology, apparently expanding pores. Kinetic implications are unclear however as desorption curves could not be fit by the spherical geometry, Fickian diffusion model. Further work is warranted using sieved samples so that particles sizes are known. Gas-liquid mass transfer may be altered by addition of steam exploded soil (small particles) to the aqueous phase. These effects, if any, must also be understood if they are rate limiting.

The work presented here has application in design of bioremediation processes. The solute-soil-water system studied is typical of remediation process where microbial degradation is employed to remove a pollutant compound. The modified ELBRO-FV method provides a engineering estimate for partition coefficients of solute for which no data is available. The gas purge apparatus has been accurately modeled and provides an effective method for collecting desorption data. The development of a fundamental mass transport model for soil organic matter systems has been started, and further work recommended. Such a model, based on soil morphology, would allow for rigorous

prediction of pollutant removal rates and aqueous concentrations which are both critical for process design.

# APPENDIX A

## APPENDIX A

## Appendix A: Sub-group representations for model SOM molecules

Slightly different sub-group representations were required to accommodate the use of molar group volumes by the method of Bondi (1968) and of Gmehling et al. (1993). Bondi molar group volumes are taken from the UNIFAC parameter set of Gmehling et al. (1982), and therefore can only be represented with sub-groups included in that parameter set for free volume term calculations. Free volume term calculations for Gmehling molar group volumes of course use the Gmehling et al. (1993) sub-group set. Sub-group representations for both molecules are listed in Table 19 through Table 22.

 Table 19: Stevenson molecule sub-group representation for Bondi molar group volumes.

CH <sub>2</sub>	1
CH	3
ACH	15
AC	22
OH	4
ACOH	13
CH <sub>2</sub> CO	2
CHO	1
HCOO	5
CH-O	6
CH <sub>2</sub> NH	1
CHNH	1
ACNH <sub>2</sub>	1

Table 20: Stevenson molecule sub-group representation for Gmehling molar group volumes.

CH <sub>2</sub>	1
CH	3
ACH	15
AC	22
OH (secondary)	4
ACOH	13
CH <sub>2</sub> CO	2
CHO	1
HCOO	5
СН-О	6
CH <sub>2</sub> NH	1
CHNH	1
ACNH <sub>2</sub>	1

Table 21: Aiken molecule sub-group representation for Bondi molar group volumes.

CH <sub>3</sub>	2
CH <sub>2</sub>	3
CH	7
C=C	1
ACH	9
AC	5
OH	6
ACOH	4
CH <sub>2</sub> CO	1
HCOO	3
СН-О	1

Table 22: Aiken molecule sub-group representation for Gmehling molar group volumes.

CH <sub>3</sub>	2
CH <sub>2</sub>	3
CH	7
C=C	1
ACH	9
AC	5
OH (primary)	3
OH (secondary)	3
ACOH	4
CH <sub>2</sub> CO	1
HCOO	3
СН-О	1

# APPENDIX B

## **APPENDIX B**

# Appendix B: MathCad worksheets for activity coefficients calculations

Three MathCad worksheets are included to illustrate the calculation of activity coefficients for benzene. Activity coefficients are calculated for each of the three phases: octanol, water and soil organic matter (Stevenson model molecule).

# Prediction of Solute Activity Coefficient in Octanol by Gmehling (1993) UNIFAC Model

Tyler T. Ames
Department of Chemical Engineering
Michigan State University
East Lansing, MI 48823

Number of Molecules Temperature, K Set mole fractions for component molecules T:=298  $x_1:=0.00001$   $x_2:=0.99999$ 

$$ln\gamma_{C_i} := 1 - V_i' + ln(V_i') - 5 \cdot q_i \cdot \left(1 - \frac{V_i}{F_i} + ln\left(\frac{V_i}{F_i}\right)\right)$$

$$\gamma_{C_i} = \exp(\ln \gamma_{C_i})$$

$$\begin{array}{ccc}
 & & \gamma \\
 & & \gamma \\
 & -0.22 \\
 & -1.392 \cdot 10^{-11}
\end{array}$$

#### Calculation of Residual Contribution to Activity Coefficient by original UNIFAC residual term:

subgroup

Set number of subgroups for Gmehling ALL (1993) parameters

$$k := 1.. nsgall$$

m := 1.. nsgall

## $g_k := READ(g_all93dta)$

Read in group designation for each

ngall := 45

Read in interaction parameter matrix from Gmehling et al (1993)

$$a_{0,p} := READ(ip\_alldta)$$

$$ag1_{\binom{a_{0,1},a_{0,2}}{0,1}} := a_{0,3} \qquad ag1_{\binom{a_{0,2},a_{0,1}}{0,2}} := a_{0,6}$$

$$ag2_{\binom{a_{0,1},a_{0,2}}{0,1}} := a_{0,4} \qquad ag2_{\binom{a_{0,2},a_{0,1}}{0,2}} := a_{0,7}$$

$$ag3_{(a_{0,1},a_{0,2})} := a_{0,5} \qquad ag3_{(a_{0,2},a_{0,1})} := a_{0,8}$$

$$a1_{m,k} := ag1_{g_m,g_k}$$

$$a2_{m,k} := ag2_{g_m,g_k}$$

$$a3_{m,k} := ag3_{g_m,g_k}$$

$$\boldsymbol{q}_i := \sum_{k} \boldsymbol{\nu}_{i,\,k} \cdot \boldsymbol{Q}_k$$

Equations from Smith and Van Ness (1987)

$$\mathbf{K}$$
 $\mathbf{G}_{\mathbf{k},\mathbf{i}} := \mathbf{V}_{\mathbf{i},\mathbf{k}} \cdot \mathbf{Q}_{\mathbf{k}}$ 

$$\theta_{k} := \sum_{i} G_{k,i} \cdot x_{i}$$

$$\tau_{m,k} := exp \left[ \frac{-\left(a 1_{m,k} + a 2_{m,k} \cdot T + a 3_{m,k} \cdot T^{2}\right)}{T} \right]$$

$$s_{k,i} := \sum_{m} G_{m,i} \cdot \tau_{m,k} \qquad \eta_k := \sum_{i} s_{k,i} \cdot x_i \qquad L_i := \frac{q_i}{\sum_{i} q_j \cdot x_j}$$

$$\eta_k := \sum_i s_{k,i} \cdot x_i$$

$$L_i := \frac{q_i}{\sum_{i} q_j \cdot x_j}$$

$$ln\gamma_{R_i} := q_i \cdot \left(1 - ln(L_i)\right) - \sum_{k} \left(\theta_k \cdot \frac{s_{k,i}}{\eta_k} - G_{k,i} \cdot ln\left(\frac{s_{k,i}}{\eta_k}\right)\right)$$

$$\gamma_{R_i} := exp(ln\gamma_{R_i})$$

$$\begin{array}{c|c}
 & 100 & R_1 \\
\hline
 & 0.893 \\
4.243 & 10^{-11}
\end{array}$$

# **Addition of Combinatorial and Residual Contributions**

$$\begin{aligned} & \ln \gamma_i := \ln \gamma \ C_i + \ln \gamma \ R_i \\ & \gamma_i := \exp \left( \ln \gamma_i \right) \end{aligned}$$



# Prediction of Solute Activity Coefficient in Water by Gmehling (1993) UNIFAC Model

**Tyler T. Ames Department of Chemical Engineering** Michigan State University East Lansing, MI 48823

**Number of Molecules** 

Temperature, K

Set mole fractions for component molecules Benzene = 1

molecs := 2

T := 298

Water = 2

i := 1.. molecs

 $x_1 := 0.00001$ 

j := 1.. molecs

 $x_3 := 0.99999$ 

#### Calculation of Combinatorial Contribution to Activity Coefficient using:

nsgfit := 85

Set number subgroups in fitted R parameter file

k := 1... nsgfit

 $R_{L} := READ(r_fitdta)$ 

 $Q_L := READ(q_all93dta)$ 

Read in fitted R subgroup parameters from file Read in fitted Q subgroup parameters from file

 $v_{1,k} := READ(benzeneall)$ 

Read in molecule 1 subgroup frequencies

 $v_2 = READ(waterall)$ 

Read in molecule 2 subgroup frequencies

$$r_i := \sum_{k} v_{i,k} \cdot R_k$$

$$q_i := \sum_{k=1}^{k} v_{i,k} Q_k$$

$$V_{i} := \frac{\sum_{j=1}^{k} r_{i,k}}{\sum_{j=1}^{k} x_{j} \cdot r_{j}}$$

$$q_{i} := \sum_{k}^{k} v_{i,k} \cdot Q_{k}$$

$$V_{i} := \frac{\sum_{j}^{k} r_{i}}{\sum_{j}^{k} x_{j} \cdot r_{j}}$$

$$V'_{i} := \frac{\left(r_{i}\right)^{\frac{3}{4}}}{\sum_{j}^{4} x_{j} \cdot \left(r_{j}\right)^{\frac{3}{4}}}$$

$$F_{i} := \frac{q_{i}}{\sum_{j}^{4} x_{j} \cdot q_{j}}$$

$$F_i := \frac{q_i}{\sum_j x_j \cdot q_j}$$

$$ln\gamma_{C_i} := 1 - V_i' + ln(V_i') - 5 \cdot q_i \cdot \left(1 - \frac{V_i}{F_i} + ln\left(\frac{V_i}{F_i}\right)\right)$$

$$\gamma C_i := \exp(\ln \gamma C_i)$$

## Calculation of Residual Contribution to Activity Coefficient by original UNIFAC residual term:

Set number of subgroups for Gmehling ALL (1993) parameters

m := 1.. nsgall

## $g_k := READ(g_all93dta)$

Read in group designation for each subgroup

ngall := 45

o := 1.. 530 p := 1.. 8

Read in interaction parameter matrix from Gmehling et al (1993)

$$a_{o,p} := READ(ip\_alldta)$$

$$ag1_{\begin{pmatrix} a_{0,1}, a_{0,2} \end{pmatrix}} := a_{0,3} \qquad ag1_{\begin{pmatrix} a_{0,2}, a_{0,1} \end{pmatrix}} := a_{0,6}$$

$$ag2_{\begin{pmatrix} a_{0,1}, a_{0,2} \end{pmatrix}} := a_{0,4} \qquad ag2_{\begin{pmatrix} a_{0,2}, a_{0,1} \end{pmatrix}} := a_{0,7}$$

$$ag3_{\begin{pmatrix} a_{0,1}, a_{0,2} \end{pmatrix}} := a_{0,5} \qquad ag3_{\begin{pmatrix} a_{0,2}, a_{0,1} \end{pmatrix}} := a_{0,8}$$

Map interaction parameter matrix into separate temperature dependent interaction parameters for groups

$$a1_{m,k} := ag1_{(g_m,g_k)}$$

$$a2_{m,k} := ag2_{g_m,g_k}$$

$$a3_{m,k} := ag3_{(g_m,g_k)}$$

Map group interaction parameters into sub-group interaction parameters

$$q_i := \sum_{k} \nu_{i,k} Q_k$$

Equations from Smith and Van Ness (1987)

$$G_{k,i} := v_{i,k} \cdot Q_k$$

$$\theta_{k} := \sum_{i} G_{k,i} \cdot x_{i}$$

$$\tau_{m,k} := \exp \left[ \frac{-\left(a 1_{m,k} + a 2_{m,k} \cdot T + a 3_{m,k} \cdot T^{2}\right)}{T} \right]$$

$$\mathbf{s}_{k,\,i} := \sum_{m} \mathbf{G}_{m\,,\,i} \cdot \boldsymbol{\tau}_{m\,,\,k} \qquad \boldsymbol{\eta}_{k} := \sum_{i} \mathbf{s}_{k,\,i} \cdot \boldsymbol{x}_{i} \qquad \boldsymbol{L}_{i} := \frac{\boldsymbol{q}_{i}}{\sum_{i} \boldsymbol{q}_{j} \cdot \boldsymbol{x}_{j}}$$

$$ln\gamma_{R_{i}} := q_{i} \cdot \left(1 - ln(L_{i})\right) - \sum_{k} \left(\theta_{k} \cdot \frac{s_{k,i}}{\eta_{k}} - G_{k,i} \cdot ln\left(\frac{s_{k,i}}{\eta_{k}}\right)\right)$$

$$\alpha = \sum_{k} exp(lnx_{i})$$

$$\gamma_{R_i} := \exp(\ln \gamma_{R_i})$$

$$\frac{\gamma_{R_i}}{1.74410^3}$$

# **Addition of Combinatorial and Residual Contributions**

$$ln\gamma_i := ln\gamma_{C_i} + ln\gamma_{R_i}$$

$$\gamma_i := \exp(\ln \gamma_i)$$

$$\frac{\gamma_i}{2.32310^3}$$

# Prediction of Solute Activity Coefficient in Polymeric Phase Using an ELBRO-FV Model w/ Gmehling (1993) Parameters

Tyler T. Ames
Department of Chemical Engineering
Michigan State University
East Lansing, MI 48823

**Number of Molecules** Temperature, K Set mole fractions for Benzene = 1 molecs := 2component molecules Stevenson 1 = 2T := 298 $x_1 := 0.00001$ i := 1 .. molecs  $x_2 := 0.99999$ j := 1.. molecs  $v_1 := READ (benzenemv) v_2 := READ (som_s1mv)$ Read in pure component molar volumes of molecules, cm^3/mole  $v_1 = 89.13$  $v_2 = 1.413 \cdot 10^3$ 

Calculation of Free-Volume/Combinatorial Contribution to Activity Coefficient using:

(1) van der Waals surface area parameters based on the method of Bondi (1968)

(2) van der Waals surface area parameters fitted/optimized by Gmehling et al (1993) . (taken from Gmehling et al, 1982) Bondi Parameters.. nsgvdw := 76 Set number subgroups in vdW R parameter file k := 1 .. nsgvdw  $R_{L} := READ (r_vdwdta)$ Read in vdw R subgroup parameters from file  $v_{1-k} := READ (benzenevdw)$ Read in molecule 1 subgroup frequencies  $v_2 := READ (som_slvdw)$ Read in molecule 2 subgroup frequencies  $\mathbf{v}_{\mathbf{w}_{i}} := \left(\sum_{\mathbf{k}} \mathbf{v}_{i,\mathbf{k}} \cdot \mathbf{R}_{\mathbf{k}}\right) \cdot 15.17$ Calculate van der Waals volume for each molecule from group contributions of subgroup  $v_{w_1} = 48.359$   $v_{w_2} = 775.905$ van der Waals volumes (Rs)  $\mathbf{v}_{\mathbf{f}_{i}} := \mathbf{v}_{i} - \mathbf{v}_{\mathbf{w}_{i}}$ Calculate free volume for each  $v_{f_1} = 40.771 \quad v_{f_2} = 637.095$ molecule  $\phi_{\mathbf{f}\mathbf{v}_{i}} := \frac{\mathbf{x}_{i} \cdot \mathbf{v}_{f_{i}}}{\sum_{i} \left(\mathbf{x}_{j} \cdot \mathbf{v}_{f_{j}}\right)}$ Calculate free volume fraction for each molecule

$$\phi_{\mathbf{f}\mathbf{v}_{i}} := \frac{1}{\sum_{j} \left(\mathbf{x}_{j} \cdot \mathbf{v}_{f_{j}}\right)} \qquad \phi_{\mathbf{f}\mathbf{v}_{i}} \\
\frac{6.4 \cdot 10^{-7}}{1} \\
\ln \gamma_{\mathbf{f}\mathbf{v}_{i}} := \left(\ln \left(\frac{\phi_{\mathbf{f}\mathbf{v}_{i}}}{\mathbf{x}_{i}}\right) + 1 - \frac{\phi_{\mathbf{f}\mathbf{v}_{i}}}{\mathbf{x}_{i}}\right)$$

$$\gamma_{\text{fv}_{i}} := \exp\left(\ln \gamma_{\text{fv}_{i}}\right) \qquad \qquad \ln \gamma_{\text{fv}_{i}} \qquad \gamma_{\text{f}}$$

$$-1.813 \qquad \qquad 0.1$$

$$-4.381 \cdot 10^{-11} \qquad \qquad 0.1$$

Calculate free volume/combinatorial contribution to activity coefficients for each molecule

#### Gmehling et al Parameters...

nsgfit := 85

kk := 1.. nsgfit

 $RR_{kk} := READ (r_fitdta)$ 

vv<sub>1 kk</sub> := READ (benzeneall )

 $vv_{2k} := READ (som_slall)$ 

$$vv_{w_{i}} := \left(\sum_{kk} vv_{i,kk} \cdot RR_{kk}\right) \cdot 15.17$$

$$vv_{w_{1}} = 34.251 \quad vv_{w_{2}} = 907.501$$

$$vv_{f_i} := v_i - vv_{w_i}$$
  
 $vv_{f_1} = 54.879 \ vv_{f_2} = 505.499$ 

$$\phi \phi_{fv_{i}} := \frac{x_{i} \cdot vv_{f_{i}}}{\sum_{j} \left(x_{j} \cdot vv_{f_{j}}\right)}$$

$$\frac{\phi \phi_{fv_{i}}}{\sum_{i} \left(n \cdot vv_{f_{i}}\right)} = \frac{\left(n \cdot vv_{f_{i}}\right)}{\left(n \cdot vv_{f_{i}}\right)} + 1 - \frac{\phi \phi_{fv_{i}}}{\sum_{i} \left(n \cdot vv_{f_{i}}\right)}$$

$$\gamma \phi_{fv_{i}} := \exp\left(n \cdot vv_{fv_{i}}\right)$$

Set number subgroups in fitted R parameter file

Read in fitted R subgroup parameters from file

Read in molecule 1 subgroup frequencies

Read in molecule 2 subgroup frequencies

Calculate van der Waals volume for each molecule from group contributions of subgroup fitted volumes (Rs)

Calculate free volume for each molecule

Calculate free volume fraction for each molecule

Calculate free volume/combinatorial contribution to activity coefficients for each molecule

Calculation of Residual Contribution to Activity Coefficient by original UNIFAC residual term with temperature dependent interaction parameters from the most current data base of Gmehling et al (1993).

nsgall := 85

m := 1 .. nsgall

k := 1.. nsgall

 $Q_{L} := READ (q_all93dta)$ 

 $g_{k} := READ (g_all93dta)$ 

ngall := 45

o := 1.. 530

p := 1..8

 $a_{0,n} := READ (ip\_alldta)$ 

 $ag1 \begin{pmatrix} a_{0,1}, a_{0,2} \end{pmatrix} = a_{0,3} \qquad ag1 \begin{pmatrix} a_{0,2}, a_{0,1} \end{pmatrix} = a_{0,6}$ 

ag2  $\binom{a_{0,1},a_{0,2}}{a_{0,1}} := a_{0,4}$  ag2  $\binom{a_{0,2},a_{0,1}}{a_{0,1}} := a_{0,7}$  into separate temperature dependence interaction parameters for groups

 $ag3 \begin{pmatrix} a_{0,1}, a_{0,2} \end{pmatrix} := a_{0,5} \qquad ag3 \begin{pmatrix} a_{0,2}, a_{0,1} \end{pmatrix} := a_{0,8}$ 

 $al_{m,k} := agl_{(g_m,g_k)}$ 

 $a2_{m,k} := ag2 (g_{m} \cdot g_{k})$ 

 $a3_{m,k} := ag3_{(g_m,g_k)}$ 

 $\mathbf{v}_{i-k} := \mathbf{v} \mathbf{v}_{i-k}$ 

 $\boldsymbol{q}_i := \sum_{\boldsymbol{k}} \boldsymbol{v}_{i,\,\boldsymbol{k}} \cdot \boldsymbol{Q}_{\boldsymbol{k}}$ 

 $G_{k,i} := v_{i,k} \cdot Q_{k}$ 

 $\theta_k := \sum_i G_{k,i} \cdot x_i$ 

 $\tau_{m,k} = \exp \left[ \frac{-\left(a \cdot 1_{m,k} + a \cdot 2_{m,k} \cdot T + a \cdot 3_{m,k} \cdot T^2\right)}{T} \right]$ 

 $s_{k,i} := \sum_{m} G_{m,i} \cdot \tau_{m,k} \qquad \eta_k := \sum_{i} s_{k,i} \cdot x_i \qquad \quad L_i := \frac{q_i}{\sum_{i} q_j \cdot x_j}$ 

 $\ln \gamma_{R_i} := q_i \cdot \left(1 - \ln(L_i)\right) - \sum_{l} \left(\theta_k \cdot \frac{s_{k,i}}{\eta_k} - G_{k,i} \cdot \ln\left(\frac{s_{k,i}}{\eta_k}\right)\right)$ 

 $\gamma_{R_i} := \exp\left(\ln \gamma_{R_i}\right)$ 

Set number of subgroups for Gmehling ALL (1993) parameters

Read in subgroup surface area parameters

for Gmehling ALL (1993)

Read in group designation for each

subgroup

Read in interaction parameter matrix from Gmehling et al (1993)

Map interaction parameter matrix into separate temperature dependent

Map group interaction parameters into sub-group interaction parameters

Equations from Smith and Van Ness (1987)

### **Addition of Free-Volume and Combinatorial Contributions**

# For Free-Volume by Bondi vdW Volumes

$$lny_{B_i} := lny_{fv_i} + lny_{R_i}$$

$$\gamma_{B_i} := \exp(\ln \gamma_{B_i})$$

## For Free-Volume by Gmehling vdW Volumes

$$ln\gamma \ G_{i}^{\ :=\ ln\gamma\gamma} \ fv_{i}^{\ +\ ln\gamma} \ R_{i}^{\ }$$

$$\gamma_{G_i} := \exp(\lim_{i \to \infty} G_i)$$

Imy G
0.642
- 3.052 10 <sup>-11</sup>

# APPENDIX C

### **APPENDIX C**

## Appendix C: FORTRAN code for batch stripping simulation

C **BATCH STRIPPING SIMULATION** C C THIS PROGRAM SIMULATES A BATCH STRIPPING EXPERIMENT. C THE EXPERIMENT CONSISTS OF FOUR PHASES: (1) A SOLID PHASE (SOIL OR SOIL ORGANIC MATTER) WHICH HAS A SPHERICAL GEOMETRY C C IN WHICH FICKIAN DIFFUSION OF A SOLUTE OCCURS, (2) A LIQUID C PHASE (WATER) WHICH IS PERFECTLY MIXED IN WHICH THE SOLID PHASE RESIDES, (3) A GAS PHASE (AIR) WHICH IS USED TO STRIP C THE SOLUTE OUT OF THE LIQUID PHASE, AND (4) THE STRIPPING FLASK C HEAD SPACE. A FILM TYPE MASS TRANSFER RESISTANCE IS INCLUDED С BETWEEN THE LIQUID AND THE GAS PHASE. C C THE MODEL IS COMPROSED OF TWO PDE(S) (DIFFUSION OF THE SOLUTE C IN THE SOIL, AND HEAD SPACE) AND TWO ODE(S) (SOLUTE MASS BALANCES

#### PROGRAM STRIP

EXTERNAL FCNUT, FCNBC
INTEGER LDY,NPDES,NX,I,J,IDO,NSPM
PARAMETER (NSPM=1, NPDES=4+NSPM, LDY=NPDES)
CHARACTER\*70 TITLE,DESCRIP
REAL A0(5),B0(5),G0(5),A1(5),B1(5),G1(5),CS0,CL0,CG0,

- + F,VH,VG,VL,VS(NSPM),KP,H,D,KLA,DELX,XBREAK(22),Y(NPDES,22),
- + GRADCS(NSPM),HINIT,T,DELT,DELTI,TFINAL,UTCH,UTCL,
- + UTCG,CGF,CGIN,RO(NSPM),RI(NSPM),
- + AT,LT,DHS,AH,LH,UTH1,UTT1,UTT0

COMMON A0,B0,G0,A1,B1,G1,F,VH,VG,VL,VS,KP,H,D,KLA,GRADCS,

+ UTCH,UTCL,UTCG,CGIN,RO,RI,

C IN THE LIOUID AND GAS PHASES).

+ AT,LT,DHS,AH,LH,UTH1,UTT1,UTT0

C>>> Open files and gather initial, boundary and model parameters

OPEN (UNIT=69,STATUS='UNKNOWN',FILE='bound.data')
DO 14 I=1,NPDES
READ (69,\*) A0(I),B0(I),G0(I)
READ (69,\*) A1(I),B1(I),G1(I)
CONTINUE
CLOSE (UNIT=69)

OPEN (UNIT=69,STATUS='UNKNOWN',FILE='init.data') READ (69,\*) CT0,CH0,CG0,CL0,CS0 CLOSE (UNIT=69)

```
OPEN (UNIT=69,STATUS='UNKNOWN',FILE='param.data')
    READ (69,86) TITLE
    READ (69,86) DESCRIP
    READ (69,*) TOL
    READ (69,*) TFINAL, DELTI, NX
    READ (69,*) F
    READ (69,*) AT,LT
    READ (69,*) AH,LH,DHS
    READ (69,*) VG
    READ (69,*) VL
    READ (69,*) KP,H,D,KLA
   CLOSE (UNIT=69)
86 FORMAT (A70)
   OPEN (UNIT=69,STATUS='UNKNOWN',FILE='soil.data')
   DO 17 I=1,NSPM
    READ (69,*) RO(I),RI(I),VS(I)
17 CONTINUE
   CLOSE (UNIT=69)
C>>>> Set initial conditions, spatial break points
   DELX=(1.0-0.0)/(NX-1)
   DO 13 I=1,NX
   XBREAK(I)=(DELX*I)-DELX
13 CONTINUE
   DO 15 J=1.NX
    Y(1.J)=CT0
    Y(2,J)=CH0
    Y(3,J)=CG0
    Y(4,J)=CL0
    Y(5,J)=CS0
15 CONTINUE
   CGF=H*Y(4,1)
   CGIN=0.0
   CL=CL0
   DO 19 I=1,NSPM
   GRADCS(I)=0.0
19 CONTINUE
   HINIT=0.0
   T=0.0
   TEND=0.0
   IDO=1
C>>>> Write header information to file
   OPEN (UNIT=69, STATUS='UNKNOWN',FILE=TITLE)
   WRITE (69,92) TEND, Y(2,NX)
```

```
C>>>> Set end-time, calc/print rel. error, calc gas film conc.,
C and write concentrations to file
16 CONTINUE
   DELT=DELTI
   IF (TEND.LT.6.0) THEN
    DELT=0.1
   END IF
   IF (TEND.LT.0.5) THEN
    DELT=0.01
   END IF
   TEND=TEND+DELT
   PRINT 84, TEND
84 FORMAT('Time = ',F12.6)
   CALL MOLCH (IDO,FCNUT,FCNBC,NPDES,T,TEND,NX,XBREAK,
         TOL, HINIT, Y, LDY)
   RERRSL=(ABS(Y(4,1)*KP-Y(5,NX)))/((Y(4,1)*KP+Y(5,NX))/2)*100
   RERRHG=(ABS(Y(2,1)-Y(3,11)))/((Y(2,1)+Y(3,11))/2)*100
   PRINT 91, RERRHG
  PRINT 85, RERRSL
85 FORMAT('% Error in partition constraint = ', F10.6)
91 FORMAT('% Error in head space b.c. = ', F10.6)
   CGF=H*Y(4,1)
   CL=Y(4,1)
   IF (IDO.EQ.3) GO TO 18
   WRITE (69,92) TEND, Y(2,NX)
92 FORMAT (T1,E15.5,',',T18,E15.5)
87 FORMAT(17E15.7)
88 FORMAT(/)
89 FORMAT(T3, 'Time', T18, 'Head Space', T33, 'Gas Phase', T48,
  +'Gas Film', T63, 'Liquid Phase', T78, 'Radius >>>', T89, 11E15.5)
   IF (TEND.GE.TFINAL) IDO=3
   GO TO 16
18 CONTINUE
   CLOSE(UNIT=69)
   END
```

#### C>>>> Subroutines required by IMSL MOLCH

## SUBROUTINE FCNUT (NPDES,X,T,U,UX,UXX,UT)

**INTEGER NPDES** 

**REAL X,T,U(5),UX(5),UXX(5),UT(5),A(1),** 

+ A0(5),B0(5),G0(5),A1(5),B1(5),G1(5)

REAL F,VH,VG,VL,VS(1),KP,H,D,KLA,GRADCS(1),UTCH,UTCL,

- + UTCG,CGIN,RO(1),RI(1),
- + AT,LT,DHS,AH,LH,UTH1,UTT1,UTT0

COMMON A0,B0,G0,A1,B1,G1,F,VH,VG,VL,VS,KP,H,D,KLA,GRADCS,

- + UTCH,UTCL,UTCG,CGIN,RO,RI,
- + AT,LT,DHS,AH,LH,UTH1,UTT1,UTT0

C>>>> Tubing between flask and detector: PFR

C>>>> Head space of flask: PFR with dispersion

C>>>> Gas phase (purging bubbles): well mixed

C>>>> Total area for each soil particle model/classification

$$A(1)=3.0*D/VL*VS(1)/RO(1)/(RO(1)-RI(1))$$

C Add additional A's here as needed

C>>>> Liquid phase: well mixed

- C Add additional terms to end of equation as needed for
- C additional soil models

UT(4)=KLA\*(U(3)-H\*U(4))-A(1)\*GRADCS(1)

- C ( No soil case liquid equation )
- C UT(4)=KLA\*(U(3)-H\*U(4))
- C ( No soil case liquid equation )

C>>>> Soil phase

$$UT(5)=D/(RO(1)-RI(1))**2*(UXX(5)+2/X*UX(5))$$

- C UT(5)=0
- C Add additional equations here for soil models as needed

UTCL=UT(4)

UTCG=UT(3)

```
IF (X .GE. (1.0-0.1*DELX)) GRADCS(1)=UX(5)
IF (X .GE. (1.0-0.1*DELX)) UTH1=UT(2)
```

#### C Add additional gradient assignments as needed

RETURN END

SUBROUTINE FCNBC (NPDES,X,T,ALPHA,BETA,GAMP)

#### **INTEGER NPDES**

REAL X,T,ALPHA(5),BETA(5),GAMP(5),

- + A0(5),B0(5),G0(5),A1(5),B1(5),G1(5),
- + F,VH,VG,VL,VS(1),KP,H,D,KLA,GRADCS(1),UTCH,UTCL,
- + UTCG,CGIN,RO(1),RI(1),
- + AT,LT,DHS,AH,LH,UTH1,UTT1,UTT0

COMMON A0,B0,G0,A1,B1,G1,F,VH,VG,VL,VS,KP,H,D,KLA,GRADCS,

- UTCH,UTCL,UTCG,CGIN,RO,RI,
- + AT,LT,DHS,AH,LH,UTH1,UTT1,UTT0

IF (X .EQ. 0.0) THEN

DO 11 I=1,NPDES ALPHA(I)=A0(I) BETA(I)=B0(I)

GAMP(I)=GO(I)

11 CONTINUE

BETA(2)=-DHS/F\*AH

GAMP(4)=UTCL

GAMP(3)=UTCG

GAMP(2)=UTCG

C GAMP(1)=UTH1

#### **ELSE**

DO 12 I=1,NPDES

ALPHA(I)=A1(I)

BETA(I)=B1(I)

GAMP(I)=G1(I)

12 CONTINUE

GAMP(5)=UTCL\*KP

GAMP(4)=UTCL

GAMP(3)=UTCG

**END IF** 

**RETURN** 

**END** 

# BOUND.DATA (Boundary conditions input file)

0.0, 0.0, 0.0

0.0, 0.0, 0.0

1.0, 0.0, 0.0

0.0, 1.0, 0.0

1.0, 0.0, 0.0

1.0, 0.0, 0.0

1.0, 0.0, 0.0

1.0, 0.0, 0.0

0.0, 1.0, 0.0

1.0, 0.0, 0.0

# APPENDIX D

For: No Soil			For: Colwood A	(whole)	
Henry's Law Coeff. (r	nass/vol.):	0.387	Henry's Law Coeff. (mass/vol.): Partition Coeff. (mass/mass):		0.387
Partition Coeff. (mass	s/mass):	0			18.6
Gas Volume (mL):	112		Gas Volume (mL):	112	
Liquid Volume (mL):	210		Liquid Volume (mL):	210	
Soil Mass (g):	0		Soil Mass (g):	1	
Solute Mass (g):	8.40E-04		Solute Mass (g):	8.40E-04	
Liquid Conc. (g/mL): 3.316E-06			Liquid Conc. (g/mL):	3.089E-06	
Gas Conc. (g/mL):	1.283E-06		Gas Conc. (g/mL):	1.195E-06	
Soil Conc. (g/g): 0.00E+00			Soil Conc. (g/g):	5.75E-05	

For: Colwood (53-125 micron)		For: Colwood (250-500 micron)		
Henry's Law Coeff. (mass/vol.): Partition Coeff. (mass/mass):	0.387 116	Henry's Law Coeff. (mass/w Partition Coeff. (mass/mass	•	
Gas Volume (mL): 112		Gas Volume (mL):	112	
Liquid Volume (mL): 210		Liquid Volume (mL):	210	
Soil Mass (g):		Soil Mass (g):	1	
<b>Solute Mass (g):</b> 8.40E-04		Solute Mass (g): 8.	40E-04	
Liquid Conc. (g/mL): 2.274E-06		Liquid Conc. (g/mL): 2.10	03E-06	
Gas Conc. (g/mL): 8.802E-07		Gas Conc. (g/mL): 8.	14E-07	
Soil Conc. (g/g): 2.64E-04		Soil Conc. (g/g): 3.	07E-04	

# LIST OF REFERENCES

#### LIST OF REFERENCES

- Abed, Y., Gabas, N., Delia, M.L. and Bounahmidi, T. (1992) Measurement of liquid-solid phase equilibrium in ternary systems of water-sucrose-glucose and water-sucrose-fructose, and predictions with UNIFAC, *Fluid Phase Equilibria* 73, 175.
- Aiken, G.R. et al.. (1985) Humic Substances in Soil Sediment and Water, Wiley, New York.
- Atkinson, B. and Mavituna, F. (1983) Biochemical Engineering and Biotechnology Handbook, Macmillan Publishers Ltd, England.
- Ball, W.P. and Roberts, P.V. (1991a) Long-term sorption of halogenated organic chemicals by aquifer material. 1. Equilibrium, *Environ. Sci. Technol.* 25, 1223.
- Ball, W.P. and Roberts, P.V. (1991b) Long-term sorption of halogenated organic chemicals by aquifer material. 2. Intraparticle diffusion, *Environ. Sci. Technol.* 25, 1237.
- Benzing, T.R. (1993) The desorption kinetics of nonionic organic compounds from hexadecyltrimethylammonium-modified soils and clays, Ph.D. Dissertation, Michigan State University, East Lansing.
- Biltz, W. (1934) Rauchemie der festen stoffe, 1. Voss, Leipzig.
- Bondi, A. (1968) Physical Properties of Molecular Crystals, Liquids and Glasses, Wiley, New York.
- Briggs, G.G. (1981) J. Agric. Food Chem. 29, 1050.
- Brusseau, M.L. and Rao, P.S.C. (1989) Sorption nonideality during organic contaminant transport in porous media, *Critical Rev. in Environ. Control* 19, 33.
- Brusseau, M.L. and Rao, P.S.C. (1991) Influence of sorbate structure on nonequilibrium sorption of organic compounds, *Environ. Sci. Technol.* 25, 1501.
- Brusseau, M.L., Jessup, R.E. and Rao, P.S.C. (1990) Sorption kinetics of organic chemicals: evaluation of gas-purge and miscible-displacement techniques, *Environ. Sci. Technol.* 24, 727.

- Brusseau, M.L., Jessup, R.E. and Rao, P.S.C. (1991) Nonequilibrium sorption of organic chemicals: elucidation of rate-limiting processes, *Environ. Sci. Technol.* 25, 134.
- Chiou, C.T. (1990) Roles of organic matter, minerals, and moisture in sorption of nonionic compounds and pesticides by soil, *Humic Substances in Soil and Crop Sciences; Selected Readings*, American Society of Agronomy and Soil Science Society of America.
- Chiou, C.T. and Shoup, T.D. (1985) Soil sorption of organic vapors and effects of humidity on sorptive mechanism and capacity, *Environ. Sci. Technol.* 19, 1196.
- Chiou, C.T., Peters, L.J. and Freed, V.H. (1979) A physical concept of soil-water equilibria for nonionic organic compounds, *Science* **206**, 831.
- Chiou, C.T., Porter, P.E. and Schmedding, D.W. (1983) Partition equilibria of nonionic compounds between soil organic matter and water, *Environ. Sci. Technol.* 17, 227.
- Cooling, M.R., Khalfaoui, B. and Newsham, D.M.T. (1992) Phase equilibria in very dilute mixtures of water and unsaturated chlorinated hydrocarbons and of water and benzene, *Fluid Phase Equilibria* 81, 217.
- Crittenden, J.C., Hutzler, N.J. and Geyer, D.G. (1986) Transport of organic compounds with saturated groundwater flow: Model development and parameter sensitivity, *Water Resources Research* 22, 271.
- Danckwerts, P.V. (1953) Continuous flow systems: distribution of residence times, *Chem. Eng. Sci.* 2, 1.
- Doong, S.J. and Ho, W.S.W. (1991) Sorption of organic vapors in polyethylene, *Ind. Eng. Chem. Res.* 30, 1351.
- Elbro, H.S., Fredenslund, Aa. and Rasmussen, P. (1990) A new simple equation for the prediction of solvent activities in polymer solutions, *Macromolecules* 23, 4707.
- Fogler, H.S. (1986) Elements of Chemical Reaction Engineering, Prentice-Hall, Englewood Cliffs, New Jersey.
- Fredenslund, Aa., Gmehling, J. and Rasmussen, P. (1977) Vapor-liquid equilibria using UNIFAC, Elsevier Scientific, New York.
- Gmehling, J., Li, J. and Schiller, M. (1993) A modified unifac model. 2. Present parameter matrix and results for different thermodynamic properties, *Ind. Eng. Chem. Res.* 32, 178.
- Gmehling, J., Rasmussen, P. and Fredenslund, Aa. (1982) Vapor-liquid equilibria by UNIFAC group contribution. Revision and extension. 2, *Ind. Eng. Chem. Process Des. Dev.* 21, 118.

- Hansen, H.K., Rasmussen, P., Fredenslund, Aa., Schiller, M. and Gmehling, J. (1991)
  Vapor-liquid equilibria by UNIFAC group contribution. 5. Revision and extension,
  Ind. Eng. Chem. Res. 30, 2352.
- Hooper, H.H., Michel, S. and Prausnitz, J.M. (1988) Correlation of liquid-liquid equilibria for some water-organic liquid systems in the region 20-250 degrees celsius, *Ind. Eng. Chem. Res.* 27, 2182.
- Hwang, Y., Keller, G.E. II and Olson, J.D. (1992a) Steam stripping for removal of organic pollutants from water. 1. Stripping effectiveness and stripper design, *Ind. Eng. Chem. Res.* 31, 1753.
- Hwang, Y., Keller, G.E. II and Olson, J.D. (1992b) Steam stripping for removal of organic pollutants from water. 2. Vapor-Liquid Equilibrium Data, *Ind. Eng. Chem. Res.* 31, 1759.
- Iwai, Y. and Arai, Y. (1989) Measurement and prediction of solubilities of hydrocarbon vapors in molten polymers, J. Chem. Eng. Japan 22, 155.
- Karickhoff, S.W., Brown, D.S. and Scott, T.A. (1979) Sorption of hydrophobic pollutants on natural sediments, *Water Research* 13, 241.
- Kontogeorgis, G.M., Fredenslund, A. and Tassios, D.P. (1993) Simple activity coefficient model for the prediction of solvent activities in polymer solutions, *Ind. Eng. Chem. Res.* 32, 362.
- Kyle, B.G. (1981) Soil-water equilibria for nonionic organic compounds, *Science* 213, 683.
- Lambert, S.M. (1968) Omega, a useful index of sorption equilibria, J. Agr. Food Chem. 16, 340.
- Lambert, S.M., Porter, P.E. and Schieferstein, R.H. (1965) Movement and sorption of chemicals applied to the soil, *Weeds* 13, 185.
- Larsen, B.L., Rasmussen, P. and Fredenslund, Aa. (1987) A modified UNIFAC group-contribution model for prediction of phase equilibria and heats of mixing, *Ind. Eng. Chem. Res.* 26, 2274.
- Macedo, E.A., Weidlich, U., Gmehling, J. and Rasmussen, P. (1983) Vapor-liquid equilibria by UNIFAC group contribution. Revision and extension. 3, *Ind. Eng. Chem. Process Des. Dev.* 22, 676.
- Magnussen, T., Rasmussen, P. and Fredenslund, Aa. (1981) UNIFAC parameter table for prediction of liquid-liquid equilibria, *Ind. Eng. Chem. Process Des. Dev.* 20, 331.

- Miller, C.T. and Weber, W.J. Jr. (1986) Sorption of hydrophobic organic pollutants in saturated soil systems, *Journal of Contaminant Hydrology* 1, 243.
- Oishi, T. and Prausnitz, J.M. (1978) Estimation of solvent activities in polymer solutions using a group-contribution method, *Ind. Eng. Chem. Process Des. Dev.* 17, 333.
- Peel, R.G., Benedek, A. and Crowe, C.M. (1981) A branched pore kinetic model for activated carbon adsorption, *AIChE Journal* 27, 26.
- Robinson, K.G., Farmer, W.S. and Novak, J.T. (1990) Availability of sorbed toluene in soils for biodegradation by acclimated bacteria, Wat. Res. 24, 345.
- Ruckenstein, E., Vaidyanathan, A.S. and Youngquist, G.R. (1971) Sorption by solids with bidisperse pore structures, *Chemical Engineering Science* 26, 1305.
- Rutherford, D.W., Chiou, C.T. and Kile, D.E. (1992) Influence of soil organic matter composition on the partition of organic compounds, *Environ. Sci. Technol.* 26, 336.
- Sandler, S.I. (1989) Chemical and Engineering Thermodynamics, John Wiley and Sons, New York.
- Steinberg, S.M., Pignatello, J.J. and Sawhney, B.L. (1987) Persistence of 1,2-dibromoethane in soils: Entrapment in intraparticle micropores, *Environ. Sci. Technol.* 21, 1201.
- Stevenson, F.J. (1982) Humus Chemistry: Genesis, Composition, Reactions, Wiley, New York.
- Tiegs, D., Gmehling, J., Rasmussen, P. and Fredenslund, Aa. (1987) Vapor-liquid equilibria by UNIFAC group contribution. 4. Revision and extension, *Ind. Eng. Chem. Res.* 26, 159.
- Wakao, N. and Smith, J.M. (1962) Diffusion in catalyst pellets, *Chemical Engineering Science* 17, 825.
- Weber, W.J. Jr., Voice, T.C., Pirbazari, M., Hunt, G.E. and Ulanoff, D.M. (1983) Sorption of hydrophobic compounds by sediments, soils and suspended solids II, *Wat. Res.* 10, 1443.
- Wu, Shian-chee and Gschwend, P.M. (1986) Sorption kinetics of hydrophobic organic compounds to natural sediments and soils, *Environ. Sci. Technol.* 20, 717.